CAPP for Hybrid Additive Manufacturing.

Zhen Hong

THESE DE DOCTORAT DE

L'ÉCOLE CENTRALE DE NANTES

ECOLE DOCTORALE N° 602
Sciences pour l'Ingénieur
Spécialité : Génie Mécanique

Par
Zhen HONG

CAPP for Hybrid Additive Manufacturing

Thèse présentée et soutenue à l'Ecole Centrale de Nantes , le 28/04/2021

Unité de recherche : UMR 6004, Laboratoire des Sciences du Numérique de Nantes (LS2N)

Rapporteurs avant soutenance :

Nicolas PERRY, Professeur des universités, Ecole Nationale Supérieure d'Arts et Métiers (Talence)

Frédéric VIGNAT, Maître de conférences HDR, Grenoble INP

Composition du Jury :

Présidente : Lihong QIAO, Professeure, Beihang University (Chine)

Examinateur : Sébastien CAMPOCASSO, Maître de conférences, Université de Toulon

Dir. de thèse : Alain BERNARD, Professeur des universités, École Centrale de Nantes

Co-dir. de thèse : Yicha ZHANG, Maître de conférences HDR, Université de Technologie de Belfort Montbéliard

Acknowledgements

Since Ph.D. study is a very challenging time period, it is never easy to finish it alone. I am grateful to have had the opportunity to study in France; it has been one of the most meaningful stages of my life. I have numerous people to give my thanks and gratitude to.

First, I give special thanks and gratitude to my supervisor, Professor Alain Bernard, and my co-supervisor Dr. Yicha Zhang, who gave me countless suggestions and encouragement with admirable and nonstop patience. I am very lucky to have two supervisors like them, and without their help, I could not have finished my work.

I am honored to have Prof. Lihong Qiao, Dr. Frédéric Vignat, Prof. Nicolas Perry, and Dr. Sébastien Campocasso as the jury members for my thesis defense. I would like to send the best regards to them for their valuable time and comments. Especially great thanks are due to two reporters Prof. Nicolas Perry and Dr. Frédéric Vignat for spending their precious time reviewing my manuscript and giving many insightful comments to improve my understanding of the research topic. I am grateful for Prof. Lihong Qiao as the president and for Dr. Sébastien Campocasso for his precious time and valuable suggestions. All of the comments and professional reputations of my jury members encourage me and inspire me greatly.

I am very grateful to Professor Nabil ANWER and Professor François VILLENEUVE, for sparing their valuable time to read my reports every year and for many professional suggestions. Thanks to the CSI meeting, I have had an opportunity to communicate with them, which has helped me to make a great progress. I am particularly thankful to Professor K. P. Karunakaran for his help when he visited ECN; I am grateful for his kind advice on writing emails, modifying slides, and encouragement in researching and improving English.

Many deep and special thanks go to my colleague and friend, Zhiping Wang, for his great help in developing the applications by using Grasshopper and his kindness. Also, I appreciate the help of Dr. Sihao Deng and Dr. Hongjian Wu for the experiments in UTBM.

I am very grateful to all of my dear friends, some of my favorite people on the planet, who come from different cultural backgrounds, who have volleyed many questions on all walks of life, and who share my nonstop enthusiasm for practicing languages and playing table tennis. I am also grateful to one very good friend, Elaheh Maleki, who helped me a lot and recommended I live with a nice French lady. Living with this lady has helped me grow in my knowledge of French culture.

A truly heartfelt and special thanks go to my best friend, confidant, and shoulder to lean on who has always been the driving force behind my perseverance and excitement in everything I do: my mother. I cannot thank my siblings more for their selfless and deep love, for supporting all of my choices financially and spiritually.

Finally, I would like to thank my Lab LS2N for the good academic environment with a high degree of internationalization. This whole period has been incredible and unforgettable, and all the people I have met and all the valuable experiences I have had will be a great treasure!

Contents

List of Acronyms

AFO: Ankle-foot-orthosis

AIMS: Additive systems Integrated with subtractive Methods

AM: Additive Manufacturing

ASTM: American Society for Testing and Materials

CAD: Computer-Aided Design

CAM: Computer-Aided Manufacturing

CAO: Conception Assistée par Ordinateur.

CAPP: Computer-Aided Process Planning

CC: Cutter Contact

CIRP: Collège International pour la Recherche en Productique

CNC: Computer Numerical Controlled

CS: Cold Spray

DASH: Direct Additive Subtractive Hybrid Manufacturing

DED: Directed Energy Deposition

DM-HAM: Digital Manufacturing-based Hybrid Additive Manufacturing processes

DMLS: Direct Metal Laser Sintering

EBM: Electron Beam Melting

FDM: Fused Deposition Modeling

FFF: Fused Filament Fabrication

FSP: Friction Stir Processing

GA: Genetic Algorithm

GH: Grasshopper

HAM: Hybrid Additive Manufacturing

HDMR: Hybrid Deposition and Micro Rolling

HLM: Hybrid Layered Manufacturing

HM: Hybrid Manufacturing

HPDM: Hybrid Plasma Deposition Manufacturing

HWMP: Hybrid WAAM and Milling Process

ICT: Immersive Computing Technologies

IV: Initial Volume

LAMP: Laser Aided Manufacturing Processes

MAT: Medial Axis Transform

MAG: Metal Active Gas

MIG: Metal-Inert Gas

MLS: Moving Least Squares

PAMPROD: Procédés Additive Manufacturing – PRODuctivité

PLCs: Programmable Logic Controllers

PBF: Powder Bed Fusion

WAAM: Wire and Arc Additive Manufacturing

WHASPs: Workstations for Hybrid Additive and Subtractive Processes

RE: Reverse Engineering

RP: Rapid Prototyping

SDM: Shape Deposition Manufacturing

SLM: Selective Laser Melting

SM: Subtractive Manufacturing

SWIFT: Solvent Welding Freeform Fabrication Technique

STL: Standard Tessellation Language/ Standard Triangle Language

USW: Ultrasonic Metal Welding

List of Figures

List of Tables

Abstract

Hybrid Additive Manufacturing (HAM) is becoming increasingly important to fabricate end-use functional components. However, a couple of problems still exist in all the stages of HAM's processing chain. This thesis reports the studies on process planning for multi-axis sequential HAM in the AM processing module. The whole research proposes a set of methods for three key tasks at a relatively general level. The main proposed methods include the generation and optimization of the initial volume, sequence planning of remaining volumes, and path planning for each subpart.

1. Initial volume generation & optimization

In the AM module of hybrid additive manufacturing processes, the process can start from an existing volume which can be fabricated with economic conventional processes. It is called initial volume in this research, which could be a simplified shape close to some subparts of the physical model. A skeleton-based decomposition method is used to generate alternative initial volumes. To avoid manufacturing constraints and ensure component quality, the coplanar and adjacent branch set is found at the first step of the optimization process. The second step is to search for the optimal initial volume, considering the material change rate, by an evolutionary optimization method, Particle Swarm Optimization (PSO) algorithm.

2. The sequence planning for AM subparts in AM processing module

After obtaining the initial volume, all the remaining volumes (the difference between the original CAD model and the initial volume), decomposed into AM subparts, are supposed to be built via an AM processing module. Hence, the HAM scope in this research is limited to a sequential process, where AM processing is adopted first based on the initial volume to obtain the near-net-shape of the CAD model and then non-AM processing is used for post-processing. To obtain a near-net-shape model, the AM subparts should be additively manufactured in a reasonable sequence to save time, material and avoid processing constraints. This research proposes a method using the initial volume and the decomposed subparts as the inputs of a variant assembly optimization problem. An optimization algorithm is proposed to solve this problem. It divides the AM subparts into a set of adjacent groups and considers two types of tool collisions (hard collision and soft collision) as constraints in the multi-axis AM scenario for optimization. For the selected AM subparts, the proposed method can automatically identify an optimal sequence for additively building the subparts in the AM processing module of sequential HAM processes. An application simulation example for a cold spraying-based HAM process is presented for method illustration.

3. Toolpath planning

To save the additive manufacturing time spent on each AM subpart, a new deposition path optimization method is proposed. In this method, the toolpath is generated based on sweeping the real deposition profile measured from the experiment which is used to set the scanning hatching space and layer thickness to ensure manufacturability implicitly. Then, contour and rastering scanning formats are used in combination to generate toolpaths for each layer with a randomly assigned rastering angle. A PSO algorithm is adopted to search for the shortest toolpath length.

To demonstrate these proposed methods above, a set of numerical simulation cases are used for demonstration. A special multi-axis sequential HAM process, cold spraying with CNC machining, is adopted to set the application requirements and manufacturing constraints in computation. However, the objective of this research is to develop generic methods for more multi-axis HAM processes, e.g., WAAM, DED, by adapting the manufacturing constraints.

Keywords: CAPP, HAM, cold spray, decomposition, initial volume, sequence planning, toolpath planning, evolutionary optimization.

Résumé

La fabrication additive hybride (HAM) devient de plus en plus importante pour fabriquer des composants fonctionnels destinés à l'utilisation finale. Cependant, quelques problèmes persistent à toutes les étapes de la chaîne de traitement de HAM. Cette thèse rapporte les études sur la planification de processus pour HAM séquentiel multi-axes dans le module de traitement AM. L'ensemble de la recherche propose un ensemble de méthodes pour trois tâches clés à un niveau relativement général. Les principales méthodes proposées comprennent la génération et l'optimisation du volume initial, la planification de la séquence des volumes restants et la planification du trajectoire pour chaque sous-partie.

1. Génération et optimisation du volume initial

Dans le module AM des processus de fabrication additive hybride, le processus peut démarrer à partir d'un volume existant qui peut être fabriqué avec des processus conventionnels économiques. Il est appelé volume initial dans cette recherche, qui pourrait être une forme simplifiée proche de certaines sous-parties du modèle physique. Une méthode de décomposition basée sur un squelette est utilisée pour générer des volumes initiaux alternatifs. Pour éviter les contraintes de fabrication et garantir la qualité des composants, l'ensemble de branches coplanaires et adjacentes se trouve à la première étape du processus d'optimisation. La deuxième étape consiste à rechercher le volume initial optimal, compte tenu du taux de changement de matériau, par une méthode d'optimisation évolutive, l'algorithme d'optimisation de l'essaim de particules (PSO).

2. La planification de séquence pour les sous-parties AM dans le module de traitement AM

Après avoir obtenu le volume initial, tous les volumes restants (la différence entre le modèle CAO original et le volume initial), décomposés en sous-parties AM, sont censés être construits via un module de traitement AM. Par conséquent, la portée HAM dans cette recherche est limitée à un processus séquentiel, où le traitement AM est d'abord adopté en fonction du volume initial pour obtenir la forme quasi nette du modèle CAO, puis un traitement non AM est utilisé pour le post-traitement. Pour obtenir un modèle de forme proche du réseau, les sous-pièces AM doivent être fabriquées de manière additive dans un ordre

raisonnable pour gagner du temps, du matériel et éviter les contraintes de traitement. Cette recherche propose une méthode utilisant le volume initial et les sous-parties décomposées comme entrées d'un problème d'optimisation d'assemblage variant. Un algorithme d'optimisation est proposé pour résoudre ce problème. Il divise les sous-parties AM en un ensemble de groupes adjacents et considère deux types de collisions d'outils (collision dure et collision douce) comme des contraintes dans le scénario AM multi-axes pour l'optimisation. Pour les sous-parties AM sélectionnées, le procédé proposé peut identifier automatiquement une séquence optimale pour la construction additive des sous-parties dans le module de traitement AM des processus HAM séquentiels. Un exemple de simulation d'application pour un procédé HAM à base de pulvérisation à froid est présenté pour illustrer la méthode.

3. Planification du parcours d'outil

Pour économiser le temps de fabrication additive passé sur chaque sous-pièce AM, une nouvelle méthode d'optimisation du trajectoire de dépôt est proposée. Dans ce procédé, le parcours d'outil est généré sur la base du balayage du profil de dépôt réel mesuré à partir de l'expérience qui est utilisé pour définir l'espace de hachures de balayage et l'épaisseur de couche pour assurer implicitement la fabricabilité. Ensuite, les formats de numérisation de contour et de tramage sont utilisés en combinaison pour générer des trajectoires d'outils pour chaque couche avec un angle de tramage attribué de manière aléatoire. Un algorithme PSO est adopté pour rechercher la longueur de parcours d'outil la plus courte.

Pour démontrer ces méthodes proposées ci-dessus, un ensemble de cas de simulation numérique est utilisé pour la démonstration. Un procédé HAM séquentiel multi-axes spécial, la pulvérisation à froid avec usinage CNC, est adopté pour définir les exigences de l'application et les contraintes de fabrication dans le calcul. Cependant, l'objectif de cette recherche est de développer des méthodes génériques pour des procédés HAM plus multi-axes, par exemple WAAM, DED, en adaptant les contraintes de fabrication.

Mots clés: CAPP, HAM, la pulvérisation à froid, décomposition, volume initial, planification de séquence, planification de trajectoire, optimisation évolutive.

Chapter 1 – The Background and Motivation

1.1 The background

Manufacturing has an evolution from concept, then to methods and tools, and can be used to produce goods for sale and end-use [1]. Till now, new methods in advanced manufacturing are emerging, and AM is one of the brightest ones illustrated in Fig. 1.1. [1] because of its capacity to manufacture parts with complex geometries by adding layers of materials without tooling and fixtures. In addition, AM also provides freedom to design, offers mass customization, and removes shipping parts and warehouse storage, reduces waste and energy consumption [1][2][3][4].

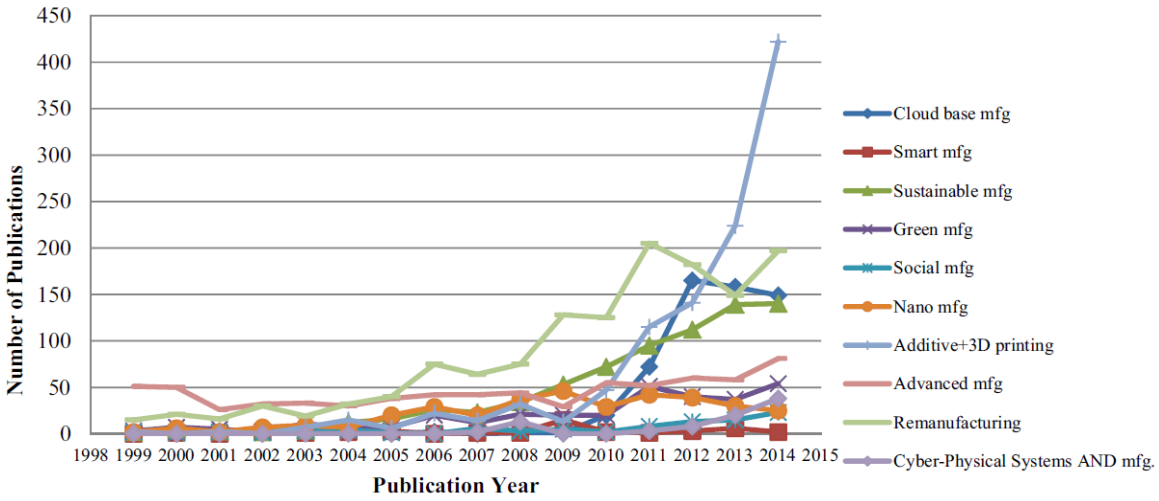

Fig. 1.1. The trend of most recent manufacturing concepts [1].

However, limitations still exist in AM processes, such as limited materials, long production time, dimensional accuracy, and surface quality [5][6]. Moreover, challenges still exist in the design, modeling, data format, standards, materials, specific software, etc. in both academia and industrial applications [3][7].

The limitations of AM can be solved by hybrid processes illustrated in Fig. 1.2. [8]. Moreover, traditional subtractive manufacturing processes have many advantages like the high quality of finish surface and high speed illustrated in Fig. 1.3. [9]. As a result, the combination of additive and subtractive manufacturing processes is a promising solution to

minimize the limitations of both AM and traditional processes [10][11]. Hybrid processes open up new opportunities and applications for manufacturing various components [12]. Hybrid Additive Manufacturing (HAM) is increasingly employed for fabricating end-use parts or remanufacturing old parts [6] [13][14][15].

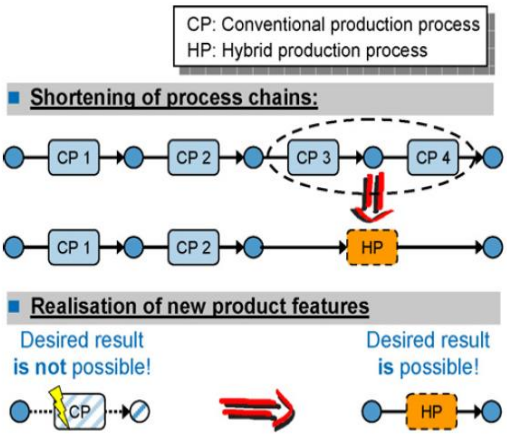

Fig. 1.2. The potential aims of hybrid manufacturing processes [8].

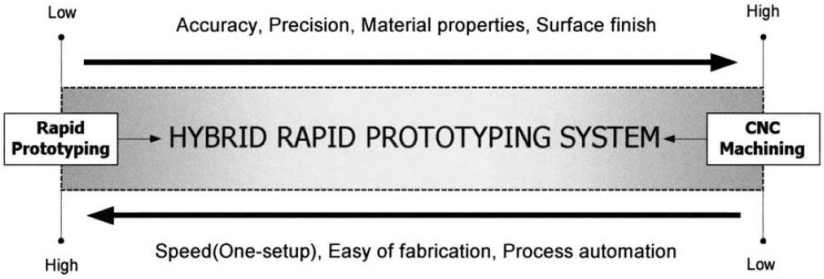

Fig. 1.3. The characteristics of RP and CNC processes [9].

Therefore, HAM is regarded as the overlap between conventional manufacturing technologies, such as machining, casting, forging, stamping, welding, etc., and additive manufacturing (AM), as shown in Fig. 1.4.

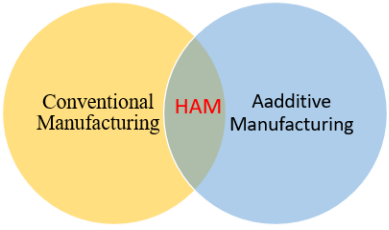

Fig. 1.4. The relationship of conventional, AM and HAM manufacturing technologies.

Then what is exactly HAM? There are many definitions, one is that “the use of AM with one or more secondary processes or energy sources that are fully coupled and synergistically affect part quality, functionality, and/or process performance” [16]. However, the AM process and Non-AM process can be operated in one machine or operated separately. Generally, the HAM processes can be classified by “type” and “timing” [17]. In detail, ”*timing*” including concurrent, main/assistive (M/S) separate, as well as main/main (M/M) separate and for the fabrication ”*type*” consisted of additive, subtractive, and the assistive process illustrated in Fig. 1.5 [17]. Furthermore, based on the concept of timing, the HAM processes include two generic groups: iterative (there are many iterations of AM and non-AM processing during the layer construction) and sequential (AM first then non-AM, or non-AM first then AM, no iteration in the layer construction) shown in Fig. 1.6.

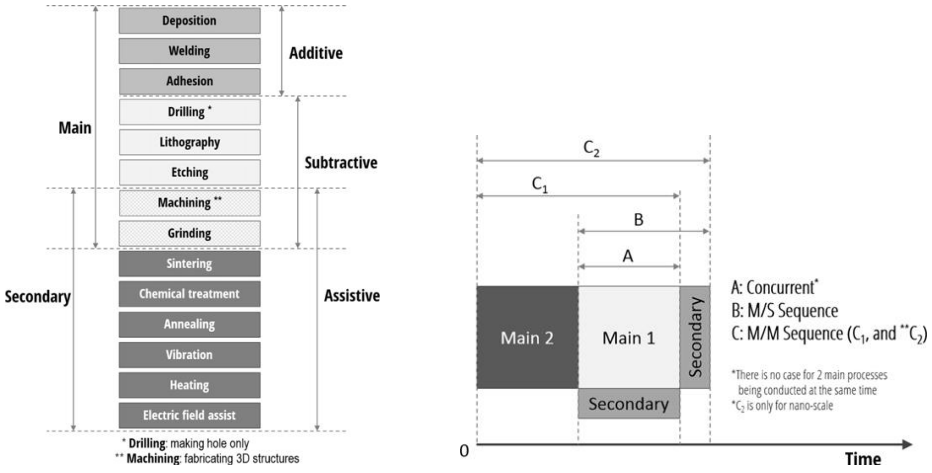

Fig. 1.5. (1). The classification by ‘**type**’; (2) The classification by ‘**timing**’ [17].

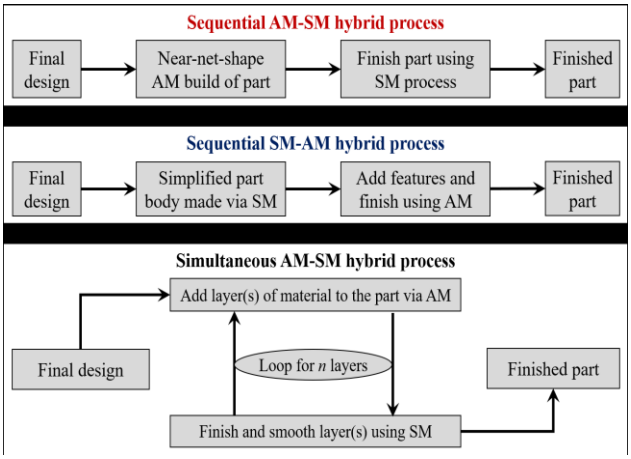

Fig. 1.6. The typical sequential and iterative hybrid AM/SM process [18].

1.2 The research scope

In this research, the research focus is on the sequential HAM process, where a near-net-shape will be obtained firstly in the AM module of a HAM system, and then the no-AM modules are used to improve surface and shape accuracy via finishing operation or improve mechanical properties via other post-processing techniques. A developing HAM process with a cold-spray-based AM module is adopted for method illustration and demonstration.

The CSHAM platform is in development at UTBM, which is a modular HAM robotic HAM platform illustrated in Fig. 1.7., where robots are used as connections to link different existing processing modules/machines. Therefore, there is no need to integrate and modify the existing machines, and it is more flexible, reconfigurable, sustainable, etc.

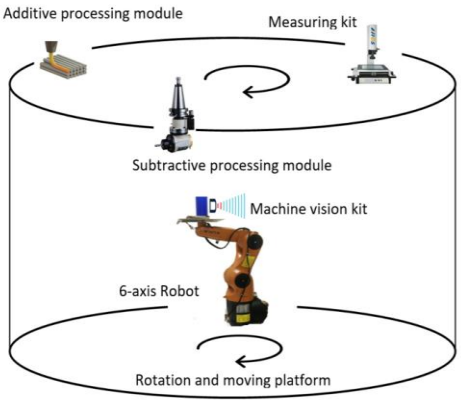

Fig. 1.7. The sequential Cold Spray based modular HAM concept in development at UTBM.

The CSAM platform is shown in Fig. 1.8., and the CS gun is fixed, robot catching the substrate to fix the initial volume (an existing volume to deposit material onto and become one part of the final component) in this research.

Fig. 1.8. The CSAM platform at UTBM.

The mechanism of CSAM [19] (illustrated in Fig. 1.9.) is that the compressed gas divides into two streams, and one passes through a powder feeder, while the other stream passes through a gas heater. Both of these two streams join together before entering a de-Laval nozzle. The gas and the powers become supersonic, so the powders project to the substrate to form a thick deposit mainly by kinematic energy. Because it is solid-state deposition, it has many specific characteristics illustrated in Table 1.1.

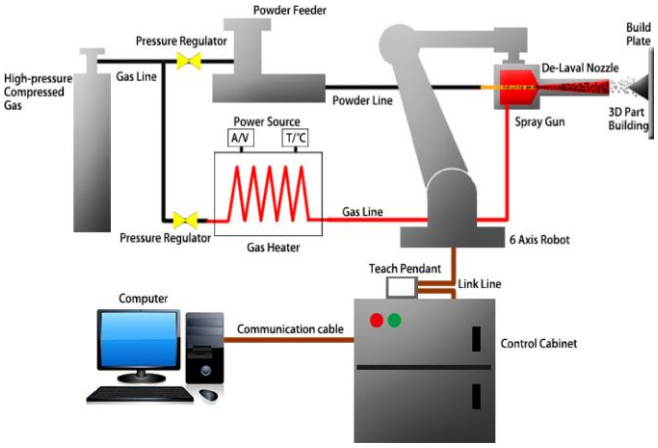

Fig. 1.9. The schematic diagram of the CSAM module [19].

Table 1.1. The CS characteristics compared with other AM processes [20]

	CSAM	**SLM**	**EBM**	**LMD**
Powder feed mode	Direct deposition	Powder bed	Powder bed	Direct deposition
Feedstock limitations	Difficulty processing high hardness and strength metals	Difficulty processing high reflectivity and poor flowability metals	Unsuitable for non-conductive and low melting-temperature metals	Difficulty with high reflectivity metals
Powder melting	No	Yes	Yes	Yes
Product size	Large	Limited	Limited	Large
Dimensional accuracy	Low	High	High	Medium
Mechanical properties (as-fabricated)	Low	High	High	High
Mechanical properties (heat treatment)	High	High	High	High
Production time	Short	Long	Long	Long
Equipment flexibility	High	Low	Low	Low
Suitable for repair	Yes	No	No	Yes

However, there are still some limitations for AM processes, including CSAM, shown in the following two examples.

Firstly, one example in the academic domain, the bracket [21], is illustrated in Fig. 1.10. It is fabricated by the CS process starting from 0, so the support structure is mandatory, and the materials are hugely wasted.

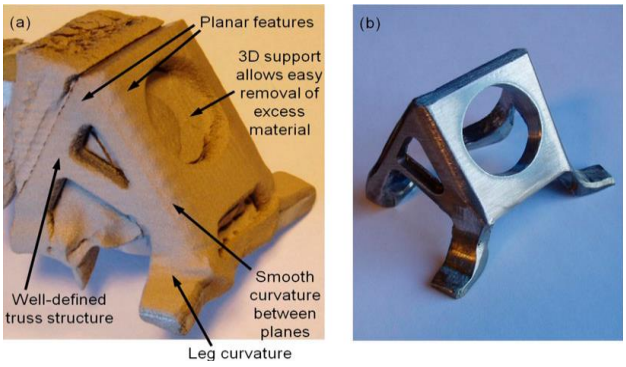

Fig. 1.10. One example from the existing research [21].

Secondly, one industrial example (illustrated in Fig. 1.11. (1)). shows that the steps of process planning (illustrated in Fig. 1.11. (2)). are still operated manually based on human's experience, which is not stable and cannot guarantee the quality either.

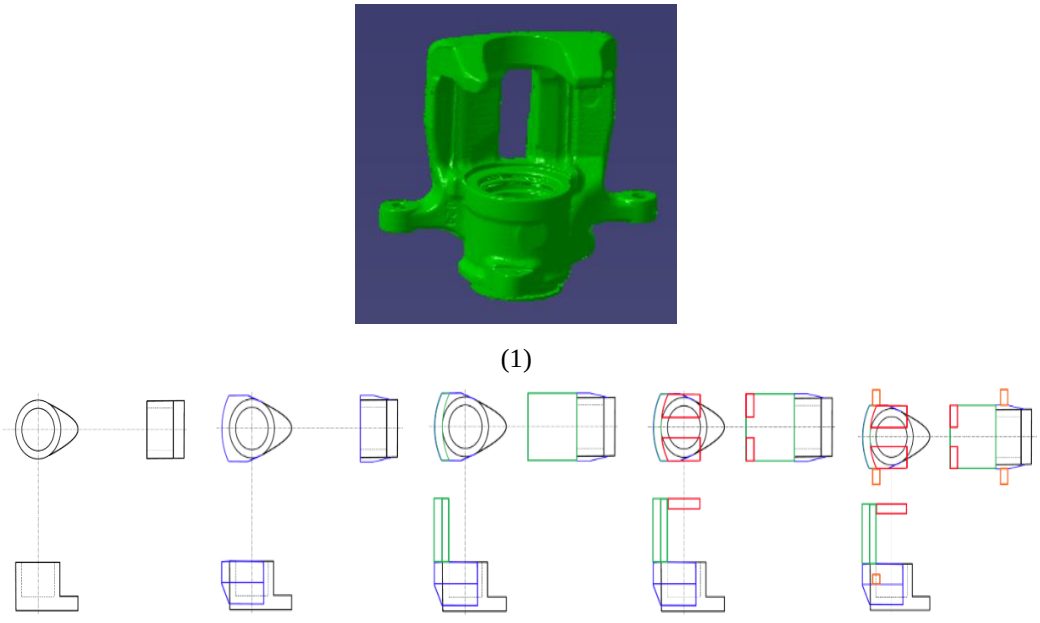

(1)

(a) Step 1 (b) Step 2 (c) Step 3 (d) Step 4 (e) Step 5

(2)

Fig. 1.11. The manual sequence planning according to experiences in an industrial manufacturing process.

Therefore, the CSAM module has some problems need to be solved as follows:

(1) Start from 0 or an existing volume (defined as an initial volume in this thesis);

(2) The sequence for subparts/remaining volume (considering collisions, spraying distance, CS gun dimensions, etc.);

(3) The toolpath to deposit material is essential, for the scanning time/length can greatly influence the cost of the manufacturing process because the CS process is expensive and cannot stop in between.

1.3 The objectives and the PhD report structure

Due to the industrial needs, when using HAM, it is necessary to start from an existing volume and it also needs an automatic process plan for saving cost and time and ensuring manufacturing quality. Currently, since the HAM is still new and under development, there are few process planning solutions available in the literature for multi-axis HAM, considering the existing volume. To fill this gap, this research is devoted to analyzing the process planning problem thoroughly to identify the general common planning tasks and tries to propose a set of methods for those identified planning tasks at a relatively general level for the AM module of multi-axis sequential HAM. As a consequence, the objectives of this research are as follows:

(1) To save the costs of AM module of CS based HAM by starting from an existing volume;

(2) To reach an optimal 'near-net-shape' CAD model in the AM module automatically;

(3) To propose a generic method that can be extended to other multi-axis processes like WAAM, DED, etc.

To present the research problem and corresponding contributions, this Ph.D. dissertation is structured as in Fig. 1.12.

Based on the objectives, the state-of-the-art of process planning for AM and HAM is presented in Chapter 2, and considering the existing contributions and limitations of CAPP for HAM, three research questions are proposed.

To solve the three questions, three corresponding methods are presented with one complex tree model as an illustrative example in Chapter 3. The first contribution relates to a new approach for the definition and the search of the optimal "initial volume", which is used as a deposit substrate for the sequential HAM process's AM processing module. The initial

volume is as a starting volume, so, probably, some remaining volumes need to be built via AM processing module to form the near-net-shape physical component of a given CAD model. Therefore, the second one is a new approach to generate the optimal sequence for building AM subparts (generated by decomposing the remaining volumes) sequence. For the building of each subpart, the toolpath directly influences the time and quality. Hence, the third proposed method is a new method for the toolpath planning in the AM module, considering the real profile of cold spray and varying the angles of rastering for each layer.

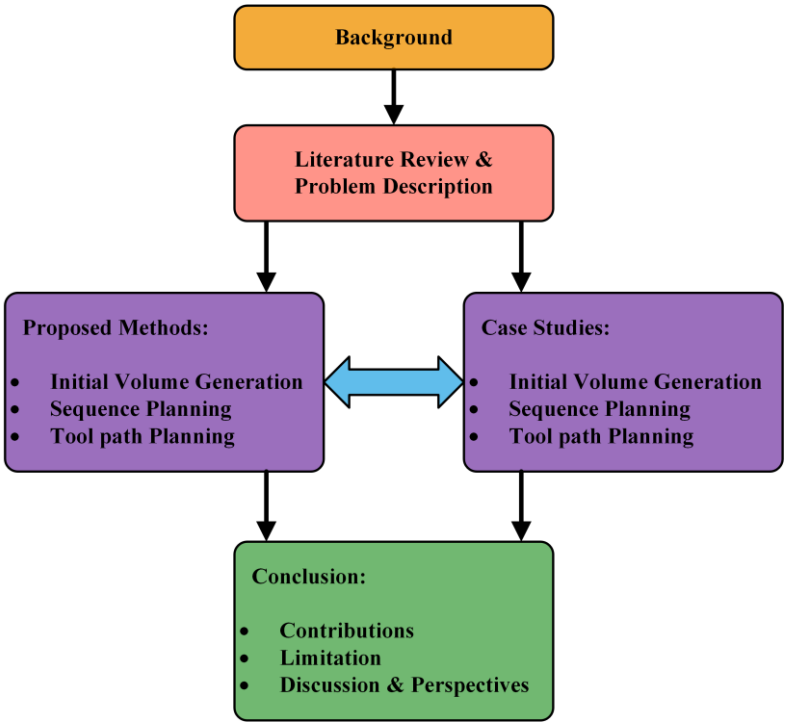

Fig. 1.12. The dissertation outline.

After the illustration of proposed methods in Chapter 3, to verify the proposed method, three models are adopted for case studies in Chapter 4.

In Chapter 5, a general conclusion is drawn based on the contributions and limitations, and the perspectives of future work are also introduced to improve the limitations of the research.

Chapter 2 – The State of the Art and Research Questions

In this chapter, based on the research objectives mentioned above, a survey on existing research is extensively conducted to extract the main research questions to be addressed in this thesis based on the contributions and limitations of the existing research.

2.1 The state of the art on AM and HAM

2.1.1 Additive Manufacturing

The term "Additive Manufacturing" was ultimately selected by the ASTM F42 committee and defined as "A process of joining materials to make objects from the 3D model, usually layer upon layer, as opposed to subtractive manufacturing methodologies, with many synonyms: additive fabrication, additive processes, additive techniques, additive layer manufacturing, layer manufacturing, and freeform fabrication" [22]. AM leads to a revolution in the way products are designed, manufactured, and distributed to end-users [3]. Therefore, AM is part of the next industrial revolution, and it has evolved from prototypes to end-use products [2][7].

Historically, the origin of AM is difficult to define and there were many activities in the 1950s and 1960s, but the associated technology (computers, lasers, controllers, etc.) developed in the early 1980s. Interestingly, parallel patents were filed in 1984 in Japan (Murutani), France (André et al.), and the USA (Masters in July and Hull in August) [4]. In addition to photo sculpture (in the 1860s) and topography (in the 1890s), modern AM techniques emerged, based on four key patents: vat photopolymerization, powder bed fusion, material extrusion, and binder jetting [23]. During these three last decades, AM had a great development thanks to the improvement and emergence of some related technologies like reverse engineering (RE), Computer-Aided Design (CAD), haptic-based technology, as well as materials, computer science, energy sources, etc. Concerning the available materials, originally, AM technology was developed with polymeric materials, waxes, and paper laminates. Subsequently, composites, metals, and ceramics were used [4]. Most recently, the American Society for Testing and Materials (ASTM) international committee F42, had classified AM technologies into seven categories: (1) material extrusion, (2) powder bed fusion, (3) vat photopolymerization, (4) material jetting, (5) binder jetting, (6) sheet lamination, and (7) directed energy deposition. For AM, the most generic process includes eight steps, shown in Fig. 2.1. [4]. Very recently, the particle spraying process, e.g. cold spray

(CS), is used as an additive manufacturing process for volume building due to a set of advanced processing characteristics [24].

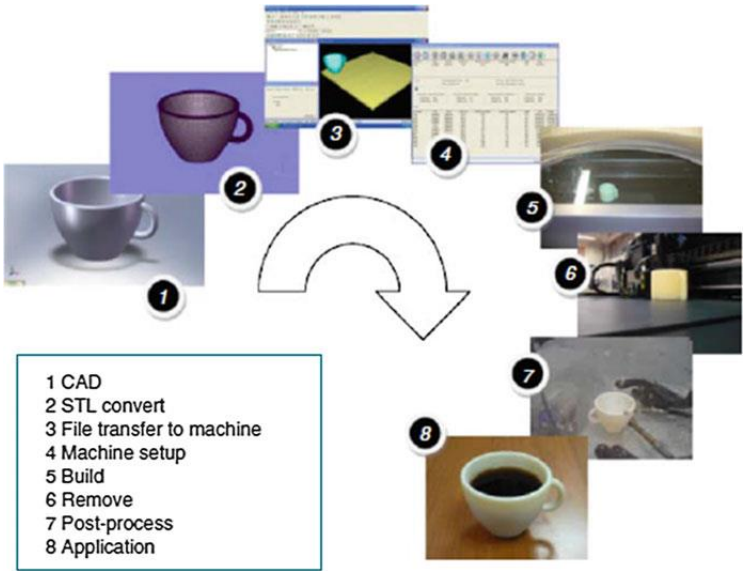

Fig. 2.1. The generic steps of AM process [4].

From the industrial perspective, AM technologies significantly influence traditional production models from industrial machinery, assembly processes, and supply chains, etc. [3][7]. It is employed in many industrial fields, such as: medical and health industry [25][26], aviation [27] and aerospace [28], food [29], clothing [30], education [31], fashion and arts [32], electronics [33], and defense [34], etc. A series of applications and cases can be found [2][4][7][33], and very complex structures and internal features can be manufactured [35][36][37].

From the perspective of the characteristics of AM, Rosen D.W. [4] summarized the unique capabilities of AM into 4 kinds of complexity: (1) shape complexity: the complex geometry (such as undercuts, enclosures, sharp internal corners) is difficult to produce with CNC, even with 5-axis interpolated control [4]. (2) material complexity: AM enables the manufacturing with multi-materials. (3) hierarchical complexity: multi-scale of features, sub-features, etc. (4) functional complexity: functional devices can be fabricated directly by embedding components.

On the other hand, many limitations of AM exist and are divided into two generic groups [5]: (1) geometric limitations because of stair-step effect; (2) process and material limitations. Even though AM can be used for finished parts instead of only for prototyping, post-processing by conventional processes like machining is most often necessary for the final

quality. Moreover, conventional processes like casting, stamping, CNC machining can be used iteratively or sequentially associated with AM processes, to take advantage of all the processes. Therefore, the hybrid AM is coming out with its necessity and strengths.

2.1.2 The hybrid AM

2.1.2.1 The definitions of HAM

Firstly, there is a need to clarify what "*hybrid*" refers to, what "*hybrid processes*" mean in practice, and how it is considered in this thesis.

The term "*hybrid*" has been widely used in many areas of manufacturing [16]. And it is used to describe several hybrid techniques: (1) hybrid processes, (2) hybrid machines, which refer to the machine platform rather than the constituent processes and (3) hybrid materials, structures, or functions, combining one or more materials to have a hybrid composition, structure, or function [38].

Moreover, the CIRP (Collège International pour la Recherche en Productique) gave a definition of the hybrid processes which is the simultaneous and controlled interaction of process mechanisms and/or energy sources/tools having a significant effect on process performance [38]. Similarly, a definition of hybrid additive manufacturing (HAM) was proposed by Michael P. Sealy et. al [16], mentioned three key features of HAM: (1) fully coupled processes, (2) synergy, (3) part and/or process improvement.

Up to date, there are a large number of researches on hybrid processes. Z. Zhu et al [12] reviewed the development of hybrid manufacturing processes and they attempted to propose possible definitions of hybrid processes and classified hybrid processes into 7 groups, shown in Fig. 2.2, based on the technology classification method, consisting of five categories, namely joining, dividing, subtractive, transformative and additive technologies given by Nassehi et al. [39]. From their viewpoint, the term "*hybrid processes*" is defined as an approach that combines two or more manufacturing operations, each of which is from different manufacturing technologies, which is a comprehensive and systematic method for the classification of hybrid processes.

Also, Won-Shik Chu et al in 2014 summarized hybrid manufacturing in micro/nanoscale and proposed a new classification method of hybrid processes in terms of both process "*timing*" and "*type*" [17]. In addition, a similar concept with "*timing*" method of Won-Shik Chu is presented according to CIRP's most recent classification efforts [38], including two major types of hybrid manufacturing processes: (1) assisted processes and (2) mixed or

combined processes. For the former classification, there exists three primary assisting processes, i.e. (1) vibration-assisted machining (implements vibration to assist with material removal or by-product/waste removal or disposal), (2) laser-assisted machining (eases machining forces by softening the workpiece), and (3) media-assisted manufacturing (uses a coolant or lubricant to assist the primary process). In terms of mixed processes, two or more processes are performed somewhat simultaneously.

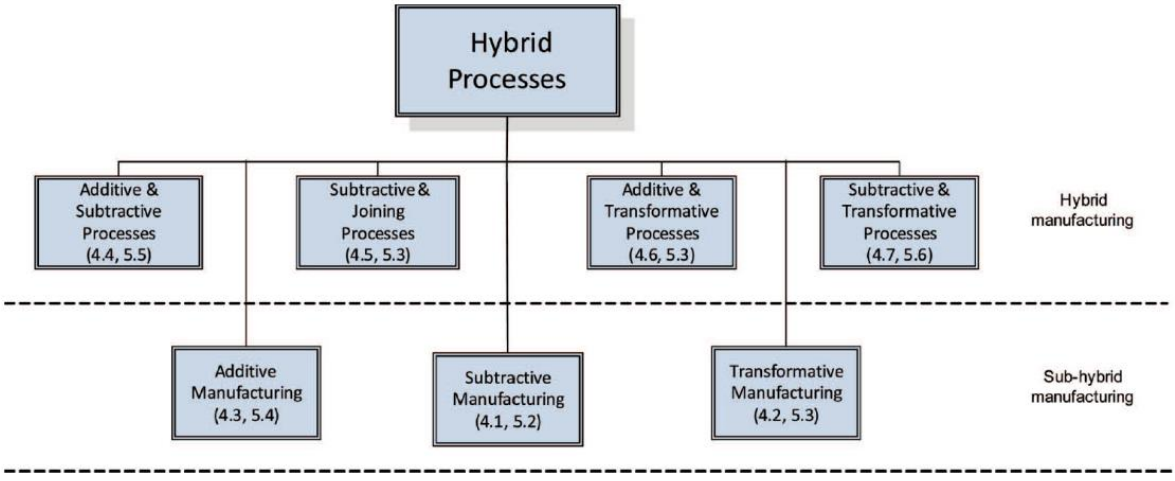

Fig. 2.2. The classification of major hybrid processes' research areas [12].

However, hybrid processes can be identified where individual processes are introduced serially or in parallel and increase the overall process capability [40].

For all the hybrid processes, if considering 'timing', as mentioned in the first chapter, they can be classified into iterative and sequential. In this thesis, the definition of HAM is considered as the AM and non-AM processing which can be sequential or iterative, and the AM and non-AM processing module can be integrated into one machine or combined like a traditional workstation in a modular way. The research scope of this research is on multi-axis sequential HAM, taking cold spray process as a specific AM process with machining (even casting, heat treatment, etc.) in a modular way.

2.1.2.2 The typical HAM machines and systems

In industrial domain, a set of commercial machines and systems have been developed, and the details of HAM processes shown in Table 2.1., namely, Hybrid-OR Creator, Matsuura's LUMEX Advance-25/ Advance-60, DMGO Mori, IBARMIA ZVH 45 L1600,

ARCONIC's Ampliforge Process, Hermle's MPA technology, Optomec's LENS 3D metal hybrid system.

Table 2.1. Some typical HAM machines

Companies	Machines	Additive processes	Non-AM processes	Sequencial-S/ Iterative-I	Ref.
OR Laser	Hybrid-OR Creator	Selective laser melting	3-axis milling	I	https://www.or-laser.com/info/laser-3d-printer
Matsuura	LUMEX Advance-25/ Advance-60	PBF	3-axis milling	I	https://www.matsuura.co.uk/additive-manufacturing/
Sodick	OPM250L/ OPM350L	PBF	3-axis milling	I	https://www.sodick.com/products/metal-3d-printing
DMGO Mori	LASERTEC 65 3D; LASERTEC S LM	Laser deposition welding; selective laser melting	5-axis CNC machining	S	https://en.dmgmori.com/products/machines/additive-manufacturing/powder-nozzle/lasertec-65-ded-hybrid
IBARMIA	IBARMIA ZVH 45 L1600	Laser cladding	5-axis milling and turning	S	https://www.ibarmia.com/en/tecnologia/add-process/
ARCONIC	Ampliforge Process	Welding	Forging	S	https://www.arconic.com/global/en/search/search.asp?q=Ampliforge+Process&page=0
Hermle	MPA technology	Thermal spray process	5-axis CNC machining	S	https://www.hermle.de/en/media/technical_press/getPrm/entry/03_03_2021_additive_machining_at_supersonic_speed/
Optomec	LENS 3D metal hybrid system	DED	5-axis CNC machining	S	https://optomec.com/3d-printed-metals/lens-technology/
Fabrisonic	SonicLayer 4000	Ultrasonic Additive Manufacturing (UAM)	3-axis vertical machining	S	https://fabrisonic.com/
IREPA LASER	PAMPROD project	DED-CLAD process; SLM + CLAD®; PBF + DED-CLAD®	Machining (post-processing)	S	https://www.irepa-laser.com/applications/fabrication-additive

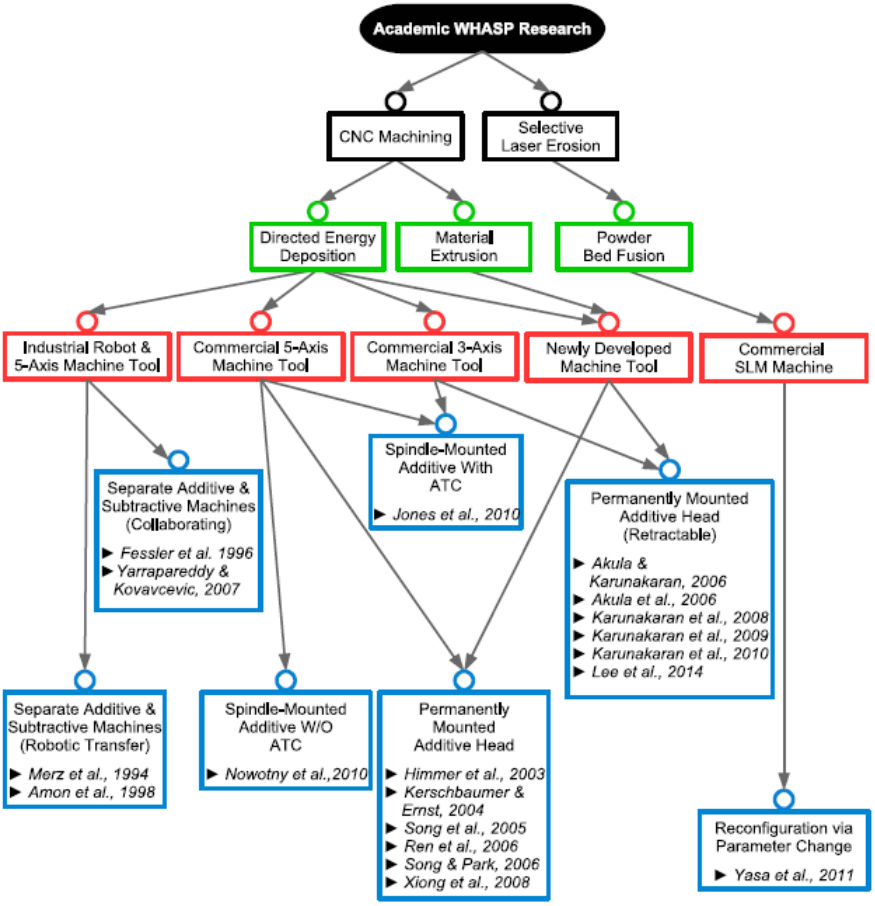

Fig. 2.3. The type of motion platform used and machine reconstruction and exchange method between additive and subtractive processes [10].

In the academic domain, there are many different types of hybrid AM processes. ‘WHASPs’ (Workstations for Hybrid Additive and Subtractive Processes) were termed, focused on metallic products by Joseph M Flynn et al. in 2016, the subdivision of hardware configurations developed in software research grouped as illustrated in Fig. 2.3. [10]. From their study, academic researches related to WHASPs are broken down into three layers: hardware, controller, and software layers [10]. Among the increasing number of WHASPs, many of these integrate directed energy deposition (DED) with subtractive CNC machining within a highly mobile multi-axis machine-tool [10] and there are also welding with Subtractive Manufacturing (SM) [11][41][42][43], as well as cladding with SM [13][44][45]. In addition, even though most HAM processes are combinations of AM with machining [46][47][48][49][50], there are also other hybrid AM processes related to thermal function, such as surface treatments, laser remelting, or erosion [51][52] and even mechanical surface treatments such as peening [53][54] or rolling. In addition, some methods combine injection

molding and milling [55], and the combination between additive and transformative manufacturing processes [52][56], as well as Ultrasonic Additive Manufacturing (UAM), with CNC machining [57].

The typical HAM systems in the academic domain are introduced in Table 2.2.

Table 2.2. Some typical HAM systems

Main Researchers	Systems	Additive processes	Non-AM processes	Start time/place	Sequencial-S/ Iterative-I	Ref.
Merz, R. et al.	Shape Deposition Manufacturing (SDM)	Thermal deposition techniques: plasma or laser-based deposition process	5-3axis CNC milling or (Deposition Manufacturing)	1994/ Stanford	S	[58]
A.G. Cooper et al.	Mold Shape Deposition Manufacturing (Mold SDM)	Solid freeform fabrication	5-axis CNC machining	1999/ Stanford	S	[59]
Chen, Y.H.	Layer Based Machining (LBM)	LM processes	7/5-degree Robot/CNC	2000/ University of Hong Kong	S	[60] [61] [62] [63]
F. W. Liou	Laser Aided Manufacturing Processes (LAMP)	Laser deposition	5-axis CNC milling	2001/ UMR	I	[64]
James B. Taylor	Solvent Welding Freeform Fabrication Technique (SWFFT)	Solvent welding	3/5-axis CNC machining	2001/ North Carolina State University	S	[65] [66]
Karunakaran et al	Hybrid-Layered Manufacturing (HLM)	Synergic MIG–MAG welding process	3-axis CNC machining	2004/ Indian Institute of Technology	S	[43]
Z. Zhu et al.	iAtractive	Additive	Subtractive and Inspection Processes	2011/ Bath university	I	[67]
Haiou Zhang et al.	Hybrid Deposition and Micro Rolling (HDMR)	Deposition	Micro rolling	2013/ Huazhong keji	I	[68] [69]
Guha	AIMS (Additive	Additive systems	Subtractive	2015/	S	[70]

Manogharan et al.	systems Integrated with subtractive MethodS) CNC-RP	(EBM/DMLS)	Methods (CNC)	Youngstown State University & North Carolina State University		
Matthew C. Frank et al.	Direct Additive Subtractive Hybrid Manufacturing (DASH)	Any direct metal additive manufacturing process	4-axis CNC milling system	2017/ Iowa State University of Science and Technology	S	[71]
Fang Li et al.	HWMP (Hybrid WAAM and Milling Process)	WAAM (wire arc additive manufacturing)	Milling process	2017/ Beijing University of Technology	S	[72]

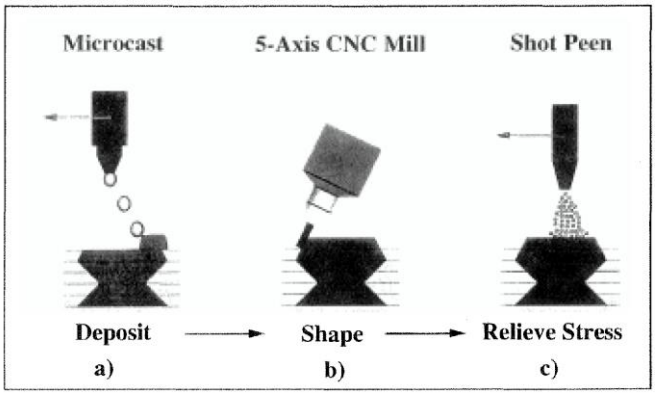

Fig. 2.4. The creation of a layer using SDM [58].

The details of some typical hybrid processes in Table 2.2. are as follows. The Shape Deposition Manufacturing (SDM) was the first HAM which can date back to 1994, shown in Fig. 2.4. [58], associated with the research on additive processes including laser deposition of metal [73] and micro-casting [74]. Then there were many studies related to this process, like robot-assisted shape deposition manufacturing [75], optimal motion planning based on the geometry skeleton instead of recursive-offset algorithms [76], process planning and

automation for SDM [77], near-optimal build orientations [78], Mold Shape Deposition Manufacturing (Mold SDM) [59], automated layer decomposition for SDM [79]. Moreover, it is used for biologically inspired hierarchical microstructures, modifying it to mold SDM to make it less labor-intensive and less difficult for handling cast materials and inserts [80]. This process is an iterative HAM process because each compact is deposited and then uses CNC and shot peen, illustrated in Fig. 2.4. After finishing one compact, the following one will be fabricated till the last one.

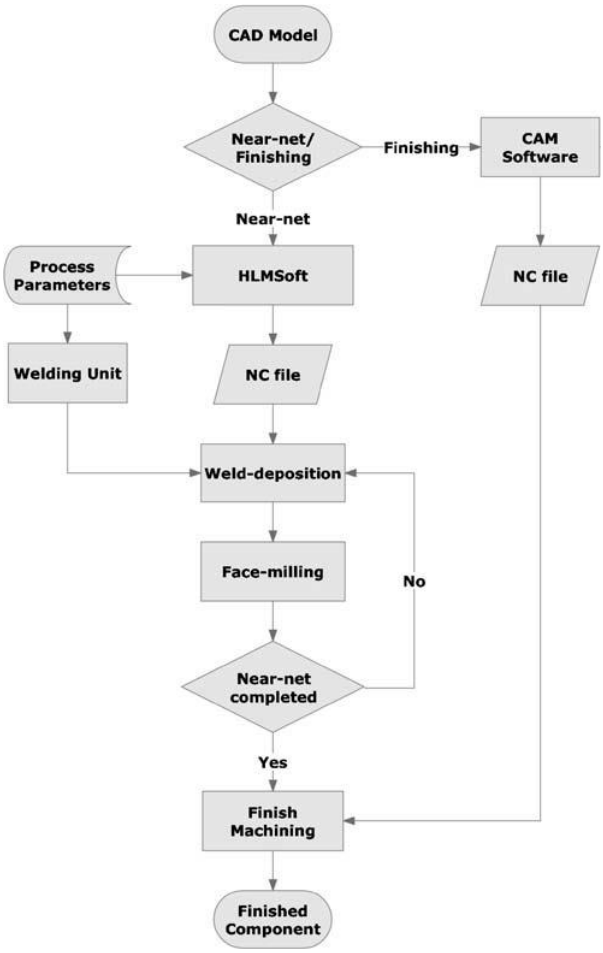

Fig. 2.5. The flow chart for ArcHLM process [43].

For the combination of welding and machining, Karunakaran et al. also have done several pieces of research on arc welding and milling, shown in Fig. 2.5., named Hybrid-Layered Manufacturing (HLM), developed for fabricating metallic dies and molds, using Metal-Inert Gas (MIG)–Metal Active Gas (MAG) welding and introducing zeroth-order edge approximation uniform slicing strategy [41][43][81]. The HLM process consists of 4 stages: (a) building a near-net-shape of the tool; (b) then rough machining the near-net shape to final dimensions; (c) heat treatment for stress relieving and strengthening; (d) finish milling to

obtain the required surface finish and quality. After they made a techno-economic analysis for HLM, proving that HLM is significantly cheaper and faster than CNC machining [42]. Moreover, the statistical process design was made, illustrating the complex cause-effect relationships between design parameters and performance [82]. Also, retro-fitment of a CNC machine for hybrid layered manufacturing named ArcHLM was presented and it is a low-cost retro-fitment to any existing CNC machine for making metallic objects [43]. This type of HAM process is sequential, because the welding process fabricates the part as a near-net-shape part, and then uses milling to guarantee the accuracy and surface quality for end-use.

F.W. Liou et al. have carried out many pieces of research on Laser Aided Manufacturing Process (LAMP), shown in Fig. 2.6. [64], from multi-axis slicing to toolpath generation and the decomposition of part, etc. This type of HAM process is multi-axis iterative.

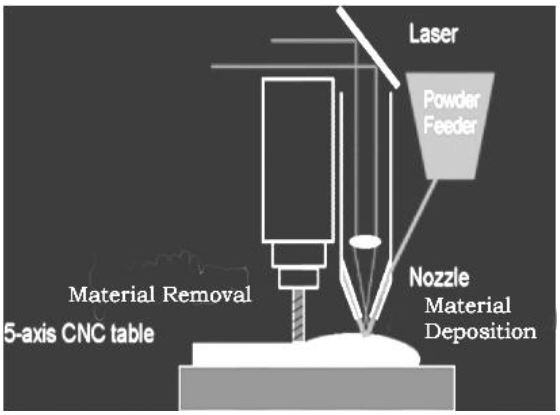

Fig. 2.6. A Five-axis LAMP system [64].

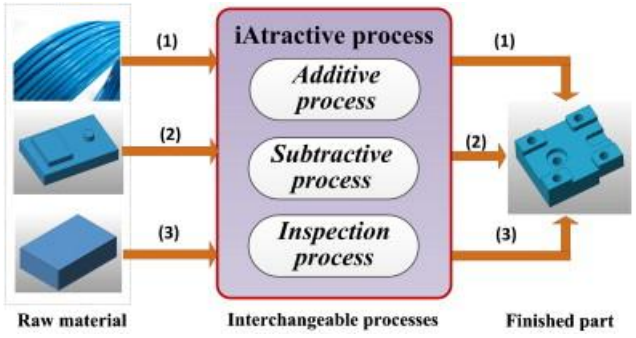

Fig. 2.7. The proposed iAtractive process [83].

Z. Zhu et al. proposed a HAM system called iAtractive, combining additive, subtractive, and inspection in 2012, shown in Fig. 2.7. [67]. They later carried out some research on process planning [83][84], and application for high precision manufacture of prismatic parts

difficult to machine [85]. This process is considered from scratch or the reuse of existing material, and it is an iterative process combining AM, SM, and inspection.

In 2013, Haiou Zhang et al. presented a new HAM process called Hybrid Deposition and Micro-Rolling (HDMR) [68][69], which combines hybrid deposition and micro-rolling and the Metamorphic Rolling Mechanism shown in Fig. 2.8. Later in 2015, they continue this research on the process using a hot-rolling process to assist the arc welding to improve mechanical property [86]. They also have done some research on the simulation of microstructure evolution during hybrid deposition and micro-rolling process [87] as well as the investigation of the mechanical properties on hybrid deposition and micro-rolling of bainite steel [88]. This is an iterative HAM process, and welding and rolling are employed iteratively.

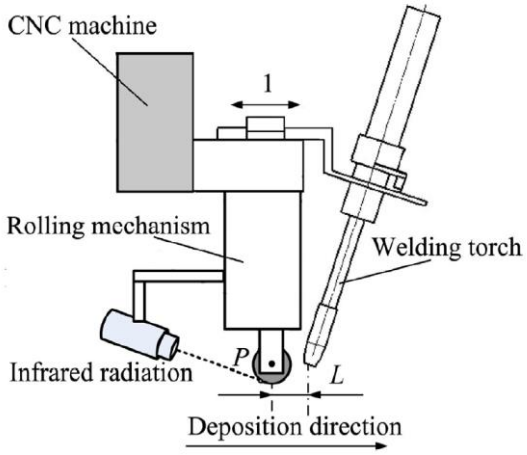

Fig. 2.8. The schematic of deposition and rolling experimental equipment [68].

In 2015, AIMS (Additive systems Integrated with subtractive MethodS) were proposed by Guha Manogharan et al., shown in Fig. 2.9. [70]. Later, Direct Additive Subtractive Hybrid manufacturing (DASH) was proposed in 2017, using both additive and then subtractive processing so that mechanical parts can be "*digitally manufactured*" to meet the final required geometric accuracy [71] and the DASH process includes 9 steps, shown in Fig. 2.10.: (a) customer model input, (b) AMF model creation with critical features identified, (c) machining setup orientation planning, (d) addition of machining allowance and sacrificial fixture supports, (e) metal AM processing, (f) clamping in CNC mill, (g) scanning and part localization, (h) automated toolpath generation, (i) finished part after support removal. These

two processes are both sequential HAM processes, and the AM process is used to obtain near-net-shape parts and CNC is employed for obtaining the finished parts.

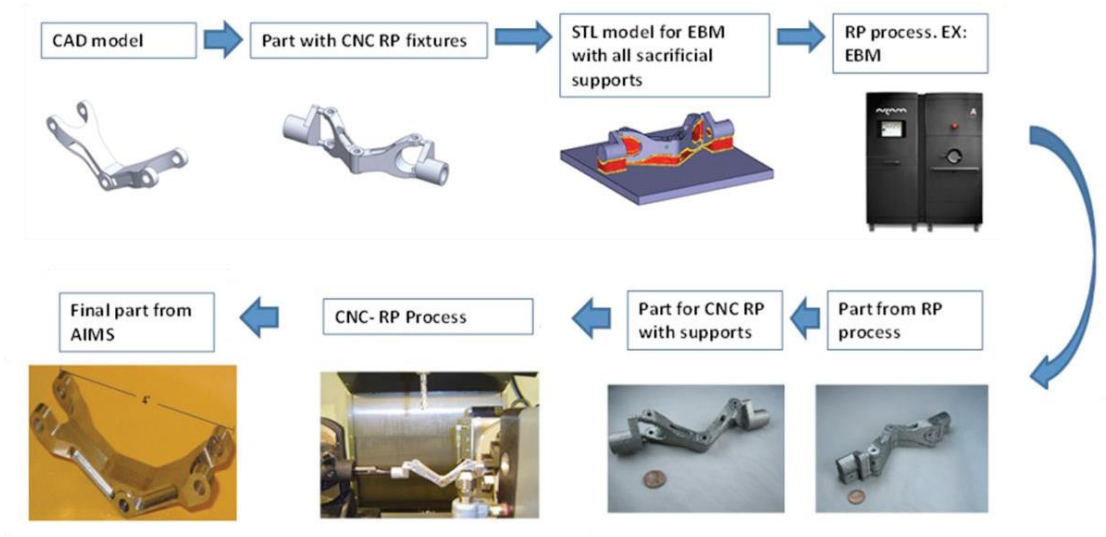

Fig. 2.9. The AIMS process [70].

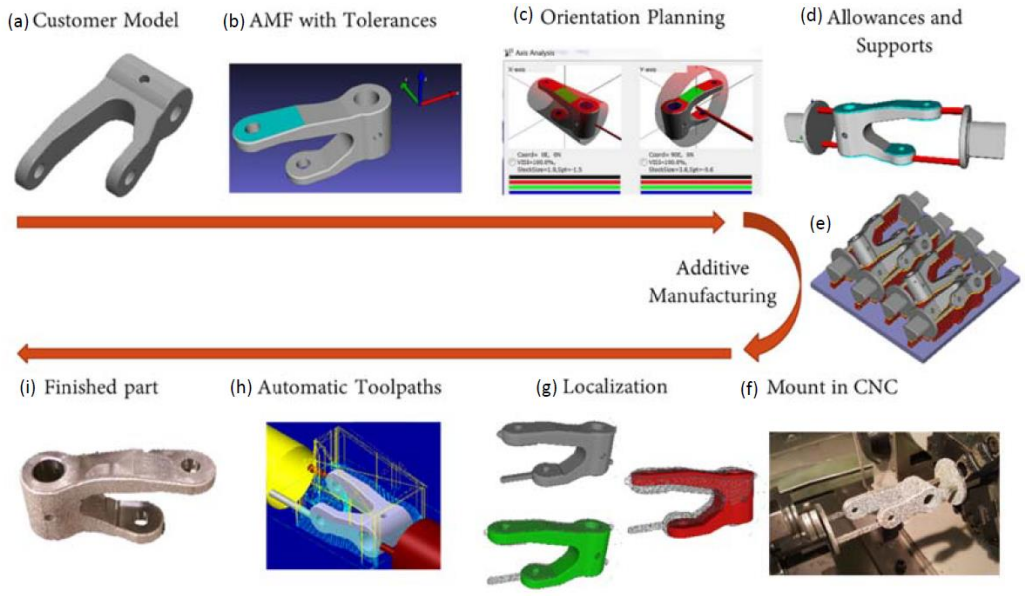

Fig. 2.10. The DASH Process Flow [71].

Therefore, even though some researchers have dedicated themselves to HAM, there still exist many problems in materials [89], cooperation of different processes [90][91], process planning [92][93], etc.. Because the process planning of HAM is very essential as mentioned above, in the next section of this chapter, the existing research on process planning for AM and HAM are collected and some typical problems are pointed out.

2.2 The state of the art on process planning for AM and HAM

In the domain of manufacturing, Computer-Aided Process Planning (CAPP) is an essential stage of the whole product life cycle which is the bridge connecting design and manufacturing stage, illustrated in Fig. 2.11. [94]. Therefore, the importance and function of CAPP for AM and HAM is similar to conventional manufacturing processes.

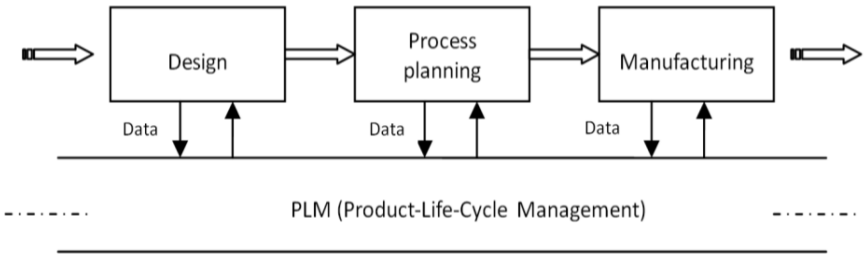

Fig. 2.11. CAPP transfers a design model to a manufacturing model [94].

Before studying the process planning for HAM, it is necessary to clarify the main tasks of process planning for AM.

2.2.1 The process planning for AM

There exist some research on process planning which can be divided into macro process planning and micro process planning [95]. The macro process planning is like manufacturability analysis [54][96], and the micro process planning is like part orientation definition [97][98][99][100][101], support generation or support-free design methods [102][103], slicing [104], path planning [105][106], etc.

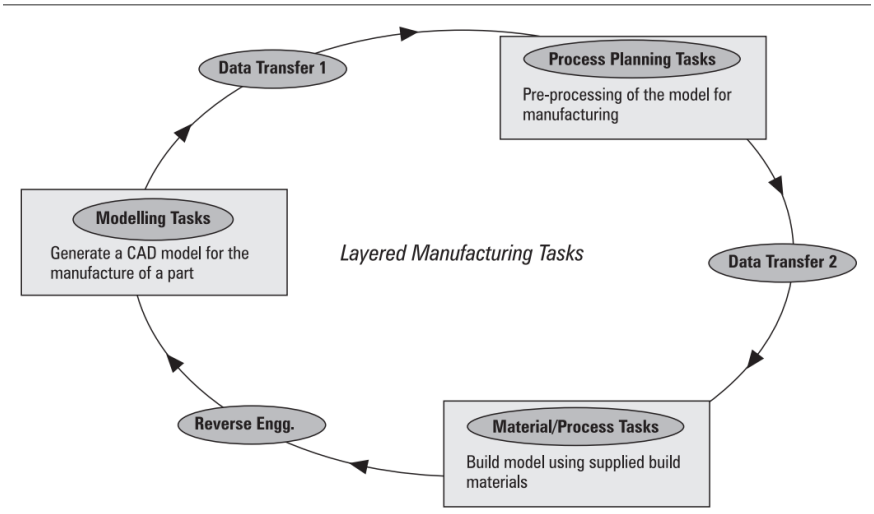

Fig. 2.12. The layered manufacturing cycle [107].

For AM processing, there are some differences from conventional processes since it is usually done in one machine, the AM printer, if post-processing is not considered. The main function of the so-called "*CAPP for AM*" is actually to transfer a design model, mostly a CAD model, into a processing model, the printing toolpath model, to complete the AM processing chain [108]. Four main planning tasks (orientation optimization, support generation, slicing, and toolpath generation) were defined as the model transformation steps for the rapid prototyping process, shown in Fig. 2.12., the initial status of AM [107]. Progressively, the rapid development and the diversity of AM technologies as well as the expansion of material selections for AM, the contents of CAPP for AM have been extended. Some researchers proposed to include manufacturability analysis, process selection, model clustering, and printing prediction as additional planning tasks to adapt to AM evolution [108][109][110][111], since these tasks are critical to solving the feasibility and suitability analysis of using AM, before printing [108]. Generally, as previously mentioned, these planning tasks can be grouped as two main global steps, macro process planning, and micro process planning, shown in Fig. 2.13. [95].

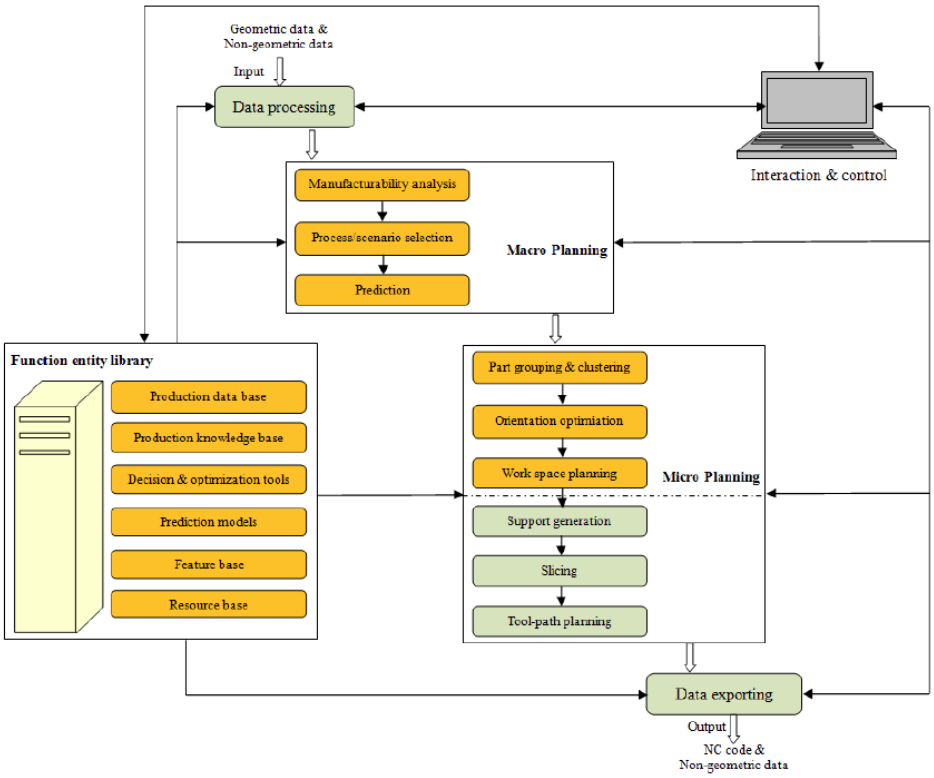

Fig. 2.13. An AM feature and knowledge based systematic process planning framework [95].

Micro process planning not only includes the four classical planning tasks, orientation determination, support structure design, slicing, and toolpath planning but also contains two additional new tasks, named part clustering/grouping and nesting, to fit the needs of simultaneous printing for multiple parts [112][113][114]. More details of existing researches are given mainly on orientation determination, support structure design, slicing and toolpath planning, and nesting.

(1) Orientation optimization

Orientation is the direction of the part to slice it into layers. It is very essential, because of the different orientations, shown in Fig. 2.14. could dramatically influence surface finish, build time, support structures, shrinkage, curling, distortion, roundness/ flatness, part tolerance, material flow, material cost, and trapped volume [107][115]. There exist much research on orientation optimization[100], and even some on multi-parts [98].

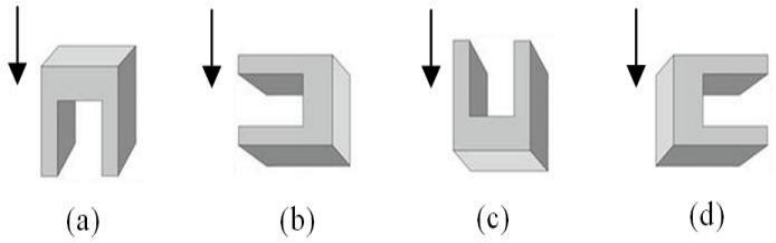

Fig. 2.14. The orientations [94].

(2) Support generation

Once the orientation of the part or parts is determined, some features are overhang, so the structure called support is needed to make the overhang features can be built onto it. Generally, supports can be internal or external, illustrated in Fig. 2.15. [107], but with some special methods like multi-axis AM processes, the use of support can be reduced or even avoided, shown in Fig. 2.16. [116].

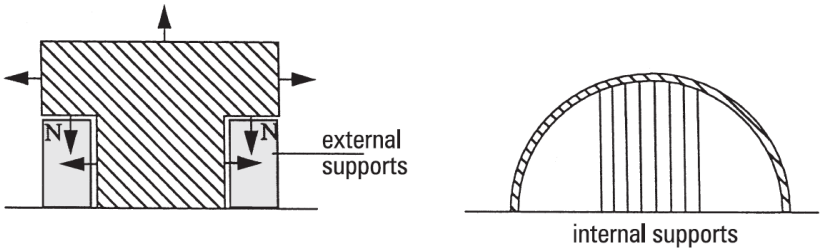

Fig. 2.15. The examples of internal or external support [107].

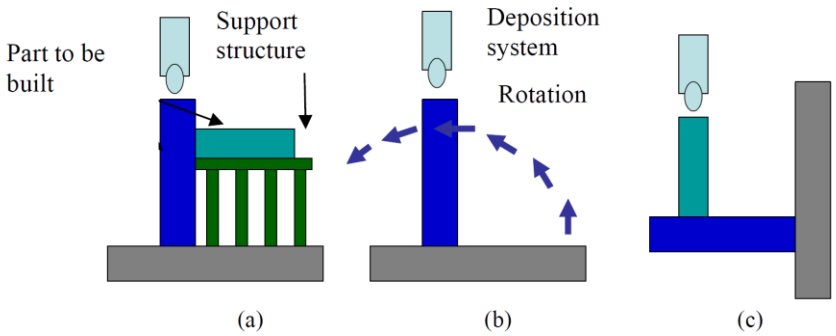

Fig. 2.16. (a) build part with support structure; (b) after building the column, the table can be rotated; (c) build the component from another direction [116].

(3) Slicing

After the determination of part orientation, the part is cut into layers and this process is called slicing. In general, slicing involves intersecting a CAD model (or the associated STL file) with a horizontal plane, illustrated in Fig. 2.17. However, with the employment of the multi-axis slicing method, the normal direction of the slicing layer changes, and the thickness can be uniform or adaptive [117]. This task is to obtain a series of layers, determining the layer thickness and the layer boundary or contours, which is used for toolpath planning.

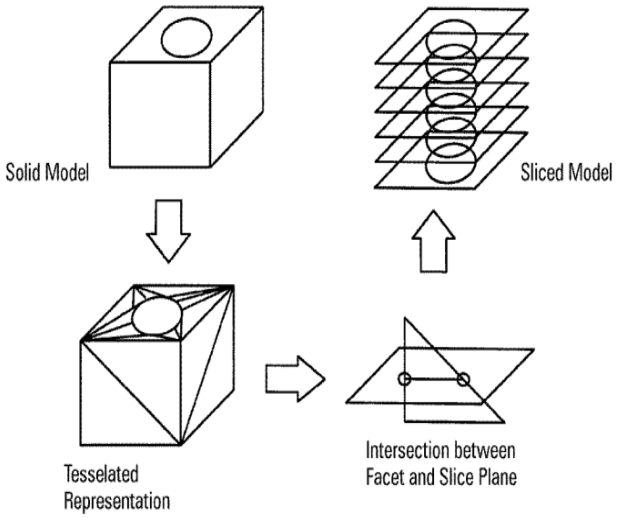

Fig. 2.17. The slicing process [118].

(4) Toolpath generation

Once the layers are obtained, each layer needs to be built with an optimal toolpath, which results in toolpath planning. It can be divided into two aspects, interior and exterior path planning, shown in Fig. 2.18., and varies due to different AM technologies. In addition, the

process of filling in the interior of the layer is accomplished employing path planning, while the external is usually by removing materials [107].

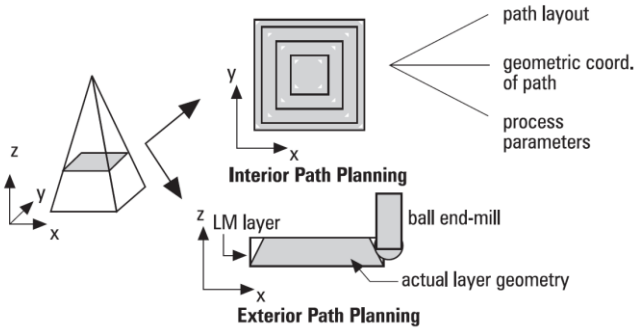

Fig. 2.18 The toolpath planning [107].

Various types of toolpath patterns from milling can be introduced into AM, such as rastering similar to zigzag, contours, spirals, and some other filling patterns [119]. And the popular types are as shown in Fig. 2.19.

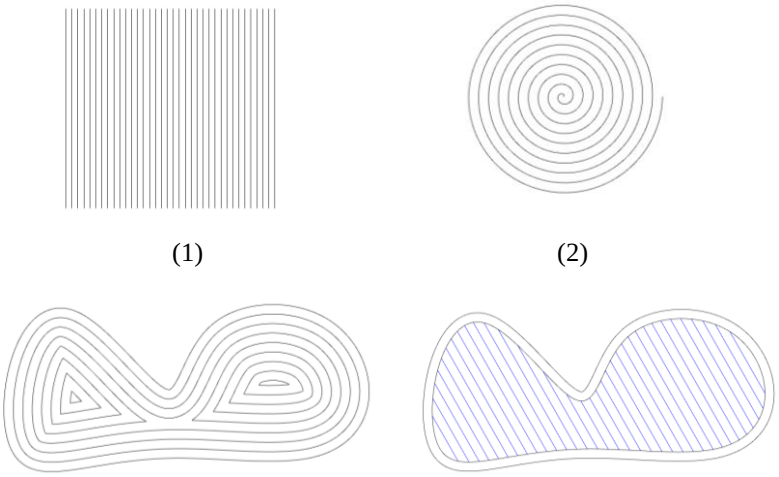

(1) (2)

(3) (4)

Fig. 2.19. Some typical toolpaths: (1) the rastering; (2) the spiral; (3) the offset; (4) the combination of more than one types.

(5) Nesting

AM machines can build many parts, no matter the parts are the same or not, within the same build envelop of an AM machine simultaneously [120]. Nesting is also an important task for AM, shown in Fig. 2.20. [121]. The workspace planning problem can be divided into 2 major categories: 2D nesting and 3D packing because some AM processes, parts can be

stacked one upon another (like laser sintering, etc.), but other processes, such as fused deposition, electronic beam melting, etc., parts cannot be like this [120].

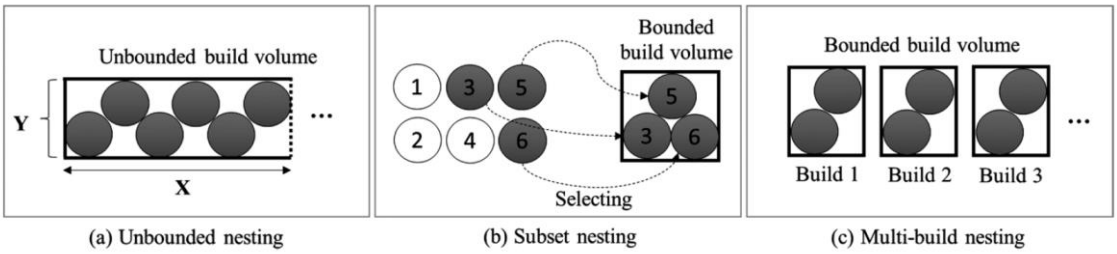

Fig. 2.20. Nesting [121].

2.2.2 The process planning for HAM

In HAM, with the introduction of a non-AM processing module/step into the AM processing, the process planning contents for HAM change and become more complicated. In this section, the reported CAPP methods for HAM and tools in literature are analyzed.

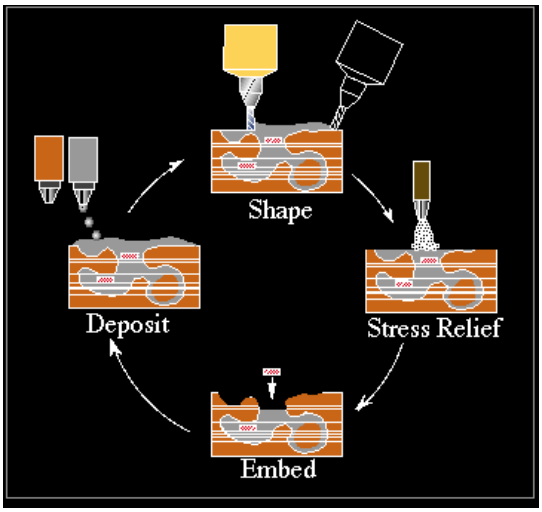

Fig. 2.21. The SDM process [5].

Krishnan Ramaswami in 1997 proposed the process planning method for Shape Deposition Manufacturing (SDM), shown in Fig. 2.21., concluding the generation of 3D layers and the generation of material deposition as well as CNC cutting-tool paths adapted to machine-specific areas of these 3D layers. In this method, the CAD model is first decomposed into 3D layers of varying thickness based upon both geometric and material criteria. Then the

layers are decomposed into manufactural volumes called compacts. Silhouette edges and silhouette loops are identified to help the decomposed models into 3D layers and compacts. The algorithm decomposes models into compacts that can be non-planar. Each compact is deposited to the near-net shape and then machined to the required shape by CNC. However, this method is not suitable for multi-axis processes. In 1998 [77], a framework for planning and execution for additive/subtractive processes of SDM was proposed, and the basic planning steps incorporate determining building directions, decomposing a part into manufacturable volumes (called single-step geometry), representing these sub-models in a structured format for allowing optimizing building sequences, depositing materials on each single-step geometry, and shaping decomposed entities. However, in this SDM method, the direction is fixed, and many supports which can be saved with multi-axis process still have to be adopted.

In 2000, K.P. Karunakaran et al. used a concept of two-level processing, which is a near-net-shape building of the layer deposition and net-shaping it by high-speed machining [122]. Therefore, this method is a sequential HAM process. Later in 2006, K.P. Karunakaran et al. proposed a HAM system which is TransPulse Synergic Metal Inert Gas (MIG)/Metal Active Gas (MAG) welding process for near-net-shape parts and CNC milling process for net-shaping. However, the authors have not considered the details of the tasks of process planning for HAM. There is no consideration of starting from an existing volume and no optimization either.

In 2001, in Laser Aided Manufacturing Process (LAMP) system, each layer is "*truly*" 3D in nature using the combination of material addition and subtraction processes by exploiting the presence of five-axis motion, with skeleton-based geometric reasoning for adaptive slicing, using face classification (non-undercut, undercut and non-monotonic), illustrated in Fig. 2.22. (1). [5] and edge classification (convex edge and concave edge), illustrated in Fig. 2.22. (2). [64]. This Lab also proposed the basic planning steps of LAMP which involve: determining the base face, extracting the skeleton, decomposing a part into subparts, determining build sequence and direction for subparts, checking the feasibility of the build sequence and direction for the machining process, and optimization of the deposition and machining [123][124]. Later in 2005, Their lab proposed the method of automatic process planning and toolpath generation of a multi-axis hybrid manufacturing system and they classified the process planning constraints into collision constraint, physical machine constraint, and continuity broken constraint [125]. In 2010, Ren et al. in the same lab

proposed a method of integrated process planning for a multi-axis hybrid manufacturing system. They have done a lot of work on process planning, including decomposition of the CAD model, improvement of the toolpath generation pattern, and collision detection algorithms. Also, the interfacing and integrating process between deposition and machining is also studied, and the centroidal axis extraction is researched, shown in Fig. 2.23., and Fig. 2.23. (a) is a solid model, Fig. 2.23. (b) is centroidal axis, Fig. 2.23. (c) is the centroidal axis with solid. However, similarly, they have not taken into account how to fabricate the parts that start from an existing volume.

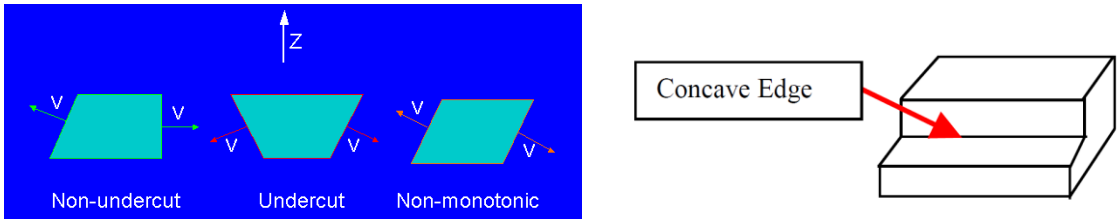

(1) (2)

Fig. 2.22. (1). The face classification [5] ; (2) The edge classification [66].

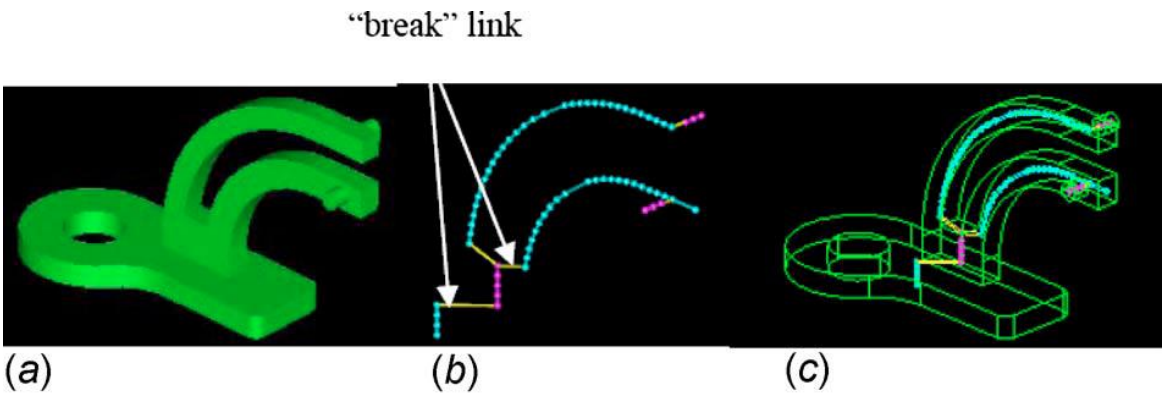

Fig. 2.23. The centroidal axis extractions [126].

In 2013, Zhu et al. proposed the iAtractive framework [83][84][85], which can manufacture high accuracy plastic parts including internal structures, combining subtractive (i.e. CNC machining), additive (i.e., Fused Filament Fabrication, FFF) and inspection operations. In their research, the complex plastic parts were decomposed into sub-parts with their build direction, which could be built and machined without tool collisions. The process planning starts with a static operation sequence, but will be further updated according to the feedback of inspection operations during the part production. Later, Newman et al. [84] proposed a re-plan process planning system for additive and subtractive processes based on

the iAtractive framework, able to generate different strategies to fabricate parts from an existing part [127]. However, they have not researched on how to generate the existing volume, neither how to generate and optimize the sequence for the remaining volumes.

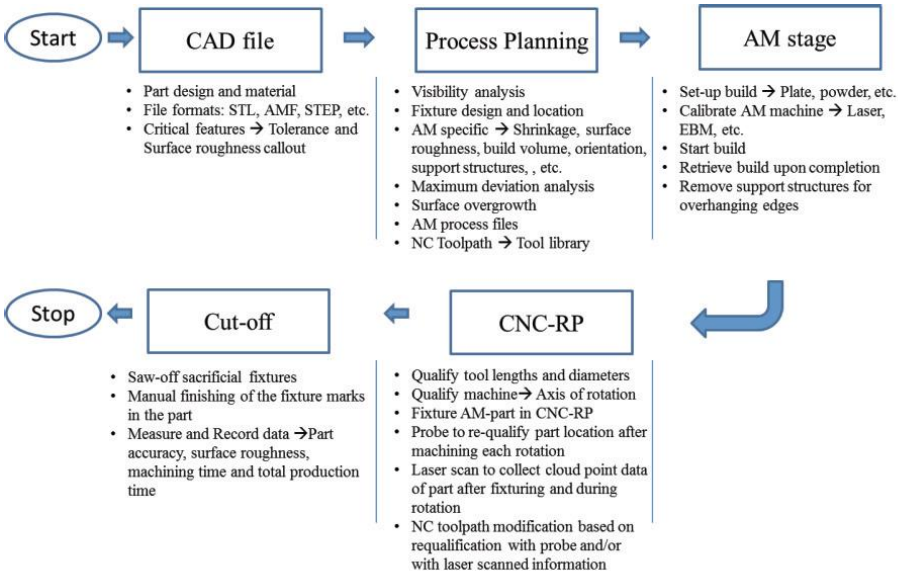

Fig. 2.24. The AIMS process flow [70].

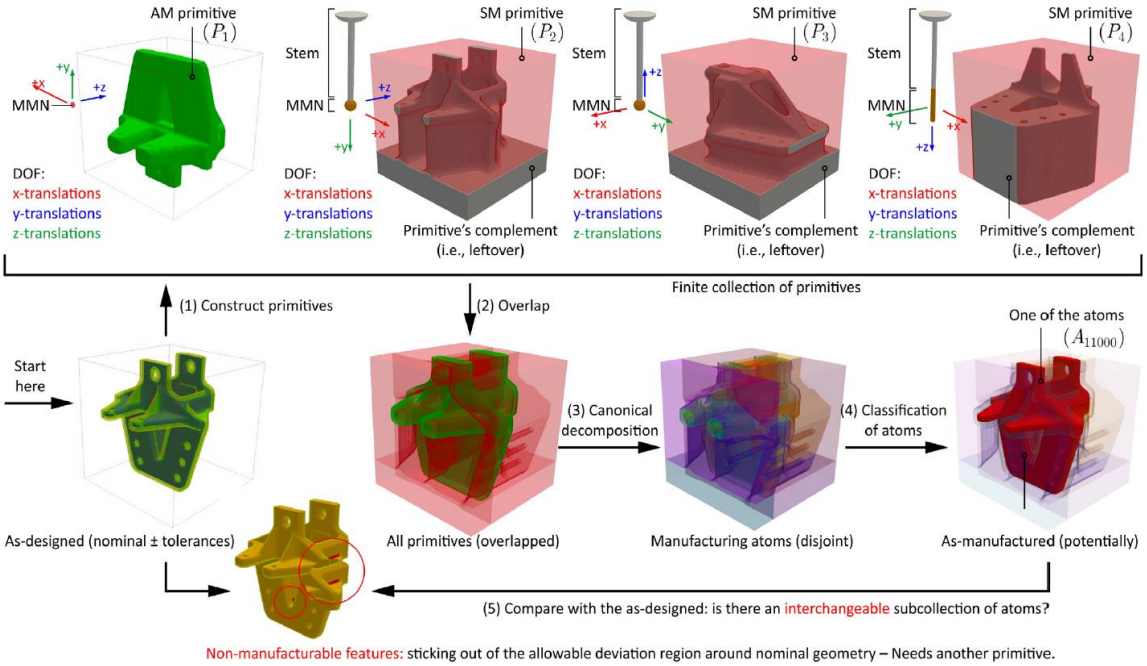

Fig. 2.25. One example including 2 AM and 3 SM primitives [128].

In 2015 and 2016, Manogharan et al. [70][129] presented a process planning framework, combining Electron Beam Melting (EBM) or Direct Metal Laser Sintering (DMLS) with SM

(CNC-RP), illustrated in Fig. 2.24. In this method, the manufacture of parts was performed in two separate phases; first a near-net shape of parts was achieved by AM processes (i.e., EBM or DMLS) and then the part accuracy was achieved by CNC-RP. This is one sequential HAM, but similarly, they have not taken the existing volume into account.

In 2018, Morad Behandish et al. proposed a systematic approach to automated CAPP for HAM (AM/SM) that can identify non-trivial, qualitatively distinct, and cost-optimal combinations of AM/SM modalities. One example is given as shown in Fig. 2.25. There are 2 AM (including raw stock, not shown) and 3 SM primitives are constructed for a 3-axis machine with a few HAM capabilities (top). The primitives are overlapped to construct an atomic decomposition whose atoms are checked against the as-designed shape to discover an interchangeable as-manufactured shape (bottom) or deviations that required to be fixed by adding more primitives to split them [128]. However, this method is not automatic as they mentioned and they did not consider the details in practice either.

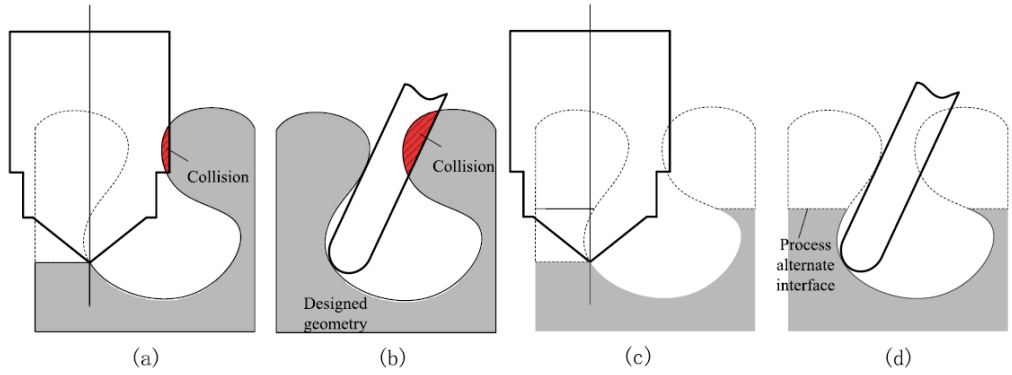

Fig. 2.26. The strategy to avoid nozzle and cutting tool induced collisions [130].

In 2020, some researchers [130] have proposed a solution to solve the collision avoidance problem in hybrid manufacturing and present a deterministic algorithm for automatically generating a collision-free sequence of hybrid manufacturing, shown in Fig. 2.26., taking into account collisions between nozzle and part (Fig. 2.26. (a)) or between cutting tool and part (Fig. 2.26. (b)) and proposing solutions (Fig. 2.26. (c): nozzle collision avoided; Fig. 2.26. (d): cutting tool collision avoided). The way to find the Tool Accessible Region (TAR) of a Cutter Contact (CC) to know the machinability is shown in Fig. 2.27. And Fig. 2.27. (a) illustrates the TAR of a given CC point for a ball-end cutter; Fig. 2.27. (b) illustrates TAR calculation taking into account shadows under a spherical light source; Fig. 2.27. (c) shows first order machinability; Fig. 2.27. (d) shows second order machinability.

This could be a method to reduce the collision to guarantee the manufacturability. However, it is especially for the part that can be represented in the columnar form, and the manufacturing process did not consider the existing volume [130].

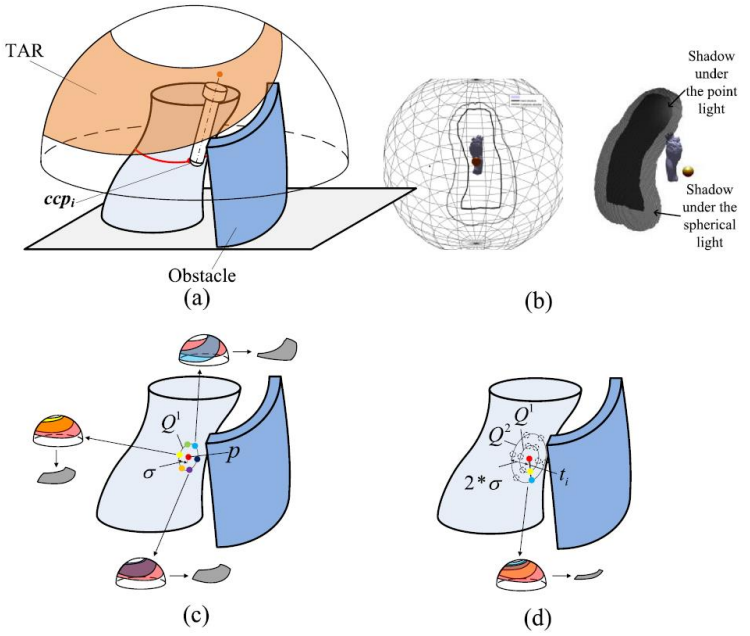

Fig. 2.27. The tool accessible region and first order second order machinability [130].

With the emerging of HAM, more non-AM processing operations and machines are introduced and considered in the processing chain. However, not so much research exists on process planning for HAM. Similarly, process planning can also be divided into macro process planning like manufacturability analysis [131][132] and selection of processes, as well as micro process planning like decomposition [79][133][134], sequence planning [6], path planning and etc. There are some new tasks of process planning for the AM module of multi-axis HAM.

Table. 2. 3. The new contents/tasks of CAPP for multi-axis HAM in the AM module.

Start from an existing volume	Sequence planning	Toolpath planning
The generation and optimization of initial volume	The sequence of depositing the remaining volumes	The optimization of toolpath for each layer

When considering HAM, the first operation is supposed to provide an existing volume which is called “initial volume” in this research, because starting from an existing volume could probably save fabrication time and cost. It could be produced by conventional technologies like casting or machining, in order to simplify the global HAM process and

reduce the cost. This is also an approach that could be considered when adding or repairing a given function on an existing part. After the existing volume is fabricated, there are still some volumes left, in order to try to find the right sequences of remaining volumes until the final part is produced. To deposit the materials for the AM module in multi-axis HAM, the toolpath is also very essential. Hence, the existing researches on the concept of existing volume, sequence planning, and toolpath planning are collected as follows.

2.2.2.1 The determination of Initial volume

For the concepts of existing volume, there exist some similar concepts with 'initial volume' (which is the definition in this research) in recent researches. However, the researches which considered existing materials/substrate/part are not common and there are only a few studies as follows.

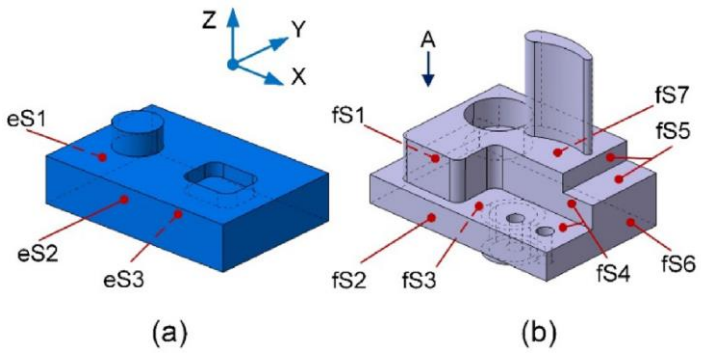

Fig. 2.28 The test parts [6].

In 2017, a method of process planning for combined additive and subtractive manufacturing technologies in a remanufacturing context is proposed. Fig. 2.28. (a) is the existing part, Fig. 2.28. (b) is the final part [6].

Zhu, Newman, et al. studied process planning for HAM from an existing material shown in Fig. 2.29. combining AM, traditional processes, and inspection process [127]. They focus on how to reuse existing parts/legacy products to save costs for the HAM process. A group of other researchers who applied HAM for remanufacturing existing physical components followed this logic [6][135]. Gradually, the benefits of starting the HAM processing from an existing volume attracted the attention of a group of researchers. Eldakroury et al. [136] tried to use primary shapes, cylinders, and cuboids, to approach the initial CAD model's sub-volume via a set of simple sequential rules to help process planners identifying the optimal

candidate substrate shown in Fig. 2.30. However, they did not analyze the solution space of the substrate and neither applied any optimization tool to enable automatic searching. The results found by them can only be subset and local optimal candidate substrates. In addition, the word, "*substrate*", may confuse the non-AM processing module's planning. Most recently, Chen et Frank [137] proposed a method to optimize the stock size for component families or groups and use the stock as the processing starting point for the following HAM processing. In their method, manufacturing begins with a base plate, where a set of subtractive steps will first create a portion of the design geometry. Next, the additive manufacturing process is planned to create geometry on the machined base plate in two opposite directions, to minimize support structure and build height. Finally, a secondary machining process is planned to produce finished surfaces on the additively manufactured near-net shape geometry. However, there is no work about how to identify an optimal stock for a given CAD model. Reichler et al. [138] did similar work, but they tried to extract a sub-volume from the initial CAD model as starting base for incremental manufacturing, where AM is applied to add customized features for the variant part. However, they did not explain how to obtain an optimal base volume automatically for the start point.

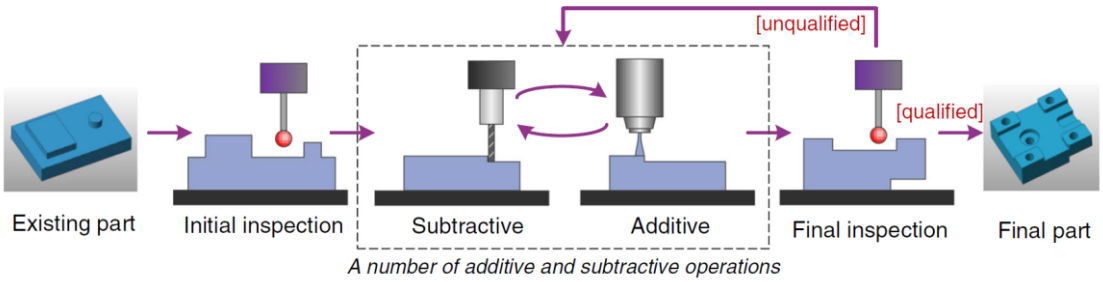

Fig. 2.29. The schematic diagram of the iAtractive process [127].

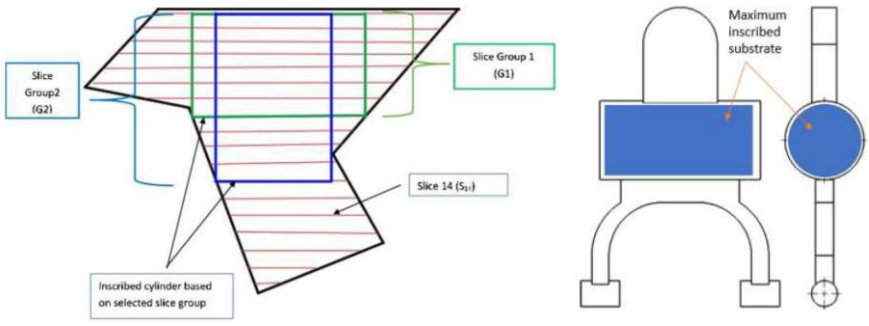

(1) (2)

Fig. 2.30. (1). The part model slicing; (2) The maximum inscribed substrate [136].

As reviewed above, there are few pieces of research addressing the question on HAM processes that start from “zero” or an existing volume, and no systematic optimization of the existing volume is proposed.

2.2.2.2 The sequence planning

Sequence planning aims to find an optimal sequence for avoiding the collisions (such as shadow effect in CS shown in Fig. 2.31.) during the fabrication process. Before making the sequence planning, the components are decomposed and the sequence of sub-volumes can be generated based on the decomposition result, shown in Fig. 2.32. [139].

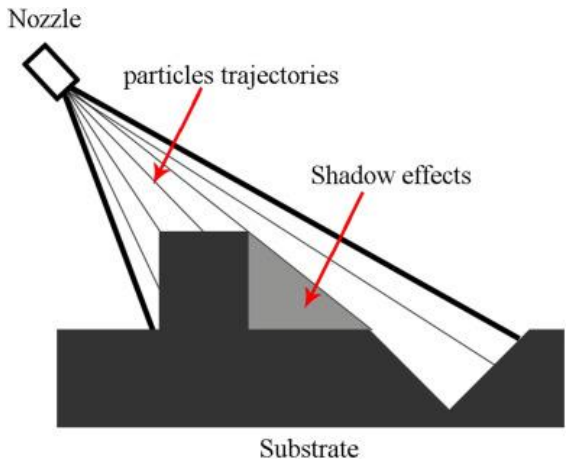

Fig. 2.31. The shadow effect [140].

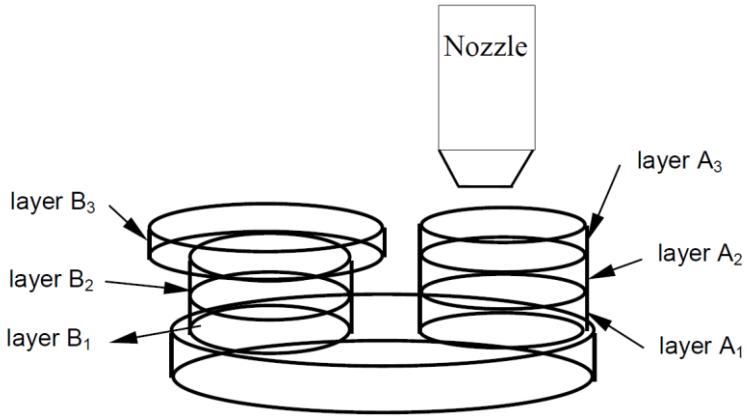

Fig. 2.32. To avoid the collision by changing layer build sequence [139].

The abovementioned researches of process planning for HAM are lack consideration of sequence planning for the remaining volume because not much research start from an existing

volume. However, there are still some similar concepts on the sequences of subparts or features. In 1998, J. Miguel Pinilla et al. [77] proposed a method for process planning, decomposing CAD models into single-step geometries, arranging these geometries into a graph representation called " *adjacency graphs*" as shown in Fig. 2.33., and automatically generating several alternative building sequences as shown in Fig. 2.34. However, their "*single-step geometries*" are manufactured along the same direction and they did not select the optimal sequence either. Moreover, they did not consider the process from an existing volume.

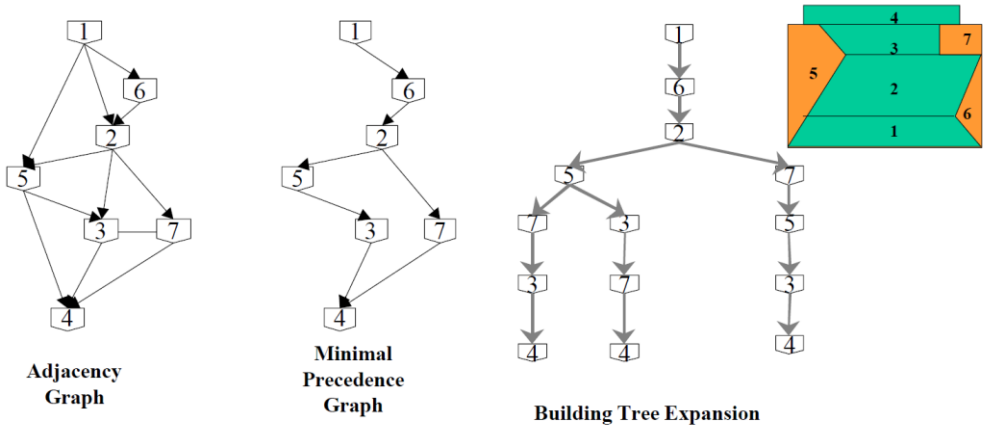

Fig. 2.33. The adjacency graph and building tree for a sample part [77].

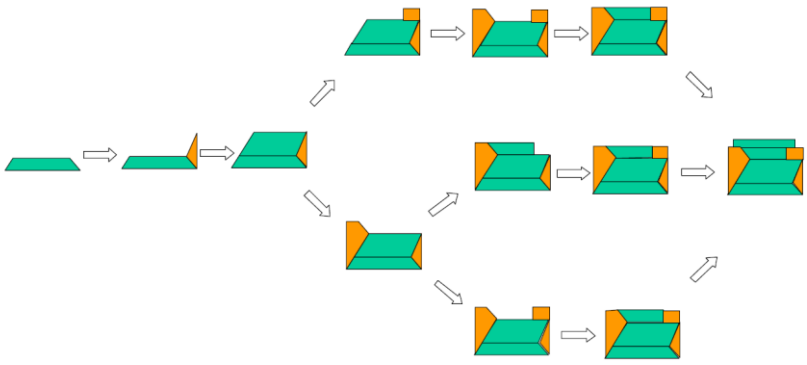

Fig. 2.34. The alternative building sequences [77].

There is still some research on the multi-axis process, and the model is decomposed shown in Fig. 2.35. (1), and based on the building relation illustrated in Fig. 2.35. (2), the building sequence illustrated in Fig. 2.35. (3), can be obtained to avoid collision [126]. However, this process did not consider building the part with a starting existing volume. Moreover, the process is not optimized for finding the optimal sequence.

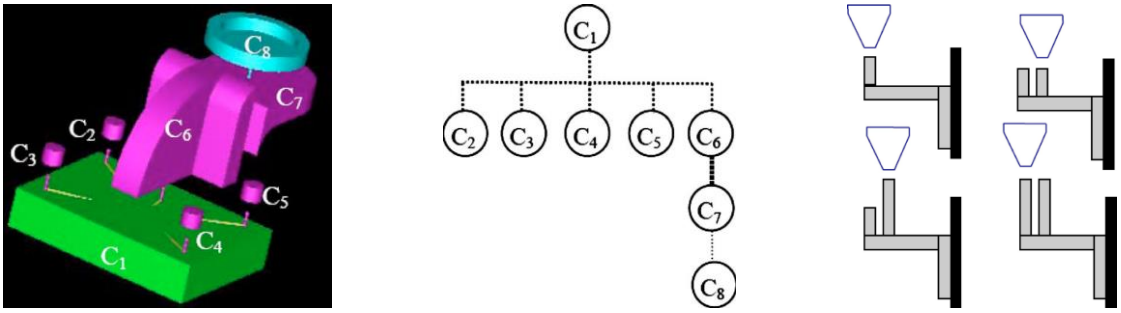

(1) (2) (3)

Fig. 2.35. (1). The decomposition; (2). The building relationship graph; (3). The building sequence [126].

In 2017, Van Thao Le et al. [6] proposed a process planning method for HAM in a remanufacturing context as shown in Fig. 2.36. and in Fig. 2.37., (a) shows the machining features (MFs) and AM features (AMFs) and (b) illustrates the relationships between the features. They carried out systematic research on sequence planning for both DED and PBF, considering the relations among different features from the perspective of topological relations, precedence relations, and geometrical relations as well as the collisions and machining force. The remanufacturing process is iterative of both AM and SM. However, their method is based on AM features and machining features, which depend on a specific classification and are not suitable for very complex freeform structures. In addition, their method is only applied according to the experience and realized manually.

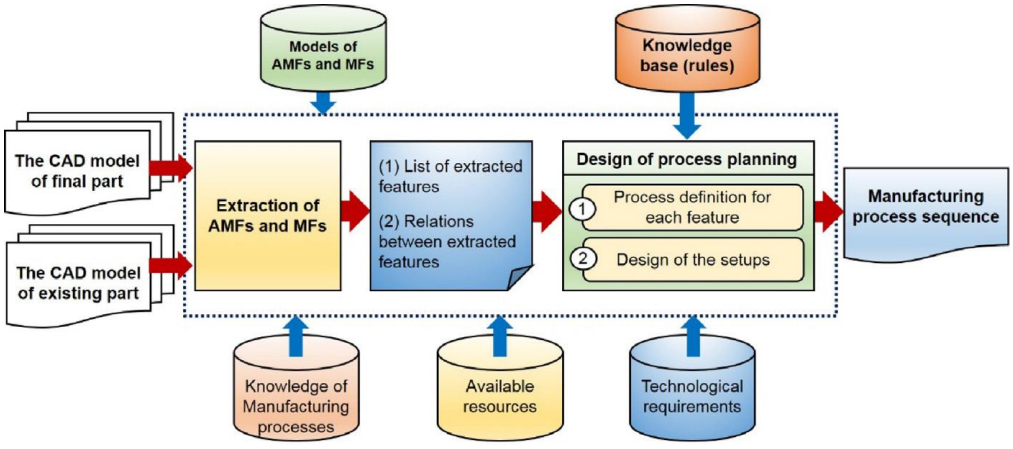

Fig. 2.36. The developed methodology for the design of AM and machining process sequence [6].

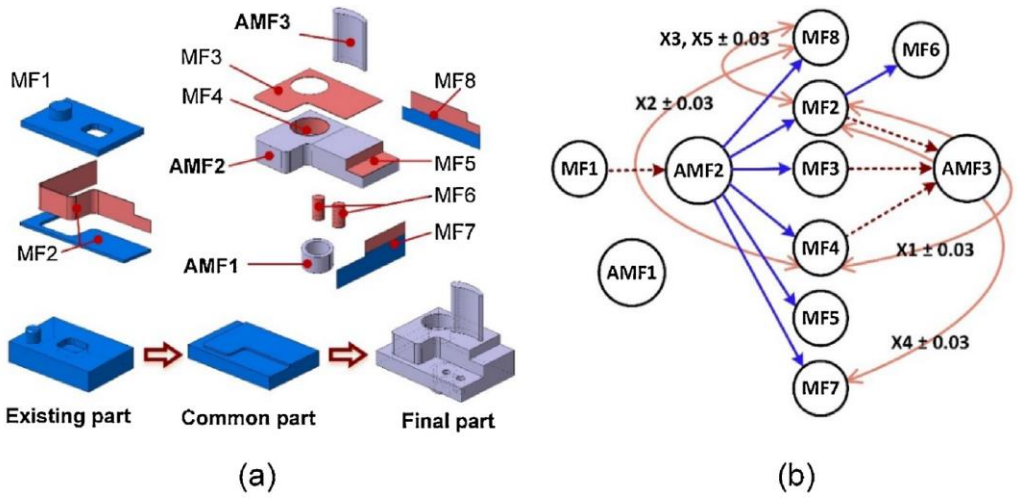

Fig. 2.37. The machining and AM features, and their relationships [6].

Similarly, In 2018, a novel process planning algorithm for additive and subtractive manufacturing was proposed based on skeleton tree matching to remanufacture disused parts [141]. The major considerations for realizing the process planning algorithm are presented with the help of a skeleton tree matching, including skeleton extraction, skeleton tree construction, feature matching, and hybrid process planning illustrated in Fig. 2.38. [141]. Then, the process routes of corresponding sub-features according to the initial machining sequence are given as shown in Fig. 2.38. (2). This process is iterative and the sequence is for both AM and SM processing. However, their method also introduced features and it is also not automatic and not optimized.

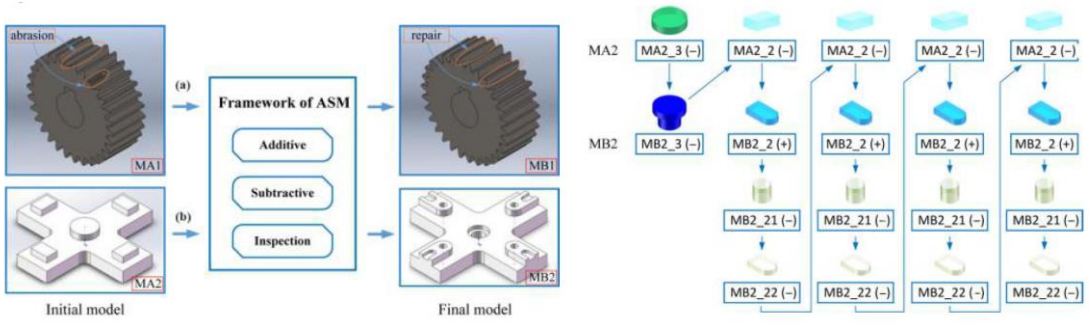

(1) (2)

Fig. 2.38. The framework of ASM and processing route [141].

Kai Tang et al. have done a lot of research on process planning for multi-axis HAM. Recently, they proposed a novel process planning framework for automatically generating a multi-axis support-free printing path for continuous 3+2-axis AM of an arbitrary freeform

part. The framework is based on the geometric processing of skeletonization and decomposition and is particularly suitable for a part with distinct multiple trunk-branch structures [134]. In this research, they realized: (1). an effective non-parallel planar slicing method based on the skeleton curve for support-free FDM printing. (2). a novel segmentation technique with consideration of both support-free and collision-free constraints for continuous 3+2-axis printing. (3). an improved algorithm for building a hierarchy tree with decomposed features and planning the building sequence illustrated in Fig. 2.39. They classify the sequence into two types which are depth-first traversal and breadth-first traversal. However, the previous calculations are not considering the initial volume and there are no details of the sequence planning.

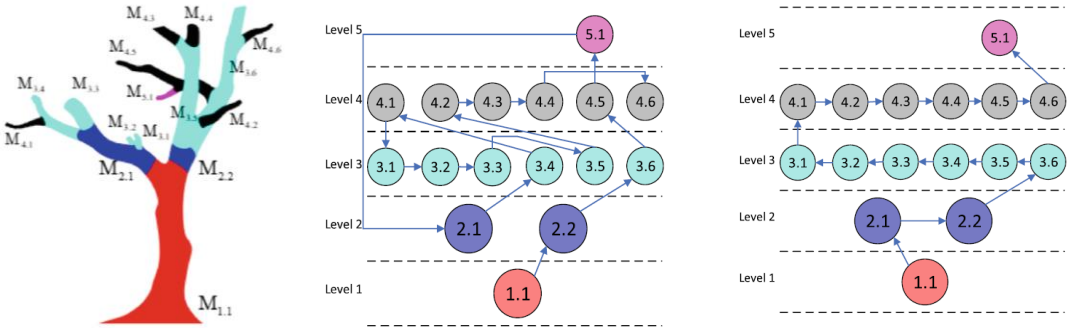

(1) (2) (3)

Fig. 2.39. (1). Decomposition and classification; (2) A depth first traversal; (3) A breadth first traversal.

Based on the existing researches, one issue to be solved relates to the automatic sequencing of the HAM process, because they lack the automatic solution for sequence generation and optimization.

2.2.2.3 The path planning

This thesis is on the AM module for multi-axis HAM. Since toolpath planning is very important for AM, there exist much research as mentioned above. Moreover, for the multi-axis AM process, the toolpath can be 3D curve paths, shown in Fig. 2.40. [142]. However, most HAM systems still adopt planar scanning.

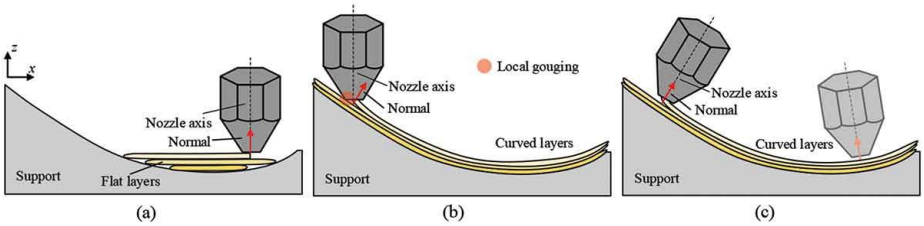

Fig. 2.40. (1) The 3D curve paths [142].

Since many HAM processes still employ planar path planning, so it is necessary to know the existing research on some basic types of the toolpath, like contour/offset, zigzag/rastering.

For the contour type of toolpath, one crucial issue to be addressed relates to offset problems along the trajectories. Problems of offset can be seen in Fig. 2.41. [143]. Void type I occurs when the area to be filled is too large for a single pass, but not large enough for another parallel offset path. Void type II occurs when corner geometry has too sharp of an angle. The angle is considered too sharp depending on specific process parameters. Void type III will occur if the offsetting algorithm generates more than one loop allowing a void between the different loops [143].

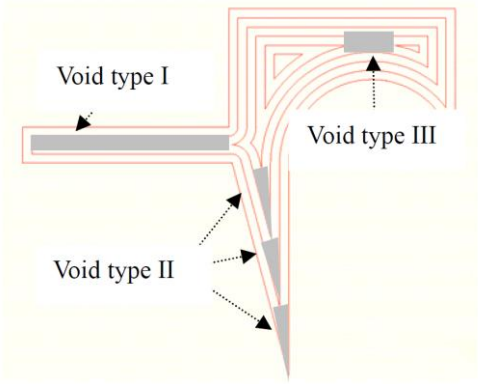

Fig. 2.41. Different types of void often happened in deposition with offset path [143].

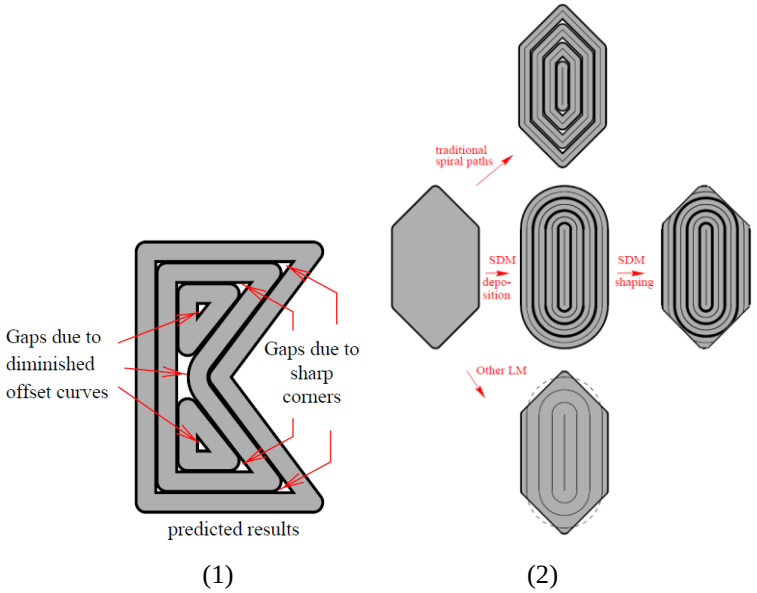

Fig. 2.42. (1). The problems produced by recursively offsetting algorithms; (2) The possible solutions [76].

The spiral path has a similar void with the offset method and a new spiral path is generated without sharp corners. The brief procedures are as shown [76] in Fig. 2.42.: (1) Obtain MAT (Medial Axis Transform) of original 2D cross-sections; (2) Re-parameterize the skeleton by arc length; (3) Solve the above optimization problem; (4) Compute spiral paths from the medial axis and the optimized radius function.

The zigzag path is also very commonly used. Liou et al. developed a hybrid manufacturing process with coverage toolpath planning, illustrated in Fig. 2.43., zigzag with interlaced direction [144]. Moreover, the rastering type is very similar to the type of zigzag.

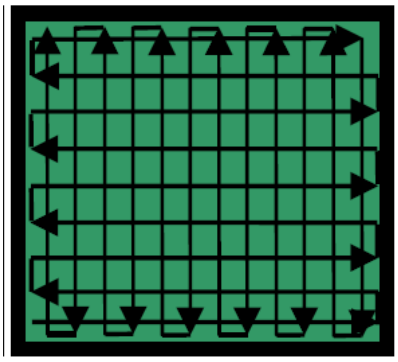

Fig. 2.43. Different toolpath generation patterns [144].

For a continuous 5-axis laser cladding process, some experiments have been proposed to study different toolpath strategies and to determine the optimal toolpath considering quantitative criteria such as the deposition rate, the height, and width of clad tracks [145]. Moreover, MAT was used for adaptive path planning of wire-feed additive manufacturing [106].

To reduce build time, a concurrent toolpath planning algorithm generates collision-free toolpaths to control the tools that deposit materials concurrently [146]. A mixed and adaptive toolpath generation algorithm has been then developed, aiming to optimize both the surface quality and fabrication efficiency in AM [147]. In the fused deposition technique, the usually applied layer filling strategies have the following characteristics: (1) the boundaries use contour filling and the interiors use vector filling; (2) the contour is laid down first, after the interior is filled; (3) the offset (distance between roads) between a vector and a contour is negative; (4) the vector angle is alternated by 90 degrees between consecutive layers [148]. Similarly, a mixed toolpath strategy is introduced to improve the boundary contour's accuracy and reduce the time for interior filling. For further improvement on fabrication quality, a tool

path adjustment is employed on the original toolpath [149]. A mixed and adaptive toolpath generation algorithm is proposed to generate contour toolpath for the boundary of each layer to make sure the surface quality, and zigzag toolpath for the internal area of the layer to reduce build time. Moreover, the best slope degree of zigzag toolpath is selected to further minimize the build time [147]. However, only six incremental degrees of slopes for the minimum build time computing are proposed ((a) 15◦; (b) 30◦; (c) 45◦; (d) 60◦; (e) 75◦; (f) 90◦ in Fig. 2.44. Similarly, another research is also on the inclinations with very few angles shown in Fig. 2.45. [150]. Therefore, there are limitations for the step length of scanning angles.

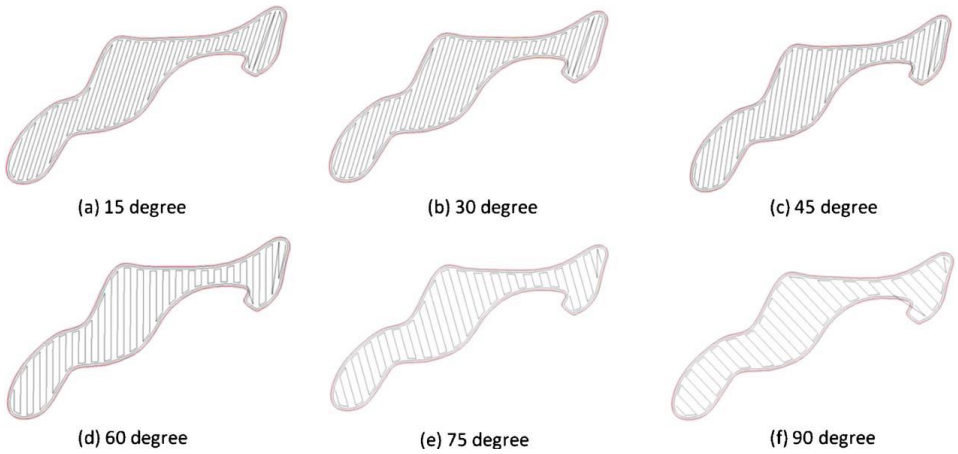

Fig. 2.44. The six incremental degrees of slopes for the minimum build time computing [147].

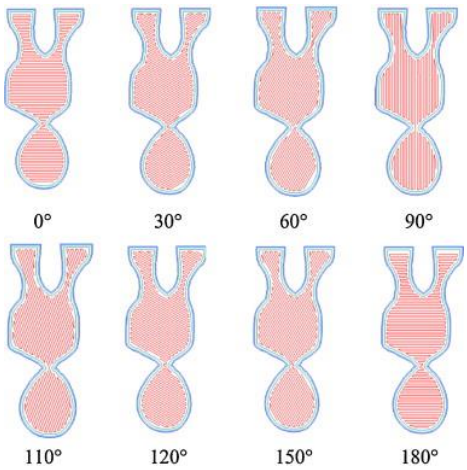

Fig. 2.45. The toolpath with 8 different inclinations [150].

Moreover, few solutions are proposed by commercial software, like AM Path Optimizer technology (https://www.plm.automation.siemens.com/global/en/our-story/newsroom/alert-additive-manufacturing-path-optimizer/66937). Similar limitations exist in commercial software, because of limited rastering angles, and the lack of considering the real physical deposition profile.

In conclusion, the existing toolpath generation methods did not consider many slope angles for optimization and the physical deposition profile. Moreover, there is no consideration of toolpath configuration for each layer (scanning type, angle, speed, energy, etc.). So, it is necessary to propose a method for toolpath generation and optimization to solve the above-mentioned limitations by profile sweeping based method, using the mixed toolpath.

2.3 The existing problems for process planning

For the initial volume generation and optimization, there are some similar concepts of existing volume: (1) Start from an existing volume; (2) Start remanufacturing from an existing feature; (3) Define a start substrate as a build base. However, very little research on initial volume generation and optimization and the existing method does not consider automatic optimization.

For sequence planning, the questions of sequence planning include how to build the remaining volumes in an optimal sequence; where to start for the remaining volume, considering the collision and tool switch length, which is very important for many AM process, e.g., CS.

For the toolpath of multi-axis AM, each layer can use 3D curve paths, however, most HAM systems still use planar scanning. For the most of existing methods, there is no valid toolpath generation, because many current methods did not consider the real deposition profile. Moreover, there is no optimization of scanning configuration for each layer.

2.4 The research questions

The whole tasks of CAPP for HAM include process identification to select the potential manufacturing processes, and manufacturability analysis to make sure the CAD models can be fabricated, but this is out of the scope of this research. Moreover, if considering the existing volume, the tasks of process planning include the selection of an optimal existing volume (defined as initial volume), the depositing sequence for the remaining volumes, and the toolpath planning, which are the main tasks of this research. The research scope includes

part skeleton generation which is prepared for initial volume generation and optimization, and AM sub-parts generation and sequence optimization, toolpath generation and optimization, shown in Fig. 2.46. The final objective of this research is the generation of the raw physical model in AM module and the near-net shape will be manufactured by non-AM processes like CNC, milling and heat treatment, etc.

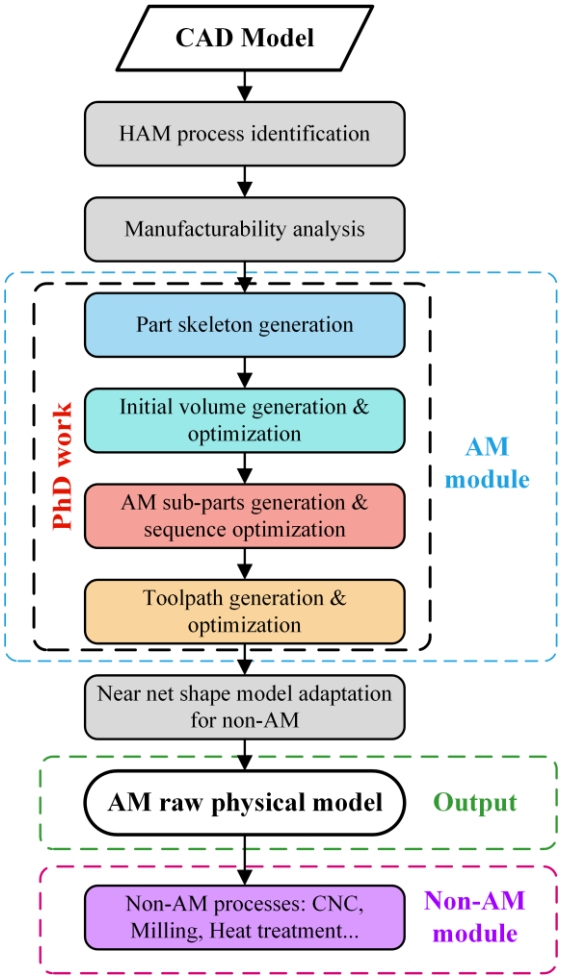

Fig. 2.46. The framework of CAPP for AM processing module in sequential HAM process.

Due to the survey of existing research, considering the objectives in chapter 1, some research questions are proposed based on the limitations of the existing research as mentioned above. In this thesis, the research work is focused on process planning for HAM mainly at the AM module and on the main following research questions:

(1) Question 1: How to consider initial volume generation and optimization for HAM from an existing volume defined in the CAD model?

(2) Question 2: How to find an optimal building sequence for the AM subparts for the processing module in a sequential HAM process?

(3) Question 3: How to generate and optimize the tool path based on the pre-optimized building sequence?

This research focuses on process planning for sequential multi-axis HAM, adopting Cold Spray (CS) as a specific AM process to describe the proposed generic methods, which can be extended to Wire and Arc Additive Manufacturing (WAAM) and DED, etc.

In the following chapter, the proposed methods are introduced in detail by adopting a complex tree structure CAD model for method implementation illustration.

Chapter 3 – The Proposed Methods

According to the previously identified problems in Chapter 2, this chapter introduces three proposed methods, i.e., initial volume generation and optimization, sequence planning of subparts, and toolpath generation & optimization in the AM processing module to solve these problems. To illustrate these methods, a complex tree structure is selected to illustrate the method workflows and technical implementation details since it is representative for collision detection and multi-axis processes.

3.1 The initial volume generation

HAM processes combine both advantages of additive processing and subtractive processing or other traditional processing like casting, stamping, etc. HAM can start from "*zero*" or an existing volume, as discussed in the former chapter. The processing from an existing volume has the potential to save material and processing time. In particular, the traditional manufacturing processes, like casting, are easy to build a fundamental physical component (an existing volume) with relatively simple shapes, called **initial volume** in this research. However, determining an optimal initial volume to save printing time, avoiding manufacturing constraints, and ensuring component quality is an open question for process planning and has rarely been investigated. To address it, this research proposes a skeleton-based model decomposition method to generate alternative initial volumes. And a set of generic evaluation criteria are defined for alternative evaluation to determine the optimal one. A multi-axis sequential HAM process, Cold Spraying (CS) with CNC, is selected as an application for method demonstration. In the CS HAM, an initial volume should be obtained by using other conventional processing processes, e.g., machining, casting, etc., and then a CS additive manufacturing module is used to build the remaining volumes onto the initial volume to form a near-net shape of the original CAD model. Finally, this model can be finished by post-processing methods, such as heat treatment, machining, laser cutting, etc. Although the application example is CS HAM, the proposed method can be adopted for other multi-axis HAM processes by introducing specific manufacturing constraints.

3.1.1 The method overview

The method includes three main steps, shown in Fig. 3.1.

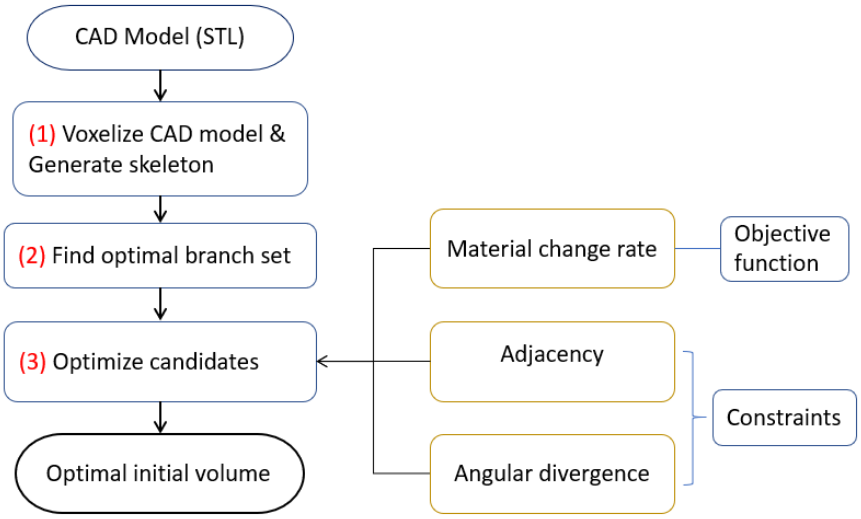

Fig. 3.1. The proposed method to generate and optimize initial volume.

(1) Voxelize a given CAD model in the format of STL to obtain a voxel model. Then generate a skeleton, the medial axis, from the voxel model to represent the general topological relationship of the original CAD model. The skeleton allows defining the "material deposition directions", which is interesting when searching "*decomposition*" of basic volumes into "*subparts*";

(2) Find the optimal branch set, which has the largest volume of the corresponding volume of the original CAD model. Decompose the skeleton into a set of branches and the CAD model into original subparts by using the intersection points on the skeleton. If necessary, remove a set of non-important sub-branches and extract the key branches, but all branches are kept in this research. The optimal branch set is a group of branches which are adjacent, and coplanar, as well as, with the largest volume of the corresponding subparts of the CAD model;

(3) Generate alternative initial volumes by a set of pre-defined 2D cross-section profiles (primary shapes, e.g., circles, polygons.) sweeping along the optimal branch set to generate 3D volumes. Considering the various size of selected 2D cross-section profiles, numerous different alternatives of initial volumes could be generated. They are called "*candidate initial volumes*"; Search the "*optimal candidate initial volume*" by using an evolutionary computational method. The material change rate is used to obtain the optimal initial volume.

3.1.2 The method implementation

At first, the original CAD model with STL format is voxelized to help obtain the model skeleton in the next step.

3.1.2.1 The voxelization generation & the skeleton generation

The CAD model with STL format is voxelized to obtain the skeleton of the CAD model in the next step.

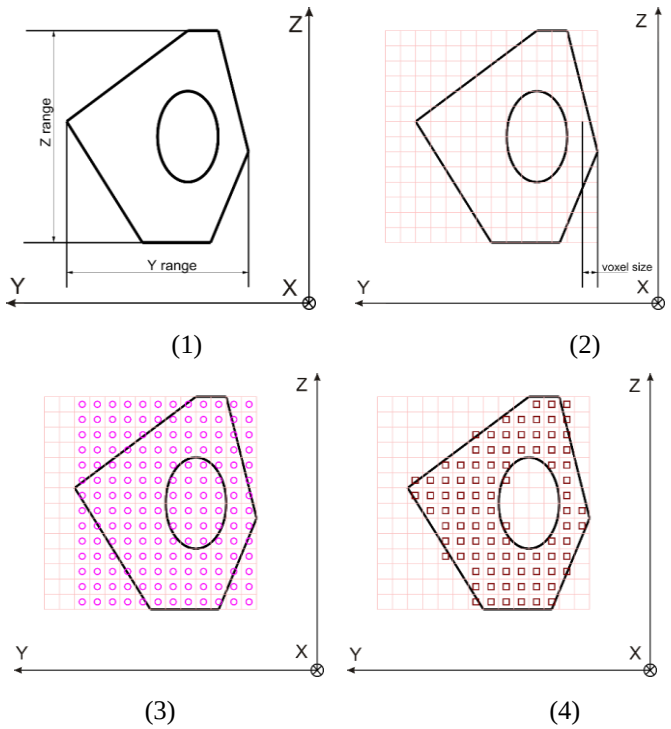

Fig. 3.2. (1). The Y range and Z range; (2). The voxel size; (3). The circle to test if the intersection is filled; (4). The filled voxels.

For the voxelization, the method proposed by Patil, S., & Ravi et al. [151] is adopted. With this method, polygonal solid models can be efficiently converted into voxel format with a maximum resolution of 1000 (one billion voxels) in less than 2 minutes. In this research, the voxelization algorithm is used to convert a solid model obtained from a CAD system in STL format. The voxel size, shown in Fig. 3.2. (2), is determined by dividing the maximum dimension of the bounding box of the STL model with a desired resolution by considering the Y range and Z range shown in Fig. 3.2. (1). The voxelization process essentially passes rays along the X-axis in a preset order (increments along Y axis first, then along Z axis) and finds their intersections with the facets illustrated in Fig. 3.2. (3). The voxels are filled if they are between an odd and the next even intersection shown in Fig. 3.2. (4). The process is carried out layer-by-layer from the minimum to the maximum Z coordinate. To demonstrate the implementation, Fig. 3.3. gives the result of the complex tree CAD model in STL format.

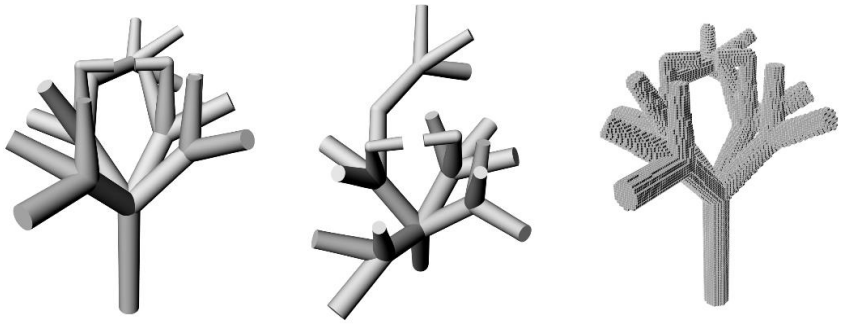

(1) (2) (3)

Fig. 3.3 (1), (2) The tree structure; (3) the voxelization result

To obtain a topology skeleton from a voxel model, a parallel 3-D medial surface/axis thinning algorithm proposed by Lee, T. C., Kashyap et al. [152] can be applied, verified for defect analysis of forging and casting. This method is an efficient three-dimensional parallel thinning algorithm for extracting both the medial surfaces and the medial axes of a 3-D object (3-D binary image). This method adopted Euler table to ensure the Euler characteristic and octree data structure of 3×3×3 lattice points are used to examine the connectivity, shown in Fig. 3.4. The implementation of this algorithm is realized by MATLAB code.

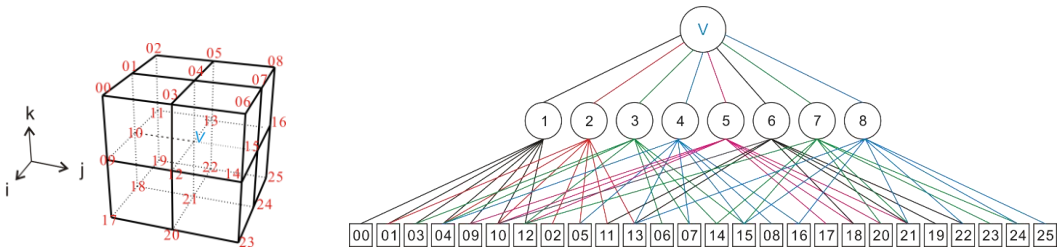

(1) (2)

Fig. 3.4. (1). The indices of the 26-neibourhood of a point v, N(v); (2). The adjacency of N(v).

The tree model is modeled in a parametric CAD tool, Rhino, a commercial 3D computer graphics and CAD software based on the NURBS mathematical model, and it focuses on producing a mathematically precise representation of curves and freeform surfaces. This tree model is generated by sweeping circles along the medial axis, i.e., each branch, shown in Fig. 3.5 (2). Based on this thinning method, the tree voxel model can be processed by MATLAB code, and the result, voxel skeleton, is achieved as in Fig. 3.5. (1).

The skeleton generated directly is made of a series of connected voxels, so it is necessary to replace it with a smoother skeleton, i.e., the voxel skeleton is hard to be used directly for generating initial volume but needs post-processing (e.g., the skeleton can be generated by connecting the voxels approximately, by like endpoints, turn points, etc.) or be replaced by

the medial axis used to generate the CAD model (e.g., the CAD model is generated by sweeping). But in this research, the smooth skeleton of the tree structure is shown in Fig. 3.5. (2), which is used during the tree CAD model generation, and it is adopted to replace the voxel skeleton, illustrated in Fig. 3.5. (1).

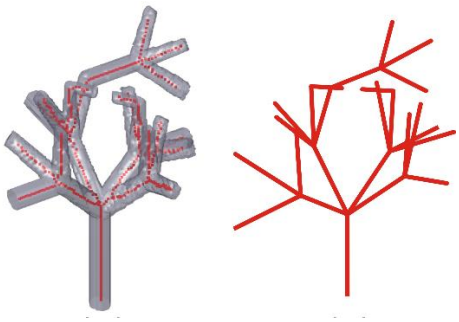

(1) (2)

Fig. 3.5. (1). The voxel skeleton; (2). The skeleton used to replace voxel skeleton.

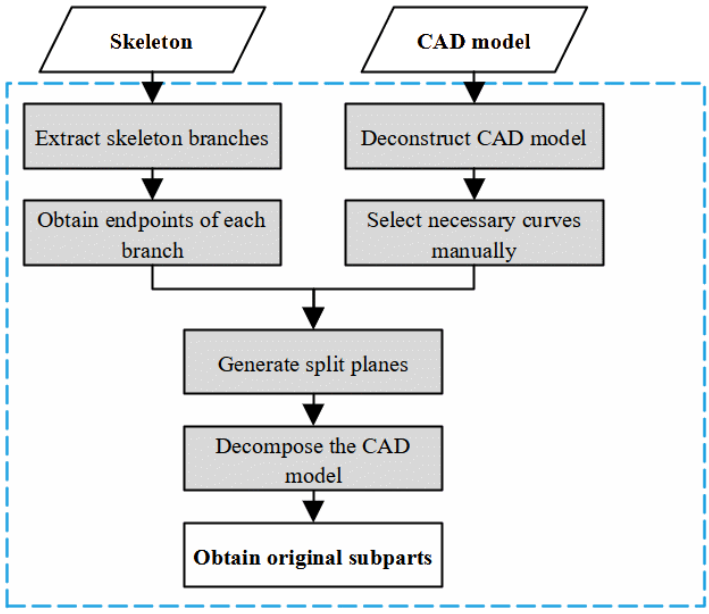

Fig. 3.6. The generation of the original subparts.

After obtaining the skeleton, the details of the second and third steps are the main research. The initial volume is generated by decomposing the skeleton and then sweeping some simple cross-sections like circles, along the selected branch set. Moreover, the corresponding volume of each branch is used to optimize the candidates, hence the model needs to be decomposed as well. As for original subparts decomposition, shown in Fig. 3.6, it is based on the skeleton and CAD model, and the end points of each extracted branches are

obtained. Meanwhile, the CAD model is deconstructed in GH (Grasshopper), so the necessary curves can be selected, manually, in this research. With the branch end points and the points of selected curves, the split planes are determined and moved to the corresponding branch points, and then the CAD model will be decomposed into many original subparts by these split planes.

Based on the original subparts and their relative branches, the optimal initial volume can be found with a two-step optimization method. First, the adjacent & coplanar criteria are adopted to find the optimal branch set which is decided by coplanar and adjacent constraints with largest volume sum of the corresponding subparts.

Then, the optimal initial volume is obtained by an evolutionary optimization method. The simple cross-sections (like circle or rectangle, etc.) can be adopted to sweep along each branch in the optimal branch set with different parameters. For the tree model, the circle cross-sections are adopted and the size of cross-sections can be searched in a range referenced with the equivalent circles (set as a fixed value in this research). The whole entities are obtained after sweeping all the branches in the optimal branch set and the optimized initial volume will be obtained by particle swarm optimization algorithm, using the criterion of the material change rate. More details are given in the following section.

3.1.2.2 Find the optimal branch set

1. Generate original subparts of CAD model

Based on the skeleton, further simplification is needed, if possible, as said above. Since the objective of using initial volume is to save time and material for the AM process, not to obtain a near-net-shape component to the original CAD model, hence, there is enough tolerance, and the initial volume should be a simple shape, geometrically close to the sub-section of the final component, which is easy to be fabricated by other non-AM processes. Based on this point, the skeleton can be simplified based on the following statements. For example, the angles between each pair of branches can be checked, considering the length and volume of the corresponding branch and its corresponding subpart. A similar consideration is given for approximate coplanarity analysis in the initial volume optimization criteria. If two connected branches have an angle larger than a certain predefined degree (e.g., 160 degrees), and their length and the relative cross-section are not very large, then the two connected branches can be replaced with one straight branch, as shown in Fig. 3.7. (1). Some angles among branches in the tree model are measured and illustrated in Fig. 3.7. (2). However, to

illustrate the proposed method, the tree model will not be simplified but keep all the branches, so the complexity of this tree structure is maintained.

Further, each straight-line segment in the skeleton is regarded as an individual branch. In other words, the decomposition uses the joint points of branches/straight lines of the skeleton. Then, based on the branches, the CAD model can be decomposed into a serial of original subparts. The tree structure with 25 branches in Fig. 3.3. is taken as an example, and hence it is decomposed into 25 subparts originally (called original subparts) illustrated in Fig. 3.8. And Fig. 3.8. (1) shows that this tree structure is cut sequentially bottom-up because this process is operated manually, from (a) to (d). If it is performed automatically, the decomposition process can be operated parallelly, so the split planes can cut the model into subparts at one time. Fig. 3.8. (2) explains the details of the split planes. Fig. 3.8. (2) (a) is the whole part which has been decomposed and a partially enlarged structure in Fig. 3.8. (2) (b) is selected to show the generation process of split planes. The split planes are decided by the intersection point in the skeleton and the points manually selected in Fig. 3.8. (2) (c), (e) on the surface of the entity. The plane in Fig. 3.8. (2). (d) is obtained by one plugin called plane fit in Grasshopper and the planes are generated by three selected points illustrated in Fig. 3.8. (2) (f). All of these planes will be translated through the intersection in the branches of these corresponding subparts.

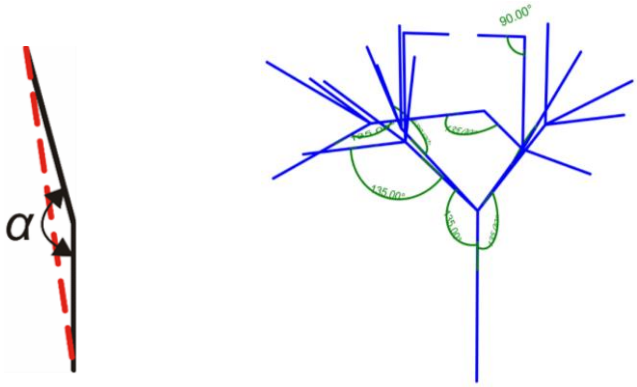

Fig. 3.7. (1). The equivalent straight line of two lines with large angle; (2). Some large angles of the tree model

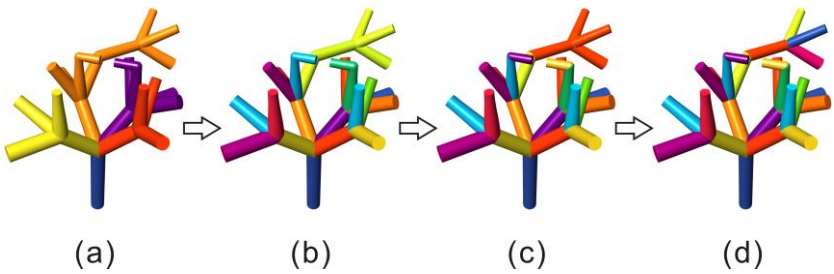

(1)

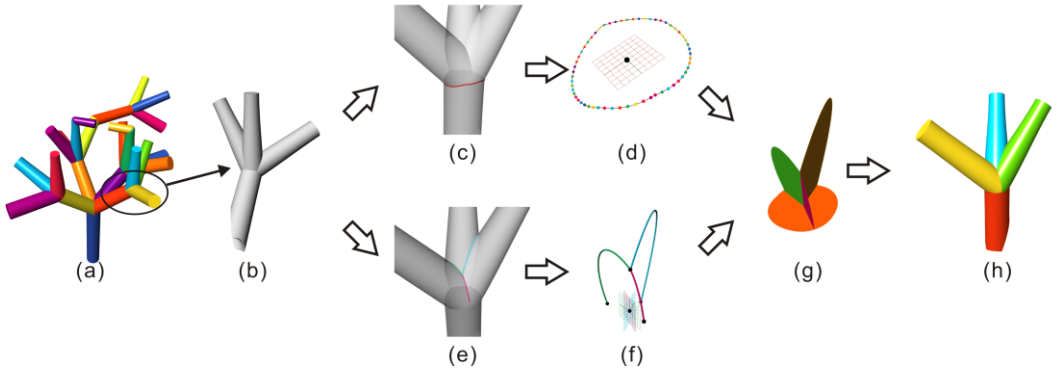

(2)

Fig. 3.8. The decomposition process and the results of tree model decomposition: (1). The main process of hierarchical decomposition, (2). The generation of split planes.

The branches of the skeleton and the original subparts are used to generate and optimize initial volumes in the next step.

2. The candidates of branch set

For searching the optimal branch set, the encoding is binary, 0 and 1, and 0 means the branch is not selected, while 1 is selected. The encoding of some candidates of branch set is shown in Fig. 3.9. (a). By altering the combination of encoding of each branch, shown in Fig. 3.9. (b), the candidates of branch set can be obtained and the corresponding volumes of selected branch can be also obtained, shown in Fig. 3.9. (c), but some of them are not continuous like (2), (4) in Fig. 3.9. (c). Therefore, the coplanar and adjacent branch sets of the skeleton are firstly found and optimized by considering the sum of original volumes of the corresponding subparts. Then, the cross-section size of each selected branch is optimized by PSO method as well in the following step to obtain the final optimal initial volume.

	0	*1*	*2*	*3*	*4*	*5*	*6*	*7*	*8*	*9*	*10*	*11*	*12*	*13*	*14*	*15*	*16*	*17*	*18*	*19*	*20*	*21*	*22*	*23*	*24*
(1)	0	0	1	0	0	1	0	1	0	0	0	0	0	1	0	0	0	0	0	0	0	0	0	0	0
(2)	0	0	1	0	0	1	0	1	0	0	0	0	0	0	0	0	0	0	0	0	0	0	0	0	0
(3)	0	0	1	0	0	1	0	0	0	0	0	0	0	1	0	0	0	0	0	0	0	0	0	0	0
(4)	0	0	1	0	0	1	0	0	0	0	0	0	0	0	0	0	0	0	0	0	0	0	0	0	0
(5)	0	0	1	0	0	0	0	1	0	0	0	0	0	1	0	0	0	0	0	0	0	0	0	0	0
(6)	0	0	1	0	0	0	0	1	0	0	0	0	0	0	0	0	0	0	0	0	0	0	0	0	0

(a)

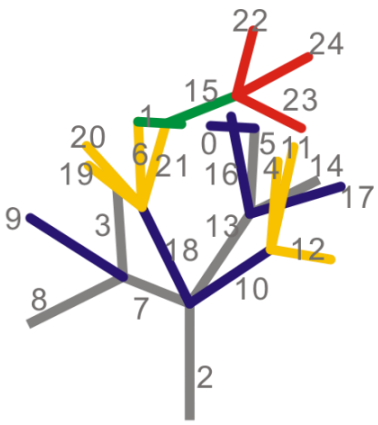

(b)

(1) (2) (3) (4) (5) (6)

(c)

Fig. 3.9. (a). The encoding of 6 candidates of branch set; (b) The skeleton of the tree model with the branch order; (c). The corresponding volumes of the 6 candidates.

3. Find the optimal coplanar and adjacent branch set

To obtain the optimal initial volume, the first step is to get the adjacent and coplanar branch set, shown in Fig. 3.10. Two main constraints need to be considered, which can be evaluated by adjacency and coplanarity, while the angular divergence is introduced to evaluate the degree of coplanarity.

(1) Adjacency

Since the candidate is generated randomly by the combination of branches, and many branch combinations are disconnected. The disconnected branches will generate more than one volume sections after the sweeping process to generate the initial volume, which means more complexity for the following AM and non-AM processing. Hence, an evaluation criterion, adjacency, is proposed for the candidates of initial volume's skeleton evaluation. It can be estimated by the number of common knots and the number of branches. If the number of knots and branches meet this formula

$$N_k - N_b \leq 1 \quad (1)$$

, the branches are adjacent and connected as the case shown in Fig. 3.11. In details, in Fig. 3.11. (1)., there are 4 branches 1-4 and 4 points a-d, Fig. 3.11. (2). 3 branches 1-3 and 4 points a-d, Fig. 3.11. (3). 3 branches 1-3 and 4 points a-d skeletons.

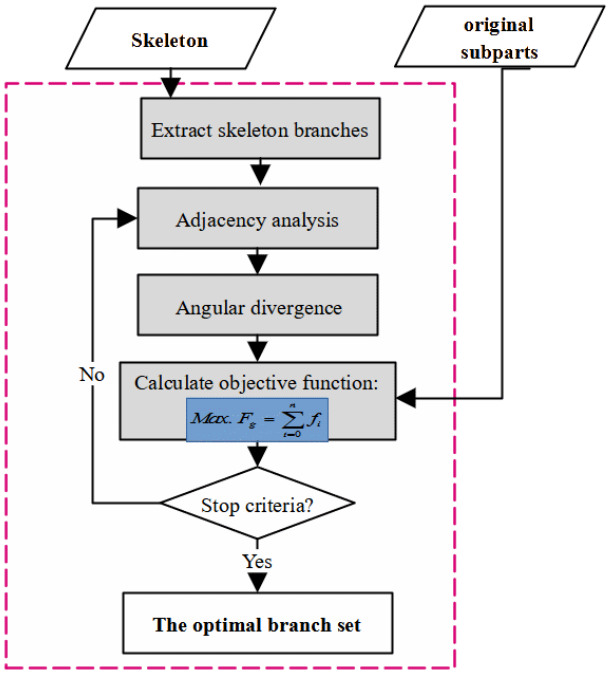

Fig. 3.10. The first step of initial volume generation--to find the optimal branch set.

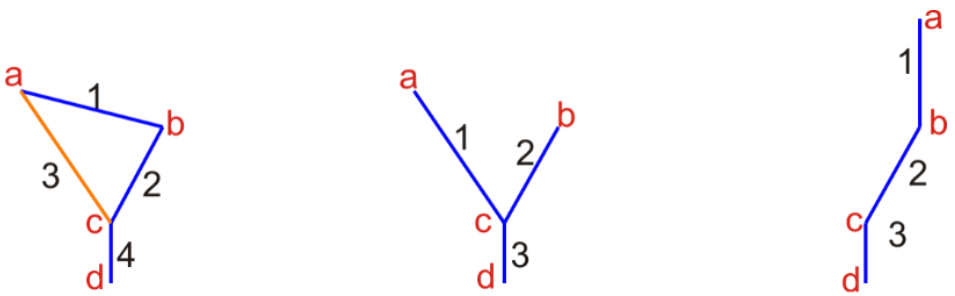

(1) (2) (3)

Fig. 3.11. The adjacent branches and the number of points and branches.

(2) Angular divergence

The other constraint is angular divergence, which is used to describe the coplanarity extent of different branches in a selective branch set of a candidate of initial volume. The coplanarity can be calculated by using the vectors of skeleton branches. For example, if given two branches i and j and their vectors, V_i and V_j, their cross product V_{ij} can be employed to do dot product with the vectors of all other vectors of the remained branches V_k (k=1,2,3…,)

of the branch set. Theoretically, if there are more branches in a candidate initial volume with small degree of divergence, to fabricate the remaining volumes, the following AM or non-AM processing would also be easier, since probably less complexity for collision detection and less reorientation of the initial volume in the following processing. Hence, there is a need to define a coplanarity to describe the criterion of angular divergence. However, generally, the degree is not easy to be absolutely 0, so the size of the cross-sections of the original CAD model should also be taken into account. Therefore, a coefficient of these branch volumes, C_v, is used to differentiate the impact of each branch of the skeleton. The value of C_v can be assigned by using experience or a ranking scheme, where long branches with big volume gain bigger weights. Therefore, the degree of angular divergence can be described by D_k, shown in formula (3).

$$V_{ij} = V_i \times V_j (i, j = 1, 2, ..., n) \quad (2)$$

$$D_k = \left(V_{ij} \bullet V_k\right) * C_v (i, j, k = 1, 2, ..., n) \quad (3)$$

As a consequence, the mean value of these D_k values can be used as an index value to describe the angular divergence of the branch sets for the candidates of initial volume. D_k can greatly reflect the degree of coplanarity with consideration of the volume of the adjacent subparts.

$$\frac{\sum_{k=1}^{m} D_k}{m} (m = n - 2, k = 1, 2, ..., m) \quad (4)$$

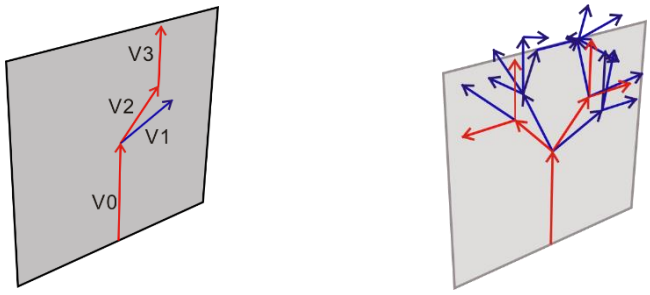

(1) (2)

Fig. 3.12. The non-coplanar and coplanar branch sets: (1). some branches from the tree model skeleton (the red branches are coplanar); (2). The tree skeleton with directions of each branch (the red branches are coplanar).

When $V_{ij} \cdot V_k = 0$, which means the branches are coplanar as the red branches, shown in Fig. 12. The structure is selected from the tree model, shown in Fig. 3.12. (1), the red

branches are coplanar and the blue branches are not in the plane of red branches. So, $D_k = V_i \times V_j \bullet V_k = 0$, when $(i, j, k = 0, 2, 3)$, which means V_0, V_2 and V_3 are coplanar, while V_0, V_2 and V_1 are not coplanar, because $D_k = V_i \times V_j \bullet V_k \neq 0$, when $(i, j, k = 0, 2, 1)$. If the value of D_k and C_v is not very big (according to the specific processes and the size, final quality of the products), the selected three lines can be seen as approximately coplanar. The vectors of each branch of the tree model are illustrated in Fig. 3.12. (2). To make it simple, D_k is set to 0, so the coplanarity is only considered absolutely coplanar in tree model. The objective function is the whole volumes of the subparts which are corresponding to selected branches, i.e., the candidate of branch set.

Max. $F_g = \sum_{i=0}^{n} f_i$ (5)

, where F_g is the sum of the volumes of subparts corresponding to the selected branch set, f_i is the volume of each subpart for the corresponding branch, and i varies from 0 to the number of branches of the selected branch set. The largest F_g is corresponding to the expected branch set.

Based on the above-mentioned two constraints, the coplanar and adjacent branches with biggest volumes of the corresponding original subparts for the tree model are obtained, shown in Fig. 3.13. The encoding is shown in Fig. 3.13. (1), and the optimal branch set of the tree model is illustrated in Fig. 3.13. (3).

0	1	2	3	4	5	6	7	8	9	10	11	12	13	14	15	16	17	18	19	20	21	22	23	24
0	0	1	1	0	1	0	1	1	0	0	0	0	1	1	0	0	0	0	0	0	0	0	0	0

(a)

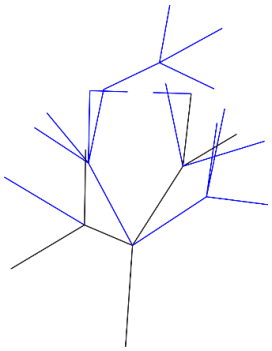

(2)

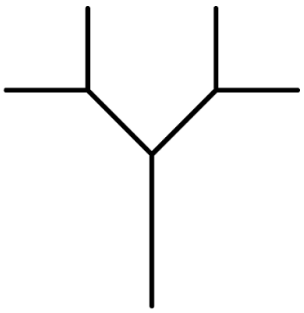

(3)

Fig. 3.13. (1). The binary encoding; (2). The original tree skeleton; (3). The optimal branch set.

3.1.2.3 Find the optimal initial volume

1. Determine the cross-section

To generate the initial volumes, it is necessary to choose relatively simple shapes or their combination for the processing by non-AM process. To generate such kind of simple 3D volume, 2D basic profiles are used, e.g., circle, polygon, and etc., to sweep along each branch of the optimal branch set so as to generate simple 3D volumes. However, each branch of the skeleton only represents the special topology of the initial CAD model's sub-part. Hence, how to find a reasonable 2D profile to sweep so as to generate an approximate 3D volume that is close to the original sub-part volume is a key question. In this research, the adopt of circle cross-section is proposed to sweep each branch of the optimal branch set for the tree model. However, it is not only circle can be selected. In the following, the range of circle profile for the tree model is presented.

Along the skeleton, the cross-sections of a CAD model are usually different, even for one branch. To obtain an equivalent cross-section profile, at first, a set of parallel planes that are perpendicular to the branch is used to cut the original CAD model's sub-part corresponding to the skeleton, and then the obtained cross-sections' profiles or approximate profiles are used to calculate. For example, if the goal is to obtain a circle equivalent profile for a branch, a set of circles, which are approximate profiles to the cross-sections, can be used. The centers of circles are on the branches, and the radius can be achieved by calculating the distances r_i between the center and the cross-section contour point j. This point can be randomly selected from the contour or respect some predefined rule. In this research, 6 points on the contours are randomly sampled in a step length of 60 degrees of rotation and the mean value of the 6 radius values is used. Then, the mean distance r_e is used as the radius of the equivalent circle.

$$\mathrm{Re} = \frac{\Sigma ri}{N},\ i = 1,2,\dots,N \qquad (6)$$

, where N is the number of cross-sections. But in some cases, a branch may be very long, and the cross-section contour diameter size may be quite different along the skeleton. In this condition, these branches of the branch set can further be decomposed and the same method is applied to calculate an equivalent circle profile for each sub-branch obtained by the decomposition, from r_e1 to r_e6 as illustrated in Fig. 3.14. (1). And again, the mean value can be used to find an approximate circle profile. The sizes of these equivalent circles are

considered as the size range for the following adopted optimal algorithm to search the best size for each cross-section. Hence, different profile shapes and diameters can also be assigned for one branch. But, to simplify, in this research, only one uniformed 2D profile is assigned for each branch. Fig. 3.14. (1). shows different cutting sections with circle profiles of one tree branch and one candidate size for this whole branch is R_e, which can be adopted as reference for optimizing the size of cross-section for the branches in the optimal branch set. Fig. 3.14. (2). shows one candidate of equivalent circle profiles for all the branches in the optimal branch set of the tree skeleton, and each branch has its own relative cross-section. However, in this research, the search range is fixed.

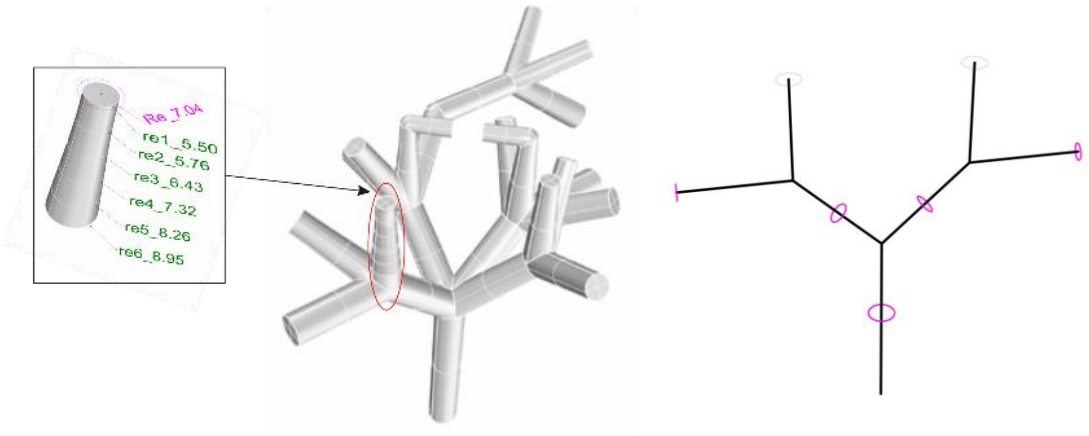

(1) (2)

Fig. 3.14. (1) Different approximate circle profiles for cross-sections along a sub-skeleton/branch; (2) One possibility of the equivalent circle profiles for the optimal branch set.

2. Determine the optimal initial volume

Once the equivalent cross-section profiles are obtained, they can act as reference to sweep along the corresponding optimal branch set to generate 3D volumes, illustrated in Fig. 3.15. The size and shape of profiles determine the final volume and the shape of the initial volume. For this illustrative tree model, an initial volume composed by a set of cylinder branches with different diameters is defined, which will be optimized by an evolutionary optimization method. Since GA (Genetic Algorithm) is very slow for iterations, Particle Swarm Optimization algorithm (PSO) is adopted for searching optimal initial volume. The flow chart of PSO is illustrated in Fig. 3.16.

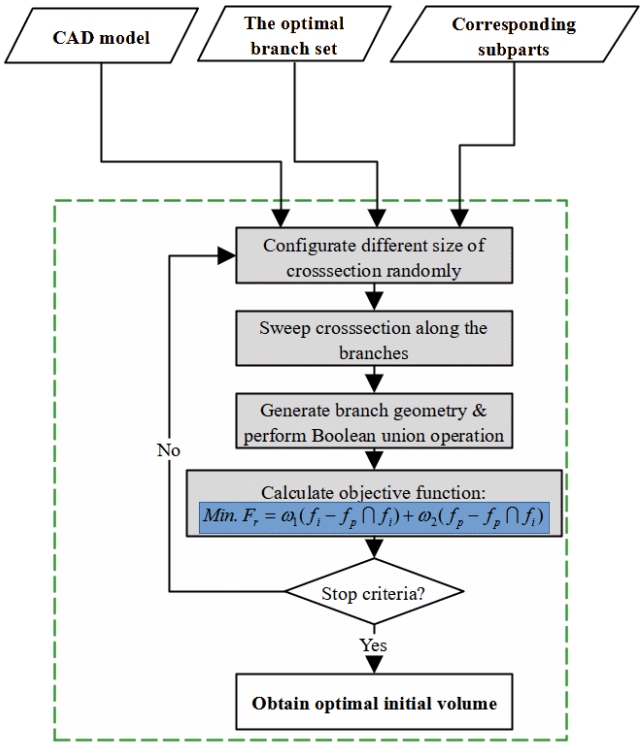

Fig. 3.15. The optimal initial volume.

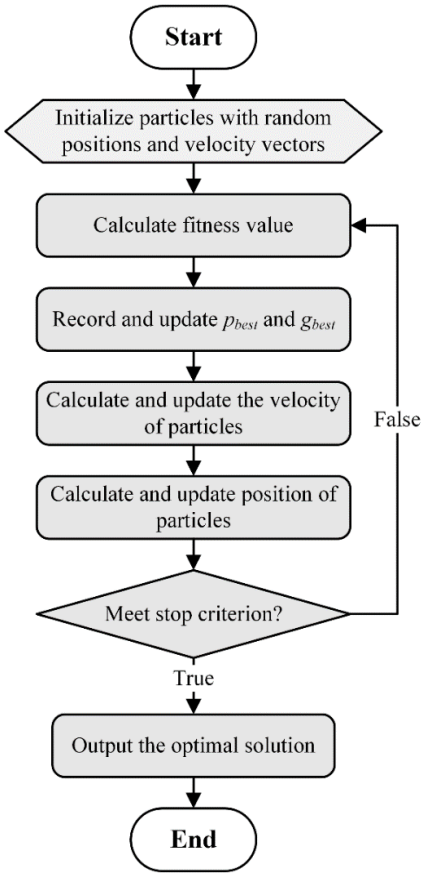

Fig. 3.16. The basic steps of PSO.

PSO is a sub-field of Computational Intelligence and belongs to the field of swarm intelligence and collective intelligence and has both ties with artificial life and evolutionary computation. It is a type of biological system, inspired by bird flocking and fish schooling and its simulation was motivated by the need to model 'human social behavior', and the collective behaviors of individuals interacting with each other and their environment form the optimization process [153]. One solver called Silvereye is introduced to realize this algorithm by visual programming in Grasshopper [154].

Based on the optimal branch set, different cross-sections with various size are adopted to sweep along the branches in the branch set, to generate the initial volume candidates. The candidates will be filtered by PSO method to obtain the optimal initial volume. As discussed above, different branches probably have different sweeping profiles with different diameters. If a branch has a tiny cross-section, then the stiffness may be not enough and cause some problems in the following AM or non-AM processing, where material deposition may cause force or cutting force, resulting in deformation of the initial volume. Hence, there is a need to check this issue. Therefore, the aspect ratio can be also introduced and used for the scoring and filtering the candidates of initial volume. Aspect ratio ϕ, defined as $\phi = L/D$, (L is the length of equivalent branches, and D is the equivalent diameter of each corresponding cross-section) is used to describe the stiffness implicitly. For example, if ϕ is too large, the stiffness is weak and the initial volume cannot support the force of fixture or the force during the fabrication process. In order to respect the aspect ratio, the following condition has to be verified: $\phi = L/D < \beta$ (β is a threshold value set according to the manufacturing constraints). To make it simple, at a generic methodology level, all the generate branches are assumed to be qualified with a fixed search range. Therefore, the encoding for this step is the size of cross-section for each branch in the optimal branch set, shown in Table 3.1.

Table 3.1. The encoding of the branches in the optimal branch set of the tree model.

Branch	1	2	3	4	5	6	7
Size	r_1	r_2	r_3	r_4	r_5	r_6	r_7

To evaluate and search for the optimal initial volume, the volume of the material needs to be deposited and removed to obtain the final product based on the initial volume will directly impact the AM and non-AM processing time. This means that the less material to be changed

(added or removed), the less time and material will be costed, because the initial volume can be obtained in a very efficient and economical way. To drive the searching, an objective function concerning the changed material volume is defined below, in equation (7):

Min. $F_r = \omega_1 \left(f_i - f_p \cap f_i \right) + \omega_2 \left(f_p - f_p \cap f_i \right)$ (7)

Where F_r is the material change rate; f_i is the initial volume (Fig. 3.17. (2)) and f_p is the volume of finished part (after AM and non-AM processing, i.e., CAD model illustrated in Fig. 3.3. (1), (2). Fig. 3.17 (3) shows the initial volume after machining from the casting shown in Fig. 3.17 (2), which is an example for the processes of Non-AM. Fig. 3.17 (4) are the remaining volumes to add materials to the modified initial volume presented in Fig.3.17 (3), and the modified initial volume considers the volume difference with the corresponding original subparts of CAD model. ω_1 and ω_2 are the weights assigned to the cost of AM, non-AM, e.g., subtractive manufacturing processes and materials, respectively. Generally, AM is more expensive than Non-AM processes. In addition, ω_1 and ω_2 meet the equation $\omega_1 + \omega_2 = 1$. In this research, the weights are set 0.95 and 0.05 as an example, by considering the cost of initial volume and its adaptation. Moreover, this function can be directly used as an objective function in the plugin called Silvereye for PSO in GH.

Table 3.2. The parameters set for PSO in Silvereye.

Option	Swarm size	iteration	Max. Velocity
Description	20	200	0.2

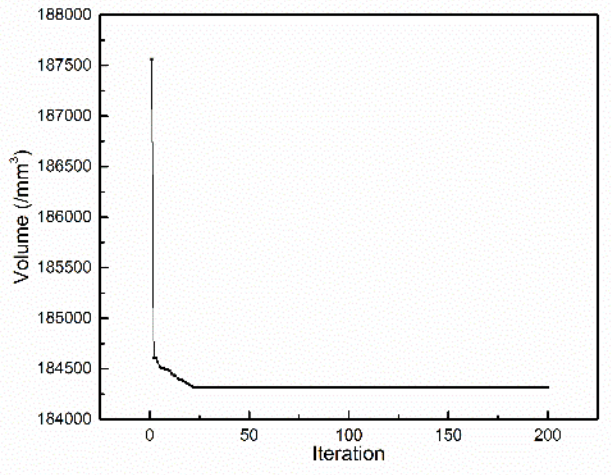

(1)

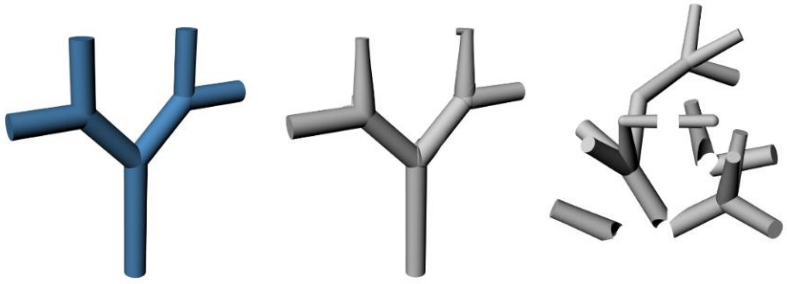

(2) (3) (4)

Fig. 3.17. (1) The calculation result in Silvereye; (2) The optimal initial volume of the tree structure; (3) The modified initial volume; (4) The volumes need to be added.

With the defined objective function and evaluation criteria, the implementation of PSO is operated in GH. The parameters are set for the initialization of algorithm, shown in Table 3.2. The process is initialized with a random population of particles and each particle represents a solution. This research chooses 20 swarm size, the same as in this research [154]. In every time step the fitness value is sampled and the velocity of each particle is updated. The velocity is constructed based on the current velocity, the best known global position (the best result sampled by the whole population - gbest) and the best position discovered by the particle (pbest) [154]. Moreover, the Max. velocity is 0.2 and the iteration is 200. This algorithm and the parameters will also be adopted in the next chapter for the study cases.

After the calculation in Silvereye with the parameters set in Table 3.2, the calculation result is shown in Fig. 3.17 (1), and the optimal initial volume is obtained in Fig. 3.17 (2).

3.2 The sequence planning

Based on the abovementioned evaluation criteria/constraints and objective function, the optimal initial volume of the tree structure is obtained. The optimal candidate is the biggest and adjacent volume (a group of 7 subparts), and the corresponding branches of subparts are coplanar as shown in Fig. 3.13. (3) and then the initial volume is modified by Boolean difference operation with CAD model shown in Fig. 3.17. (3). As this research is on the multi-axis process, the remaining volumes need to be decomposed to the AM subparts, shown in Fig. 3.18. Then, it is necessary to find the optimal sequence of these AM subparts in the AM module for sequential HAM. These AM subparts are obtained slightly differently from the original subparts as in the previous section. They are generated using the original subparts as a guide because of the possible complex tiny volumes after the Boolean difference between the CAD model and the modified initial volume, but the details are out of the scope of this

research. The split planes shown from Fig. 3.18. (c) to (g) are generated similarly to the original subparts.

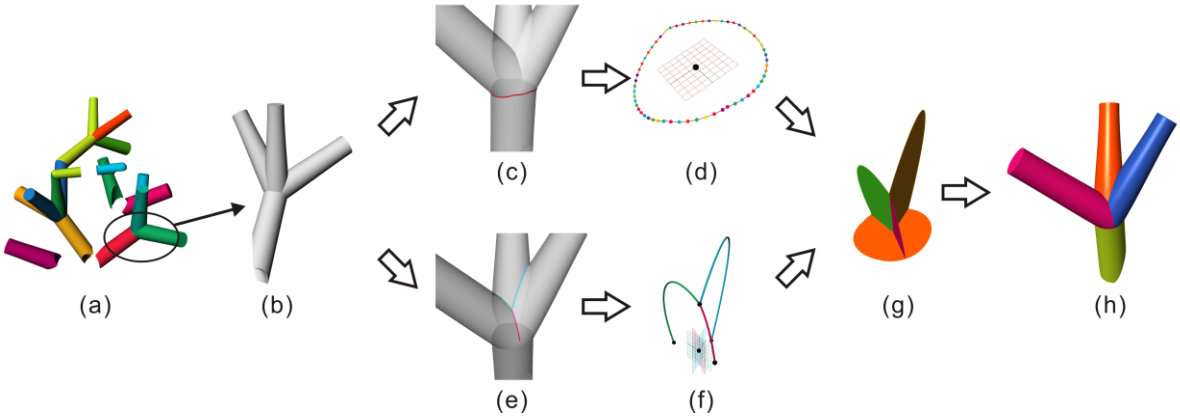

Fig. 3.18. The process of AM subparts generation after the Boolean difference operation between CAD model and modified optimized initial volume.

As introduced above, the initial volume is the starting volume of processing for AM module. This volume is different from the original CAD model, and the difference volumes (the Boolean difference of CAD model with modified initial volume) are called the remaining volumes in this thesis. Hence, the remaining volumes (decomposed into several volumes called AM subparts and added to the modified optimal initial volume), the CAD model volume subtract the obtained modified optimal initial volume, maybe discontinuous, and all the subparts may result as different disconnected volumes. These remaining volumes are decomposed into AM subparts considering the skeleton branches and the original subparts, as mentioned before. Therefore, to build all the remaining volumes, it needs to operate different manufacturing actions to achieve the near-net-shape of the CAD model by adding materials onto the optimized initial volume. A sequence-planning problem comes up for building all of the AM subparts. In this section, a sequence planning method is introduced to find an optimal sequence for building the AM subparts to deposit the remaining volumes in the AM module of multi-axis sequential CSHAM platform. The objective is to simplify the sequencing requirements.

3.2.1 The method overview

After selecting the optimized initial volume, some volumes still left and need to deposit material onto the initial volume. Hence, a new feature-free sequence planning method is proposed in this research. The AM subparts of the remaining volumes should be classified

into several groups by adjacency relationship to minimize the AM sequence solution space. The initial volume is considered as the start point, and the AM subparts in different groups are built hierarchically from the group adjacent to the initial volume, then to other groups until the end. The proposed method of sequence planning for AM subparts includes three main modules shown in Fig. 3.19.: AM subparts group module, inter-group collision analysis module, and sequence planning module.

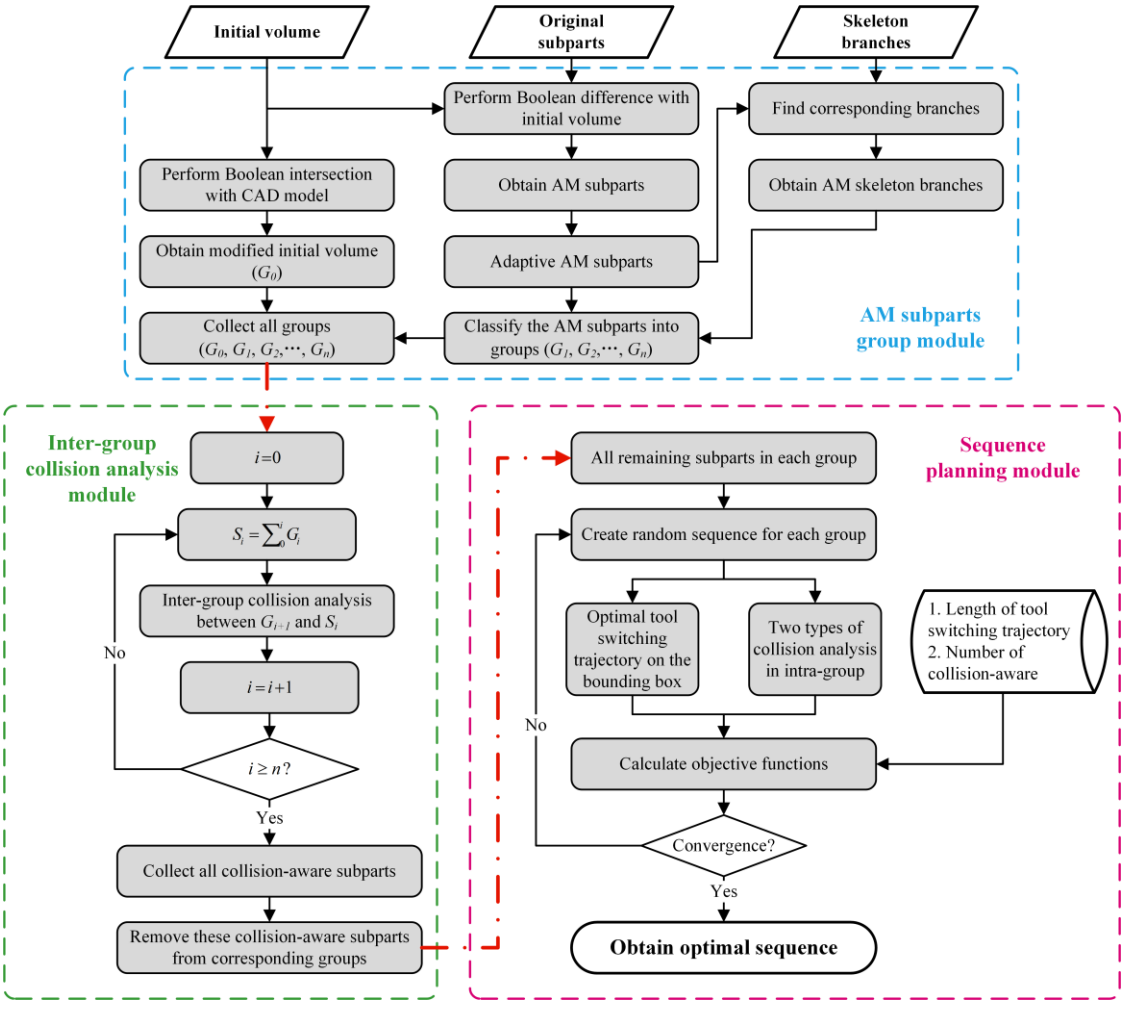

Fig. 3.19. The proposed method for sequence planning (inter-group: between two or more groups; intra-group: inside one group).

The AM subparts are obtained by decomposing the remaining volumes with the original subparts as a guide. Then, these subparts are classified into different groups (G1, G2, …, Gn). Since collisions are very important for manufacturing process, they will be detected among different groups (inter-group) first. For the subparts which have collisions with the existing volumes of other groups, they will be manufactured with support base. Therefore, they will be

removed from their own groups and not considered for sequence planning of the subparts in the sequence planning module. For the remaining subparts which do not need support base, they will be calculated by Genetic Algorithm (GA), with two criteria: the length of total tool switch trajectory and the number of intra-group (inside one group) collisions. Finally, the optimal sequence for the AM subparts which do not have inter-group collisions.

The following sections will implement the proposed method. The tree structure example used above is still applied here to explain the details of this method to optimize the sequence for AM subparts.

3.2.2 The method implementation

3.2.2.1 The group classification

In detail, the original initial volume needs to be modified by operating Boolean intersection operation. In practice, some conventional processes can be adopted, e.g., CNC, milling, to remove the extra material or to make it close to corresponding original subparts. The remaining volumes which need to be added onto the initial volume can be obtained by performing Boolean difference operation between CAD model and the modified initial volume. To fulfill the capacity of multi-axis platform, the remaining volume need to be decomposed as in the previous chapter based on the skeleton branches. However, the curves of the remaining volume may be very complex to select, so it is not easy to decompose it totally the same as in the previous chapter. Interestingly, the remaining volumes are quite close to the corresponding original subparts. In addition, their skeleton branches are the same among the original subparts and AM subparts, respectively. Therefore, the former original subparts can be used as guides to generate the AM subparts. Probably, the AM subparts need to be adapted, because of the complexity and discontinuity by adding or removing tiny volumes in the original subparts, but this is out of the scope of this research.

For the AM subparts, each of them has one direction based on the corresponding branch of skeleton. If there exist collisions between the CS gun and the part (even the fixture of the part) in the processing, subparts need to be re-decomposed or the orientation of the subparts have to be changed, but this point is out of the scope of this thesis.

Then, based on the adjacent relationship of skeleton branches, the AM subparts are classified into several groups (G1, G2, …, Gn). The classification method of AM subparts is similar with the method for reconstruction assembly proposed in [155], because both of these two cases start from one start point to add other volumes onto the existing volumes

hierarchically, using topology and adjacent relations to assemble subparts shown in Fig. 3.20. (1), (2). As a consequence, the initial volume can be seen as G0, and the AM subparts which are adjacent to the initial volume is G1, and the ones which are adjacent to G1 is G2, etc., till the last group Gn. This process is iterative and all the groups of tree model are shown in Fig. 3.21.

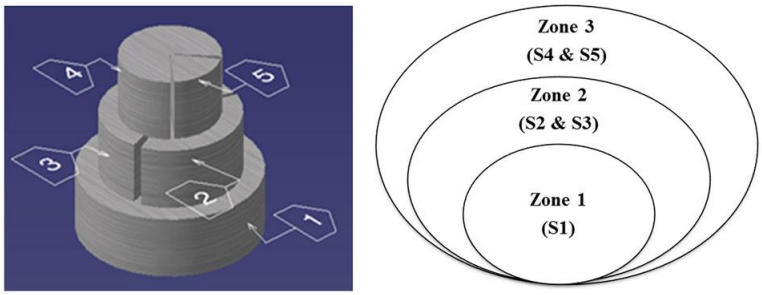

(1) (2)

Fig. 3.20. (1), (2). The segments classification for a broken object [155].

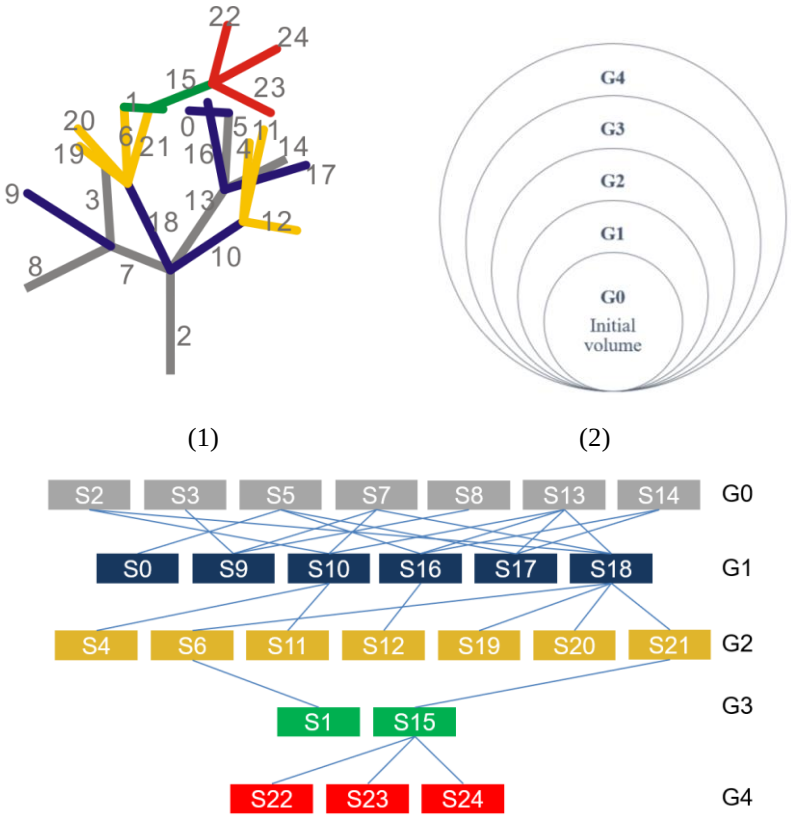

(1) (2)

(3)

Fig. 3.21. The classification result for tree model based on the adjacent relation: (1) the branches of tree skeleton; (2) all four groups of the AM subparts; (3) the adjacent relation of different groups.

The classification result of tree model is illustrated in Fig. 3.22. The first group Fig. 3.22. (3) is the subparts need to be deposited onto the initial volume (Fig. 3.22. (2)), whose relative branches are 7 grey branches shown in Fig. 3.22. (1). Then, other branches, in different colors, are corresponding to the subparts which will be manufactured hierarchically from group 1 to group 4 in Fig. 3.22 (3), (4), (5), (6).

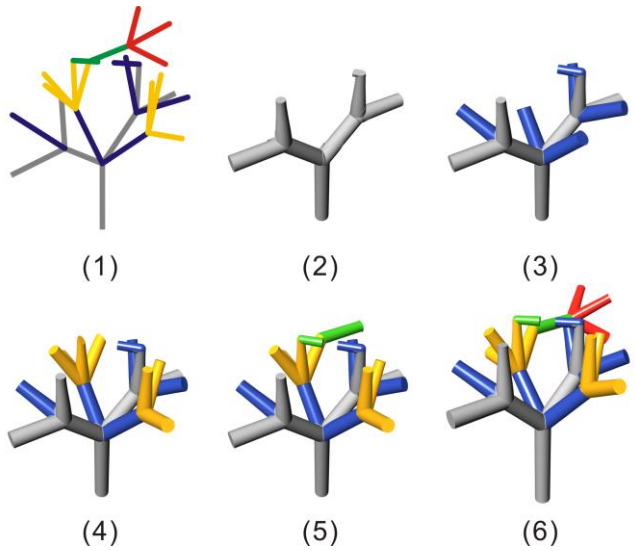

Fig. 3.22. Tree model with four groups of subparts and the initial volume: (1). Skeleton; (2). Initial volume (Group 0); (3). Group1 with group 0; (4). Group 0 to group 2; (5). Group 0 to group 3; (6). Group 0 to group 4.

3.2.2.2 Collision detection and collision avoidance by bounding box

To generate valid processing sequence, the collision detection is operated first to check the collisions between different groups. For the AM subparts which do not collide the subparts of the previous groups, their sequence will be optimized in their own group. However, the collisions may also occur among the subparts in the same group. In this research, a bounding box strategy is applied to avoid collisions when the CS gun switch from one subpart to the following one. The idea is to use a bounding box, shown in Fig. 3.23. (c), to envelope the existing volumes, i.e., the initial volume and part A, shown in Fig. 3.23. (a) and the tip points, shown in Fig. 3.23. (b). Moreover, the CS gun switch points will be replaced by the nearest points on the bounding box surfaces, which is very easy to realize in Grasshopper. Then the processing nozzles/tools can move on the surfaces from the just finished subpart to the next one. Therefore, the collisions can be avoided during the tool switch. The convex polygon connection of tip points P_A, P_B in Fig. 3.23. (b), is a set of the alternative moving trajectories of the processing nozzles/tools. When the nozzle or tool

switches from one surface to another, a rotation of the precedent structure or reorientation is generated. When one branch is finished, the gun moves to the next one on the surface of the bounding box, and the trajectory of processing tool switch is shown as in Fig. 3.23. (d), (e). To make the tool switch trajectory shorter, it is assumed that the smaller bounding box probably has the shorter length. So, the bounding box is optimized roughly by changing the angles. Another solution is to keep the tool switch trajectory as a straight line after unfolding the bounding box, shown in Fig. 3.23. (d), (e).

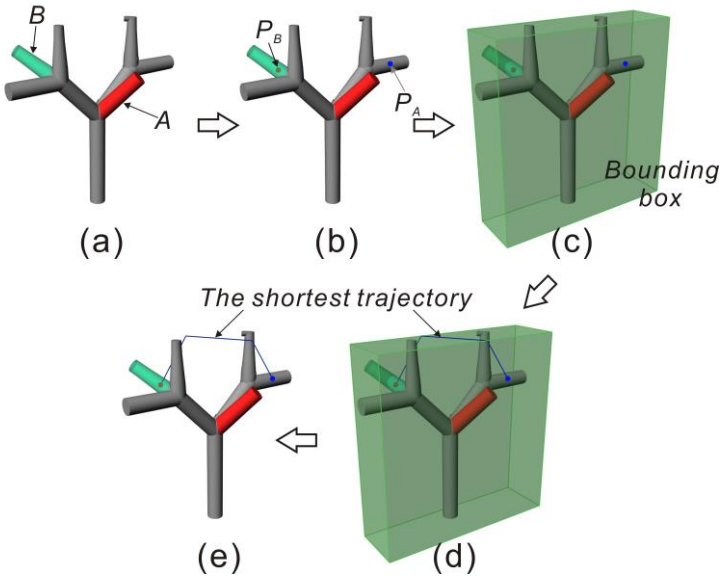

Fig. 3.23. The bounding box of initial volume with existing subparts: (a). Subpart A has been manufactured; (b). PA and PB are tip points of tool; (c). The bounding box envelop subpart A and existing initial volume; (d), (e). The tool move from PA to PB on the surface of bounding box and trajectory is a line when the box is unfolded to plane.

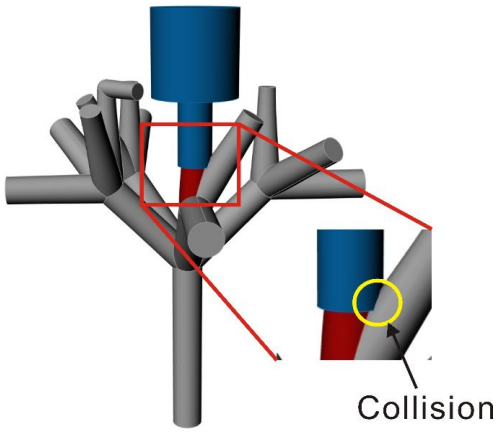

Fig. 3.24. A description of collision between CS gun and the existing volume.

Even though many collisions can be avoided by bounding box, but there are still some intra-group collisions left among the AM subparts inside one group. To simulate the collision, the model of a CS gun with the shape of the projected powder is built to test the collision with the existing volumes, shown in Fig. 3.24. Even though the collisions during the CS process can be divided into two types, i.e., soft collision and hard collision of inter-group or intra-group types, both of these collisions can be tested by this method. In detail, the collisions of CS gun with the built parts or the fixtures are called hard collisions, illustrated in Fig. 3.24., while the shade of powder particles by the built part or fixtures are called soft collisions in this research, shown in case study in Fig. 4.18. (b). The CS gun is simplified as two cylinders in dark blue and the red cylinder is the projected powder, shown in Fig. 3.24. The gun has two cylinders: the bigger cylinder is with the diameter and the length 10mm and 30mm, respectively; the diameter and length of the smaller cylinder are 4mm and 10mm, respectively. For the shape of the projected powder, the length is 30 mm and the diameter is 1mm. All these parameters are parametric in the programming, so different configuration can be adjusted easily.

3.2.2.3 GA for sequence planning optimization

After defining the main principles of the sequence planning, it is necessary to optimize it. As said above, the tip points on the bounding box may generate many alternative connections along the surfaces for the processing tool/nozzle's moving. Hence, the tool/nozzle trajectory length for each processing step (the AM subpart building step) and the total length may be different but important to the final total processing time. Specially for CS, it is hard to stop projecting materials during the period of tool switch. Hence, to find an optimized solution, where the total trajectory length and the minimum number of collisions, GA is adopted for this optimization problem.

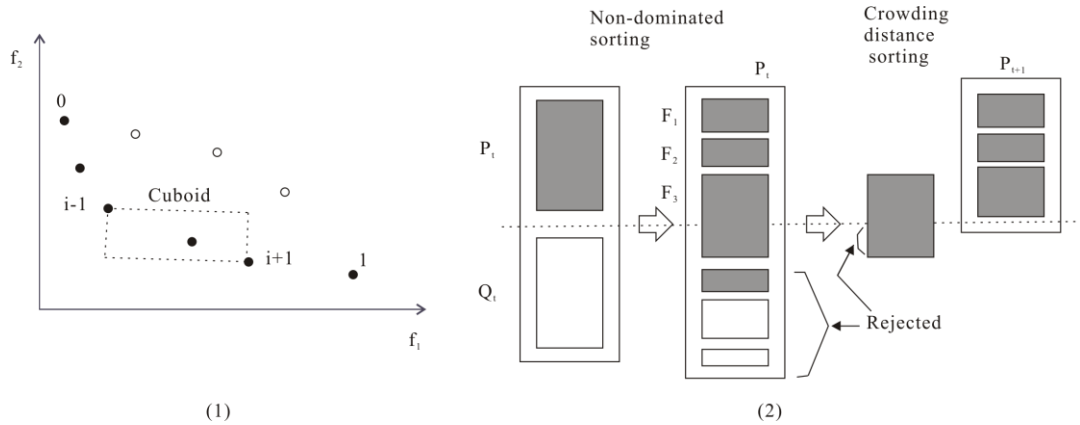

Fig. 3.25. (1). The crowding-distance calculation; (2). The NSGA-II procedure [156].

The Wallacei X plugin in GH is employed with the NSGA-II algorithm schematically represented in Fig. 3.25. (2) [156], because NSGA-II can solve constrained multi-objective problems efficiently. This is a nondominated sorting-based Multi-Objective EA (MOEA), which alleviates the difficulties: 1) High computational complexity of nondominated sorting; 2) Lack of elitism; and 3) the need for specifying a sharing parameter. Fig. 3.25. (1) shows the crowding-distance calculation and points marked in filled circles are solutions of the same non-dominated front.

Since the AM processing sequence in this research is an ordinal sequence, which is similar to constrained traveler salesman problem (TSP) in Fig. 3.26. [155]. Therefore, ordinal representation used in TSP problem is also used for encoding to optimize the processing sequence.

RouteList	FreeList
( )	(A B C D E F)
(1)	(B C D E F)
(1 4)	(A B C D F)
(1 4 3)	(A B C E F)
(1 4 3 1)	(A C D E F)
(1 4 3 1 2)	(A B C D E F)
(1 4 3 1 2 1)	(A B D E F)

Ordered Cities	A	B	C	D	E	F
Representation	1	4	3	1	2	1
Route	A	E	D	B	F	C

$j \in \{1, 2, \ldots, n - i + 1\}$

Fig. 3.26. The ordinal representation for an alternative route in TSP problem [155].

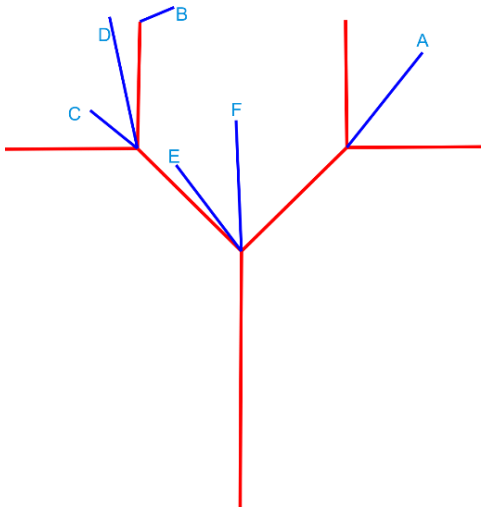

Fig. 3.27. The ordinal branches of group 1 of the tree model.

To explain this process, the first group of the AM subparts from tree model is chosen, and the six branches are ordered from A to F, shown in Fig. 3.27. Two ordinal representations are given as two parents in Fig. 3.28. To produce more variance for the solution space, traditional single-point crossover operation can be operated on the ordinal representations, shown in Fig. 3.29., by randomly choosing a crossover position in a string section and exchange the ordinal codes. Moreover, single-point mutation operation is adopted to change the number of the selected point, shown in Fig. 3.30. In addition, tournament selection operator is applied for the evolutionary searching process of optimization.

Ordinal Rep.	Subparts
()	(A B C D E F)
(1)	(A B C D E F)
(1 1)	(A B C D E F)
(1 1 1)	(A B C D E F)
(1 1 1 1)	(A B C D E F)
(1 1 1 1 1)	(A B C D E F)
(1 1 1 1 1 1)	(A B C D E F)

Subparts	A	B	C	D	E	F
Representation	1	1	1	1	1	1
Sequence of parent 1	A	B	C	D	E	F

(1)

Ordinal rep.	Subparts
()	(A B C D E F)
(4)	(A B C D E F)
(4 2)	(A B C D E F)
(4 2 2)	(A B C D E F)
(4 2 2 1)	(A B C D E F)
(4 2 2 1 1)	(A B C D E F)
(4 2 2 1 1 1)	(A B C D E F)

Subparts	A	B	C	D	E	F
Representation	4	2	2	1	1	1
Sequence of parent 2	D	B	C	A	E	F

(2)

Fig. 3.28. (1) The ordinal representation of parent 1; (2) The ordinal representation of parent 2.

For the crossover operation, the crossover point is chosen at B and the result is shown in Fig. 3.29. The sequences of these two children are DBACEF and ABDCEF, respectively.

Subparts	A	B	C	D	E	F
Rep.parent 1	1	1	1	1	1	1
Rep.parent 2	4	2	2	1	1	1

Subparts	A	B	C	D	E	F
Rep.child 1	1	2	1	1	1	1
Rep.child 2	4	1	2	1	1	1

Fig. 3.29. The crossover operation.

For mutation operation, parent 1 is chosen and mutates it from 1 to 3 at B gene location, shown in Fig. 3.30. The processing sequence is changed from ABCDEF to ADBCEF.

Subparts	A	B	C	D	E	F
Rep.parent 1	1	1	1	1	1	1
Rep.child	1	3	1	1	1	1

Fig. 3.30. The mutation operation.

The objective functions are given below, shown in equation (8), where l_i is the length of processing tool's moving on the bounding box from the processed part to the following AM subpart to be processed. C_i is used to describe whether the collision occurs between nozzle tool or the powder shape model and the existing subparts with initial volume and the processed part during depositing i[th] AM subpart. When the collision exists, C_i is 1, otherwise it is 0.

$$\min \begin{cases} L=\sum_{i=1}^{n} l_i \\ N=\sum_{i=1}^{n} C_i \end{cases} (i=1,...,n) \quad (8)$$

The parameters are set in GH, illustrated in Table 3.3, and the generation size is 20, the generation count is 40 and the population size is 800, the crossover probability is 0.9, mutation probability is 0.3, crossover distribution index is 20, mutation distribution index is 20.

Table 3.3. The parameters of GA.

generation size	generation count	population size	crossover probability	mutation probability	crossover distribution index	mutation distribution index
20	40	800	0.9	0.3	20	20

After the optimization calculation for tree model in GH, the optimized sequence is illustrated for each group, shown in Fig. 3.31.

The final sequence is shown in Fig. 3.32. and the three red subparts indicate the subparts that the processing tool interfere with the processed subparts which need support base. The shortest tool switch trajectories are the lines with colors, shown in Fig. 3.32.

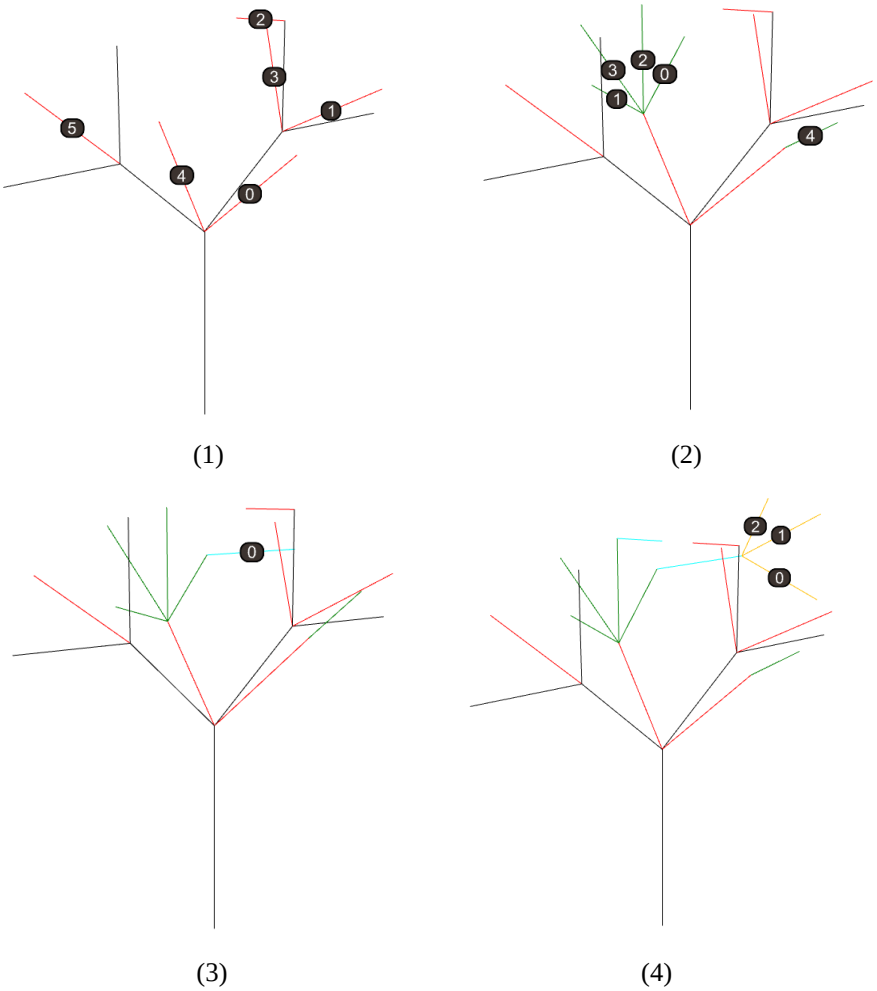

(1) (2)

(3) (4)

Fig. 3.31. The optimal sequence of AM subparts from group 1 to group 4.

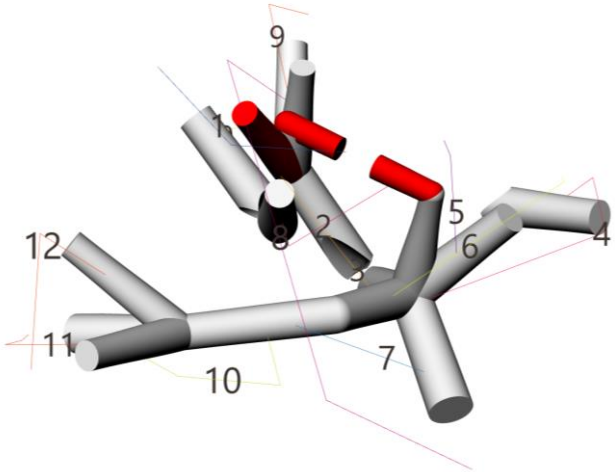

Fig. 3.32. The optimized sequence with tool switch trajectories (the subparts with support are in red).

3.3 The toolpath generation

When the optimal sequence for the AM subparts has been found, the toolpaths have to be defined for each layer of every AM subpart. From the existing methods in the literature mentioned in chapter 2, for planar toolpath, combining different path types can lead to good quality with less fabrication time. However, for rastering/zigzag, very few angles of rastering are adopted. So, the method of mixed toolpath can adopt contour for the first one or two pass trajectories from the boundary of each layer and use contour or other types like rastering (similarly, zigzag), spiral, etc. to fill the inside. In this research, only contour for the two passes outside and rastering for filling the inside are employed and the total toolpath length is optimized by varying the rastering angles with a small step length, 0.1 degree, by a PSO method, illustrated in Fig. 3.33.

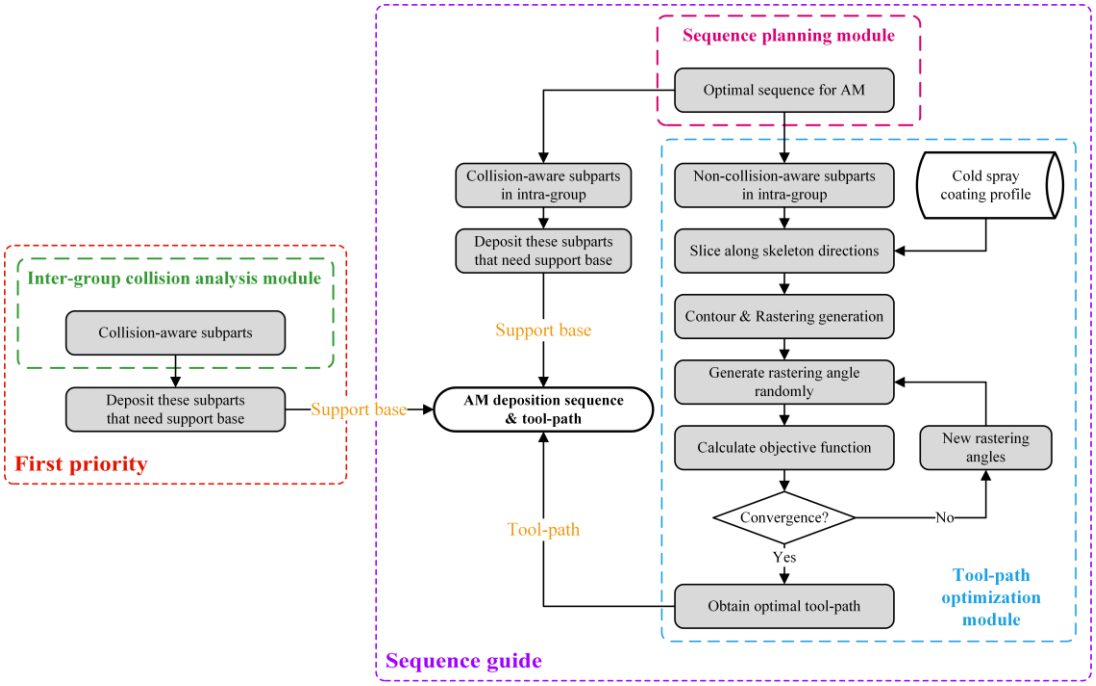

Fig. 3.33. The proposed method for toolpath planning.

The toolpath generation is based on the results, from the previous sections, like the AM subparts and their corresponding skeleton branches, the optimal sequences of the AM subparts without the need of support bases. The subparts are manufactured one by one according to the sequence optimized from the sequence planning module. The slicing process is operated along the skeleton direction evenly. The sliced layers with a fixed thickness referred from the experimental results of cold spray [140]. The layers will be filled by the combined toolpath,

which includes two passes of contour at boundary, and the rastering with different angles inside. The whole toolpath length of one subpart is adopted as the objective to optimize the angle.

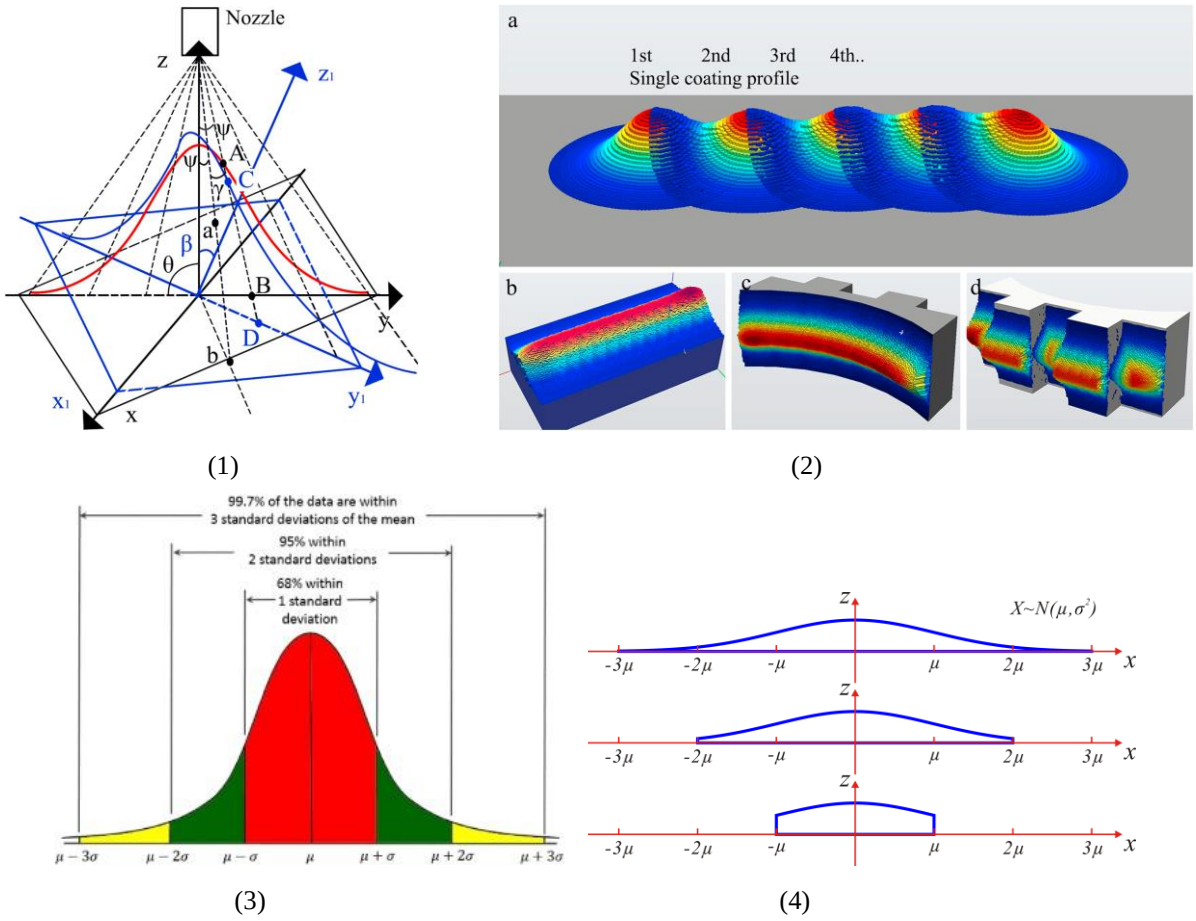

Fig. 3.34. (1). The schematic of single coating profile model; (2). The different kind of overlaps on various surfaces [140]; (3) The Gaussian curve [19]; (4) The Gaussian distribution in GH.

In this research, the cold-spray-based HAM process is considered. The toolpath generation is based on coating profile proposed by Hongjian Wu et al. [140]. The deposition material volume is a three-dimensional geometric model based on Gaussian distribution and the 2D cross-section profile is shown in Fig. 3.34. In Fig. 3.34. (1), a schematic representation of single coating profile model on X-Y plane (red line) and X1-Y1 plane (blue line) is proposed. θ and β are the spray angle on X-Y plane and X1-Y1 plane respectively. a is the angle between Z axis and Z1 axis. ψ is the deflection angle (the angle between Z axis and ab line, as well as AB line). γ is the angle between ab line and AB line. Fig. 3.34. (2) (a) shows discrete single coating profile with overlaps, Fig. 3.34. (2) (b) shows continuous single coating profile on a flat surface, Fig. 3.34. (2) (c) shows continuous single coating profile on a

curved surface, and Fig. 3.34. (2) (d) shows continuous single coating profile on a complex surface. The Gaussian distribution profile (Fig. 3.34. (3)) [19] is generated in GH as in Fig. 3.34. (4). The section of 2μ is used as a reference to define the layer thickness and the hatching space.

The idea is to use the adopted experimental deposition cross-section profile to sweep along the generated toolpath to form 3D volume for the AM processing. The sweeping profile along the toolpath. For each layer, the process starts from outside to inside and the first two contour trajectories are used for the layer boundary to guarantee its accuracy. Contour and raster which are commonly used, so they are taken for the mixed toolpath. The contour is for the outside, and the raster is filling inside the boundaries of two contour passes, shown in Fig. 3.35. The objective is to minimize the length of the total toolpaths for each subpart. The raster angles are optimized for all the layers of the AM subpart with a step length of 0.1 degree for rastering, because of the limitation of robot move precision. The following section introduces the PSO implementation for toolpath length optimization.

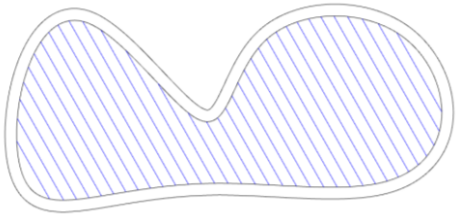

Fig. 3.35. The toolpath strategy: the contour with rastering.

3.3.1 Optimize the toolpath

The optimization method is the same as for the initial volume, which is PSO algorithm. For the encoding, each layer is one chromosome gene, so one subpart is a chromosome, shown in Table 3.3.

Table 3.4. The encoding of one subpart.

Layer	1	2	3	4	5	6	7	....	...	n
Angle	α_1	α_2	α_3	α_4	α_5	α_6	α_7	....	...	α_n

In the optimization process, the objective function is the total toolpath length, shown in equation (9):

Min: $L = \sum_{i=1}^{n} l_i^{\alpha_j}$ (9)

$\alpha \in [0°, 180°)$

where, L is the total length of all toolpaths; α is the rastering angle and $l_i^{\alpha_j}$ is i[th] layer's toolpath length with a rastering filling angle of α_j.

To illustrate the method, the tree structure CAD model used above is again employed. In the implementation, a PSO plugin Silvereye is also used the same as for initial volume optimization and the parameters are set as in Table 3.5.

Table 3.5. The parameters set in Silvereye.

Parameter	Swarm size	Iteration	Max. Velocity
Value	20	1000	0.2

After the calculation of 1000 iterations, the corresponding shortest length of each iteration is shown as in Fig. 3.36.

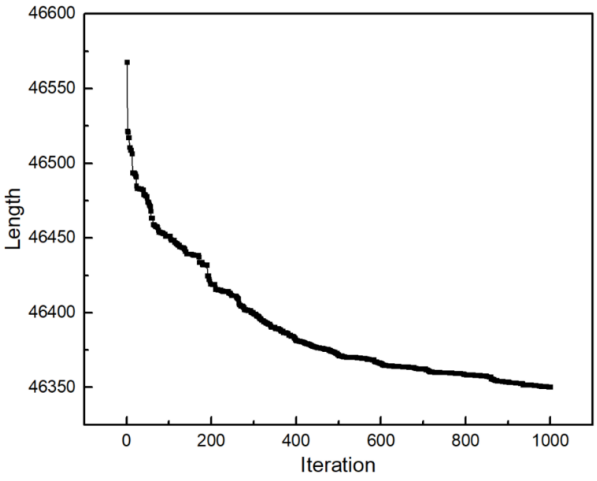

Fig. 3.36. The shortest toolpath length of each iteration.

For each subpart, the layers are obtained by the normal plane which is perpendicular to the corresponding skeleton cut evenly according to layer thickness obtained from the Gaussian model, shown in Fig. 3.34. The process starts to deposit materials onto the initial volume with the optimal sequence obtained by using the methods proposed above. For the tree model, the first subpart of the first group is chosen for demonstration, illustrated in Fig. 3.37 (1). One layer is selected to show the details of toolpath, shown in Fig. 3.37. (2), (3). For the layer with the same cross-section, the angles are the same (the white cylinder), shown in Fig. 3.37. (2). Fig. 3.37. (4), (5) show several layers of the first subpart of tree model. The

finished result for all the AM subparts (except the three subparts which need support bases, shown in Fig. 3.31) is illustrated in Fig. 3.38.

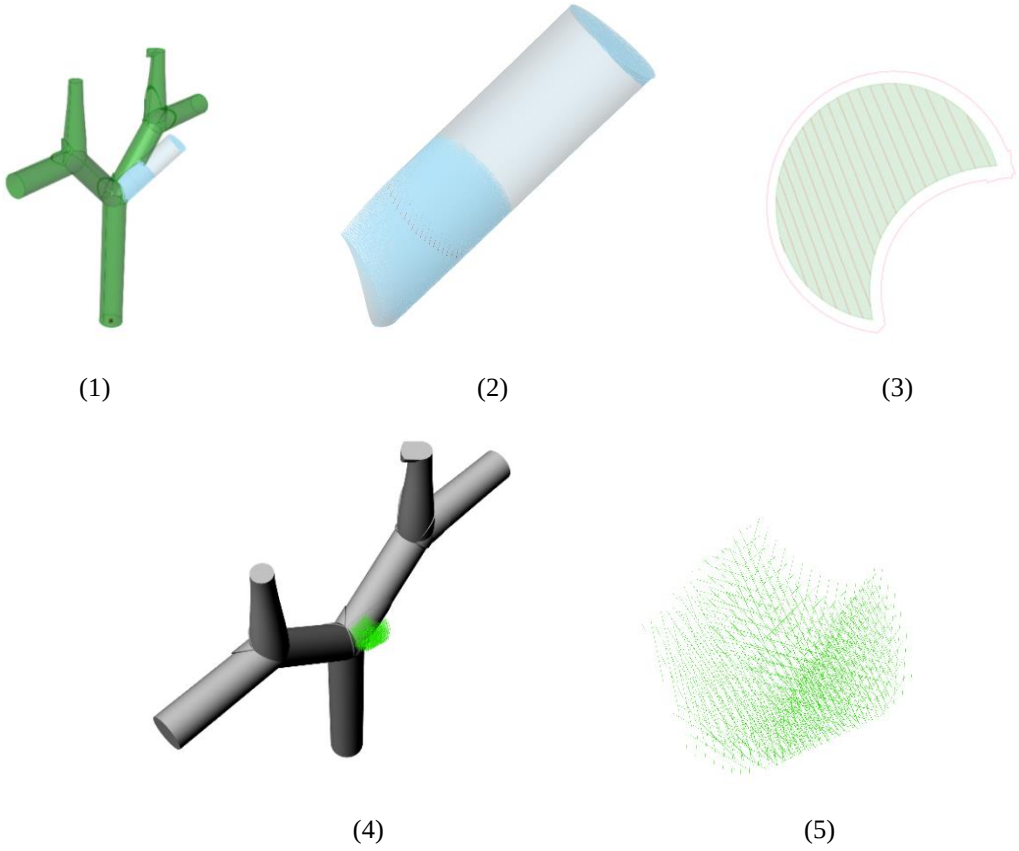

Fig. 3.37. (1). The fist subparts with the path; (2), (3). One layer is selected to show the details of toolpath; (4), (5). Several layers of the first subpart.

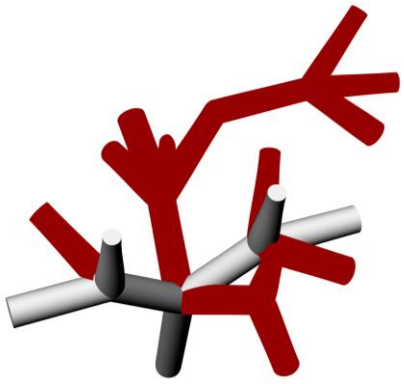

Fig. 3.38. The toolpath of the AM subparts that do not need support.

In conclusion, in this chapter, three methods have been proposed to solve the three corresponding research questions defined in chapter 2. All of these three solutions for initial volume, sequence planning and toolpath planning are implemented with one complex tree model that has 25 branches. In the following chapter, three case studies are operated to show the application of the proposed methods and also to show their relevance and their limits.

Chapter 4 Case Studies

To verify the three methods proposed in the previous chapter, three examples are adopted at different complexity levels to test the implemented algorithms. This first model is quite simple to show the basic steps of the proposed methods, illustrated in Fig. 4.1. (1). The second one is selected from a published paper [21], illustrated in Fig. 4.1. (2), to prove the benefits of the proposed methods. The third one is a part of the planes, which is complex and challenging to manufacture because of collisions and the lack of fabrication bases, illustrated in Fig. 4.1. (3). The following sections will show the details and the related results of each case to demonstrate the advantages and limitations of the methods.

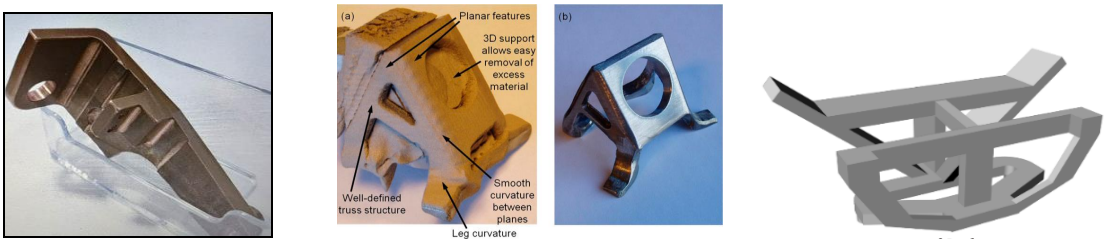

(1) (2) (3)

Fig. 4.1. The three cases adopted for case studies.

4.1 Case 1

4.1.1 The initial volume generation and optimization

The three cases are first used to verify the method to generate and optimize initial volume. This method is the same as in chapter three. The skeleton is first prepared for decomposing the CAD model into original subparts and the skeleton into branches. Then based on the skeleton branches and the volumes of the subparts, the adjacent and coplanar branch set with the largest volume sum of the corresponding subparts is selected manually in GH. After obtaining the optimal branch set, the size of the cross-section will be optimized by calculating the least material change rate, and the optimal initial volume will be finally determined automatically in GH. For the first case, the details of each step for initial volume generation and optimization are as follows.

4.1.1.1 CAD model & skeleton generation

The first case is shown in Fig. 4.1. (1), and its CAD model is illustrated in Fig. 4.2. (1). The CAD model is modified to make it simple, filling the small hole, shown in Fig. 4.2. (2),

to obtain a skeleton in the following step. The CAD model is generated in the software called Rhino, based on the medial axis and cross-sections.

(1) (2)

Fig. 4.2. (1). The CAD model with hole; (2). The CAD model without hole.

The skeleton can be obtained from MATLAB coding, and the results are shown in Fig. 4.3, but it is made of voxels, so it is not smooth and cannot be used directly. Fig. 4.3. (1) shows the skeleton of the CAD model with a hole after the voxelization by MATLAB code. Fig. 4.3. (2) is the CAD model without a hole. In this research, the medial axis is shown in Fig. 4.3. (3), which is used for generating the CAD model is adopted to replace the voxel medial axis for the next steps of finding an optimal initial volume.

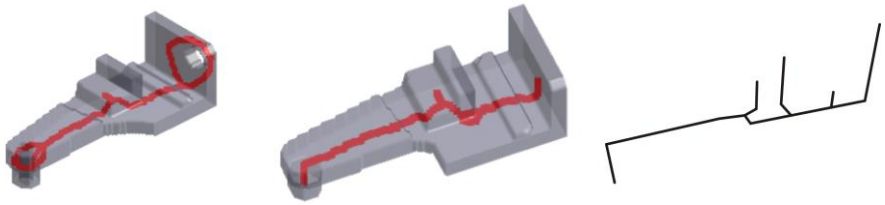

(1) (2) (3)

Fig. 4.3. (1). The voxelization and voxel skeleton of case 1 with hole; (2). The voxelization and voxel skeleton of case 1 without hole; (3). The media axis used to generate the CAD model.

4.1.1.2 Generate subparts and determine the optimal branch set

The original subparts are obtained by decomposing the CAD model based on the joint points of branches, and the decomposition result of case 1 is illustrated in Fig. 4.4 (1). And the optimal branch set is chosen shown in Fig. 4.4 (2).

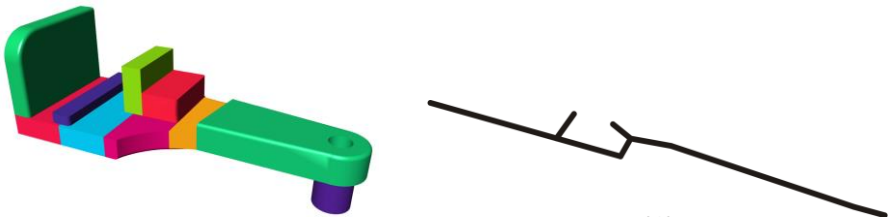

(1) (2)

Fig. 4.4. (1) All the original subparts of case 1; (2) The optimal branch set.

4.1.1.3 Generate and optimize initial volumes

To obtain the optimal initial volume, the first step is to get the adjacent and coplanar branch set, shown in Fig. 4.4 (2) with the largest volume sum of corresponding subparts. It is selected manually according to the constraints mentioned above. The final objective is to obtain an initial volume with the least material change rate calculated by the PSO algorithm in one plugin of GH, Silvereye. The parameters are set the same as for the tree model, except that the iteration is 50. After calculation, the best result of each iteration is achieved, shown in Fig. 4.5.

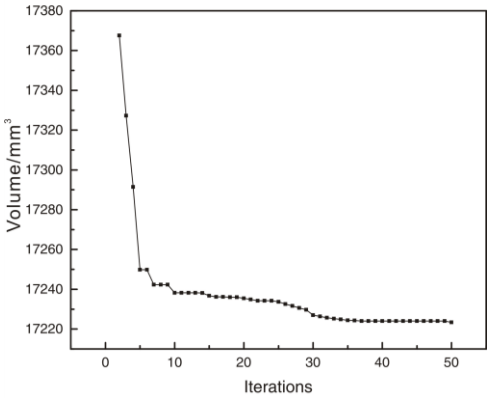

Fig. 4.5. The best result of each iteration in Silvereye.

The optimal initial volume considering the criteria as mentioned earlier is achieved, shown in Fig. 4.6. The method uses 2D cross-sections to sweep along the branch set to generate 3D volume, shown in Fig. 4.6 (1). To make the whole process simple, the cross-section in this case study is the circle, and the balls are employed as joints of the adjacent subparts, shown in Fig. 4.6 (1). However, it needs to cut the directly sweeping result by two planes parallel to the plane generated by the adopted coplanar branch set. The result is illustrated in Fig. 4.6 (2). At last, the modified optimal initial volume of case 1 is adapted, shown in Fig. 4.6 (3) by Boolean intersection operation with the original CAD model.

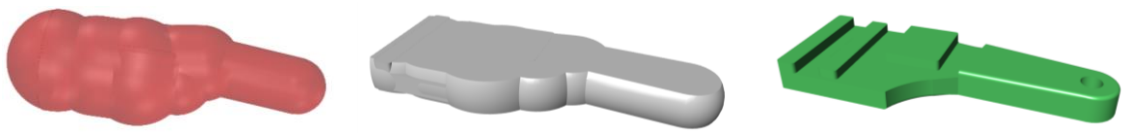

(1) (2) (3)

Fig. 4.6. The result of initial volume: (1). The direct sweeping result; (2). The optimal initial volume cut by two parallel planes; (3). The modified initial volume.

4.1.2 The sequence planning for the AM subparts

After obtaining the initial volume, there are still some volumes left, illustrated in Fig. 4.7. (2) (the volume in green is initial volume), and based on the adjacent relation, these remaining volumes can be classified into 1 group, shown in Fig. 4.7. (1), (2). Therefore, the sequence of each AM subpart (obtained by decomposing the remaining volume), is necessary to be optimized to save time and material during the CS.

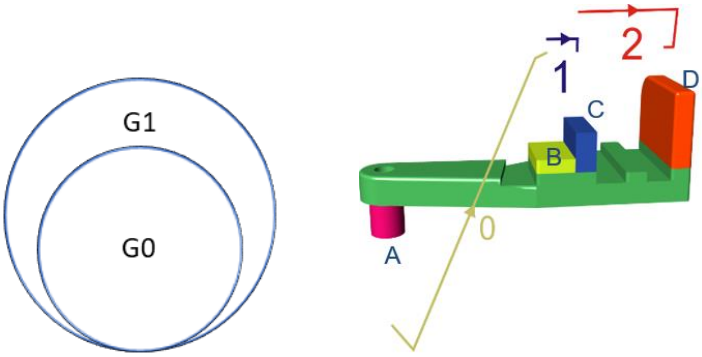

(1) (2)

Fig. 4.7. (1). The only one group of AM subparts; (2). The optimal processing sequence with tool switch trajectories.

The sequence planning for the case study is also similar to the tree model, and the optimization method is the NSGA-II algorithm. The objective functions are the length of the tool switch trajectory and the number of collisions. The parameters set for optimization calculation, in this case, are the same as for the tree model, shown in table 3.2. These parameters are set in the plugin of GH, Wallacei X: the generation size is 20; generation count is 40; the population size is 800; the crossover probability is 0.9; mutation probability is 0.3; crossover distribution index is 20; mutation distribution index is 20. After the calculation in GH, the result is obtained.

This case is simple and only has one group, illustrated in Fig. 4.7. (1), including four subparts from A to D (the initial volume is green), shown in Fig. 4.7. (2). The tool switch trajectories are the lines with colors, and the numbers show the tool switch order, illustrated in Fig. 4.7. (2).

4.1.3 The toolpath planning

Based on the optimal sequence of AM subparts, for the AM subparts which do not need support bases, the shortest toolpath for each subpart is necessary to be determined by

changing the rastering angles for each layer. The evolutionary optimization algorithm PSO is adopted, and the calculation is operated in the plugin, Silvereye. The parameters are set the same as for the tree model.

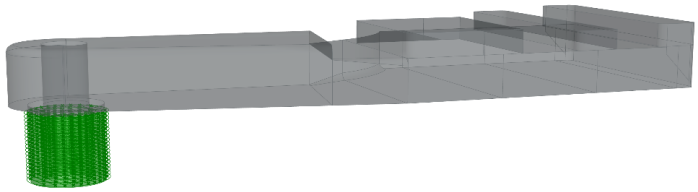

(1)

(2)

Fig. 4.8. (1). The toolpath of subpart 1; (2). One layer of toolpath of subpart 1.

Because the cross-sections are even for the subparts, these angles are the same for all layers and only one angle for a whole subpart, shown in Fig. 4.8. and Fig. 4.9. For the first case, the shapes of subparts include cylinder, the first AM subpart, shown in Fig. 4.8 (2), and cuboid, the second AM subpart, in Fig. 4.9 (2).

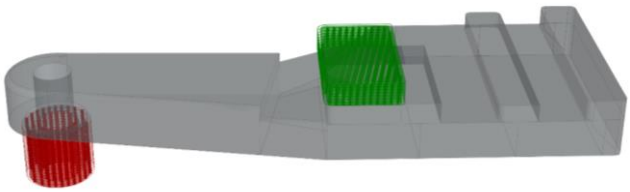

(1)

(2)

Fig. 4.9. (1). The toolpath of subpart 2; (2). One layer of toolpath of subpart 2.

Since this case is simple and no collision exists, all the four AM subparts need to be considered to optimize their toolpath by the proposed method. For the other two AM subparts,

the process is similar, and the optimal toolpath for all the four AM subparts is shown in Fig. 4.10.

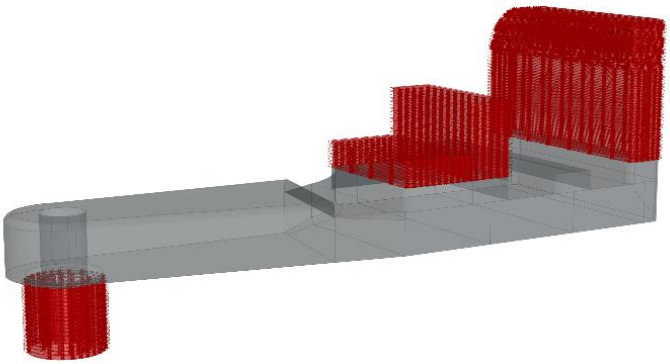

Fig. 4.10. The toolpath of all the subparts.

4.2 Case 2

This model is from the existing research, a bracket manufactured with a cold spray process shown in Fig. 4.1 (2) [21]. The whole model is built from scratch in their method, which needs an extensive support structure and causes many wasted materials.

4.2.1 The initial volume generation and optimization

However, suppose this case adopts the methods proposed in this thesis. In that case, a large initial volume can be fabricated by traditional economic methods, so only very few remaining volumes, the small complex structures like the four feet of this bracket, need to deposit material onto the initial volume. Hence, the employment of initial volume can save much material and time.

To obtain an optimal initial volume, the skeleton is first prepared for decomposing the model into original subparts and the skeleton into branches. Then, based on the skeleton branches and the volumes of the original subparts, the adjacent and coplanar branch set with the largest volume sum of the corresponding original subparts is selected manually in GH. After obtaining the optimal branch set, the size of the cross-section will be optimized by the least material change rate, and the optimal initial volume will be finally determined automatically in GH. For the second case, the details of each step for initial volume generation and optimization are as follows.

4.2.1.1 CAD model & skeleton generation

The CAD model of the bracket is made in Rhino, shown in Fig. 4.11, which is generated similarly as the first case by sweeping cross-sections along the medial axis, shown in Fig. 4.12 (2).

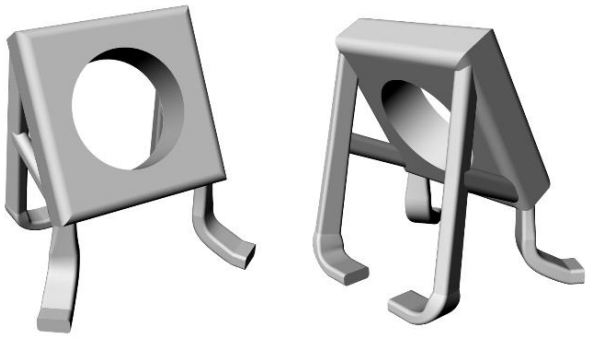

(1) (2)

Fig. 4.11. The CAD model of bracket in Rhino.

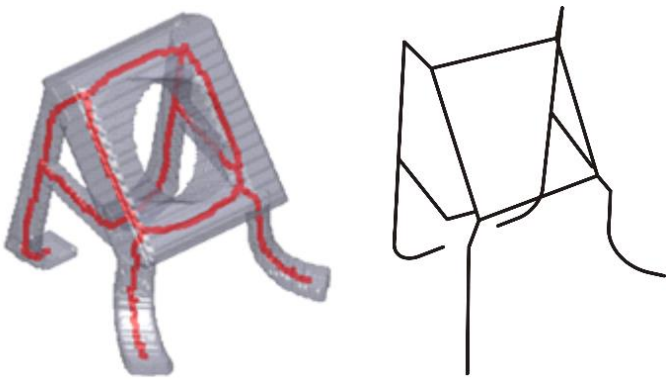

(1) (2)

Fig. 4.12. (1). The voxelization and voxel skeleton; (2). The medial axis used to generate the CAD model.

Based on the CAD model of the bracket, the voxelization can be obtained in MATLAB and then the voxel skeleton is generated, illustrated in Fig. 4.12. (1). In this research, the medial axis, shown in Fig. 4.12. (2), used for generating CAD model, is adopted to replace the voxel skeleton for the following steps.

4.2.1.2 Generate subparts and determine the optimal branch set

The original subparts can be decided by the branches based on the joint points, similarly with the tree model and case 1, and the original subparts of the bracket are shown in Fig. 4.13 (1), (2). And the optimal branch set is chosen, shown in Fig. 4.13 (3).

(1) (2) (3)

Fig. 4.13. (1), (2). The original subparts of bracket; (3). The optimal branch set.

4.2.1.3 Generate and optimize initial volumes

To obtain the optimal initial volume, the first step is to get the adjacent and coplanar branch set, shown in Fig. 4.13 (3). with the largest volume of corresponding subparts. The final objective is to obtain an initial volume with the least material change rate calculated by the PSO algorithm in Silvereye. The parameters are set the same as for the tree model, but the iteration is 100. After calculation, the best result of each iteration is achieved, shown in Fig. 4.14.

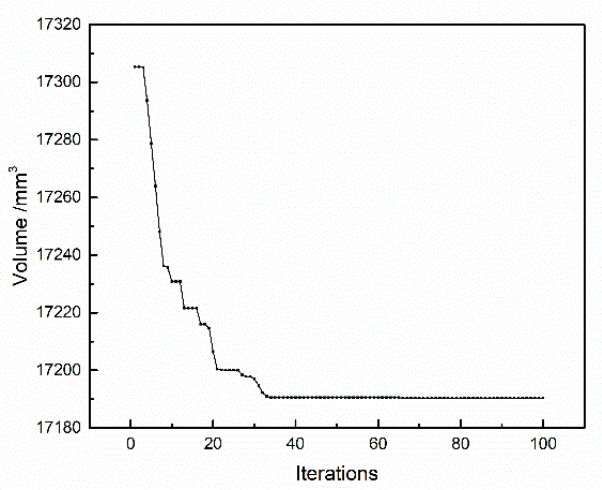

Fig. 4.14. The best result of each iteration in Silvereye.

The optimal initial volume considering the criteria mentioned above is achieved, shown in Fig. 4.15. Since the method is using 2D cross-sections to sweep the branch set, the 3D volume is generated. The cross-section in this case study is the circle, and the balls are used as

joints of the adjacent branches, shown in Fig. 4.15. (1). However, it needs to cut the directly sweeping result by two planes that are parallel to the plane generated by the selected branch set, and the result is illustrated in Fig. 4.15. (2). At last, the modified optimal initial volume of case 2 is adapted, illustrated in Fig. 4.15. (3), by Boolean intersection operation with the original CAD model.

(1) (2) (3)

Fig. 4.15. (1). The directly sweeping result; (2). The optimal initial volume cut by two parallel planes; (3). The modified optimal initial volume.

4.2.2 The sequence planning for the AM subparts

Except for the initial volume, there are still some volumes left illustrated in Fig. 4.16. (1), and based on the adjacent relation, these volumes can be decomposed into AM subparts and classified into three groups shown in Fig. 4.16. (2), (3).

The sequence planning is similar to the tree model and case 1, and the optimization method is also the NSGA-II algorithm. The objective functions are the length of the tool switch trajectory and the number of collisions. The parameters set for optimization calculation are the same as for the tree model and case 1, shown in table 3.2. The parameters of the Wallacei X plugin in GH are as follows: the generation size is 20; generation count is 40; the population size is 800; the crossover probability is 0.9; mutation probability is 0.3; crossover distribution index is 20; mutation distribution index is 20.

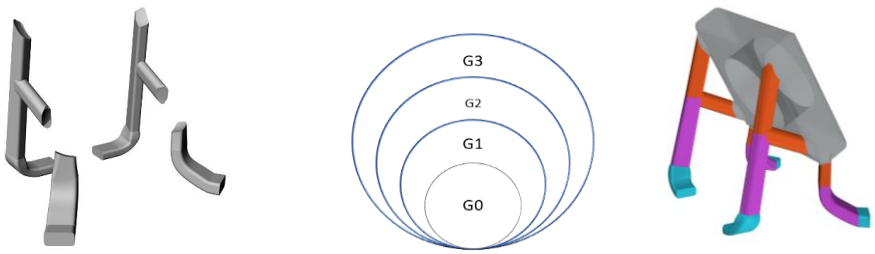

(1) (2) (3)

Fig. 4.16. (1). The remaining volumes; (2), (3). The three classified groups of case 2.

After the optimization calculation, the three groups of AM subparts and their sequences are illustrated in Fig. 4.17. (1), (2), (3). Fig. 4.17. (4) shows where collisions exist, and the red subparts collide with the CS gun.

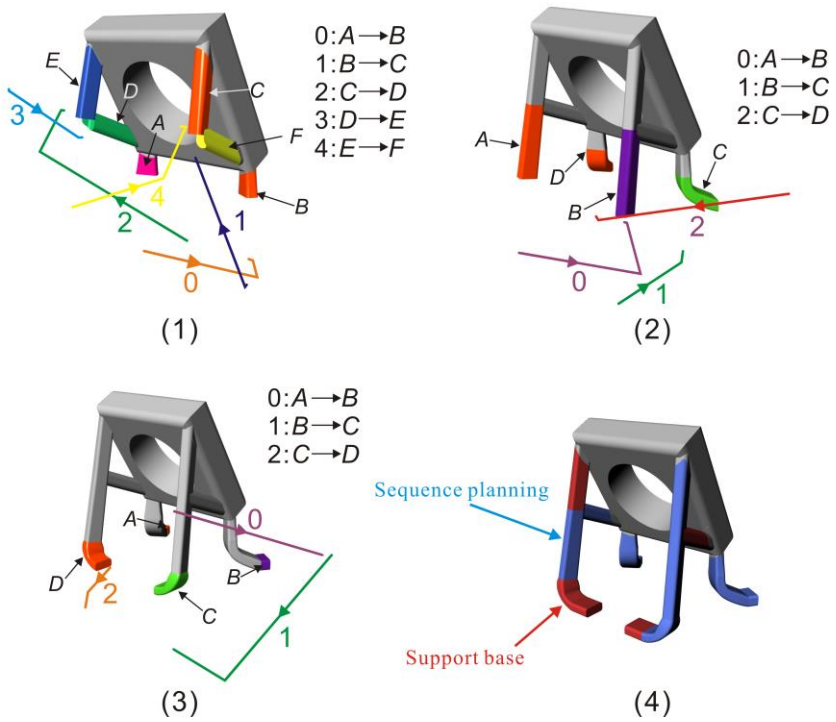

Fig. 4.17. (1), (2), (3). The sequence of three groups; (4). The three red subparts have collisions.

Moreover, the collision of group 1 is taken as an example, shown in Fig. 4.18., which is a soft collision. Here, the soft collision means that the collision happens because the powder beam (purple in Fig. 4.18. (b)) is blocked, and the material deposition is not entirely achieved, but the gun has not touched the entity.

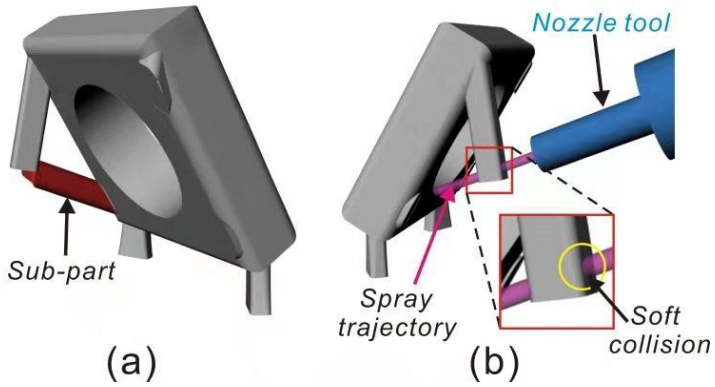

Fig. 4.18. One example of soft collision in case 2.

4.2.3 The toolpath planning

Based on each group's sequence planning result, the subparts that have no collisions will deposit material with an optimal toolpath. The first subpart is chosen as an example, and one layer is selected to show the details, illustrated in Fig. 4.19.

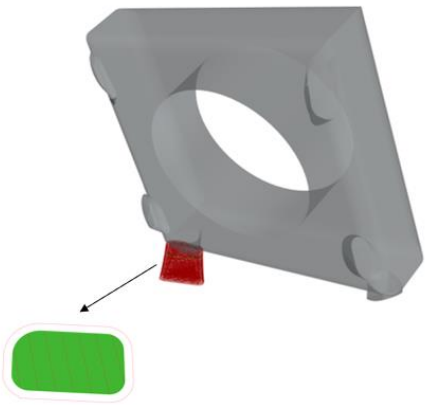

Fig. 4.19. The toolpath of subpart 1 and one layer of toolpath.

Fig. 4.20. The toolpath of all subparts that do not have collisions in case 2.

Moreover, in this case, three red subparts have collisions, shown in Fig. 4.17. (4). These three subparts are not considered for optimizing the toolpath, so only other AM subparts are manufactured by this method. The final optimal toolpath of all these subparts is illustrated in Fig. 4.20.

4.3 Case 3

This model is more complex compared with the two cases mentioned above. All of the three proposed methods will be verified with this case as well.

4.3.1 The initial volume generation and optimization

To obtain an optimal initial volume, the skeleton is first prepared for decomposing the model into original subparts and the skeleton into branches. Then based on the skeleton branches and the volumes of the subparts, the adjacent and coplanar branch set with the largest volume sum of the corresponding original subparts is selected in GH. After obtaining the optimal branch set, the size of the cross-section will be optimized by the least material change rate, and the optimal initial volume will be finally determined in GH. For the third case, the details of each step for initial volume generation and optimization are as follows.

4.3.1.1 CAD model & skeleton generation

This model is more complex with many branches, shown in Fig. 4.21. It is modeled in Rhino by sweeping cross-sections along the medial axis, shown in Fig. 4.22 (2).

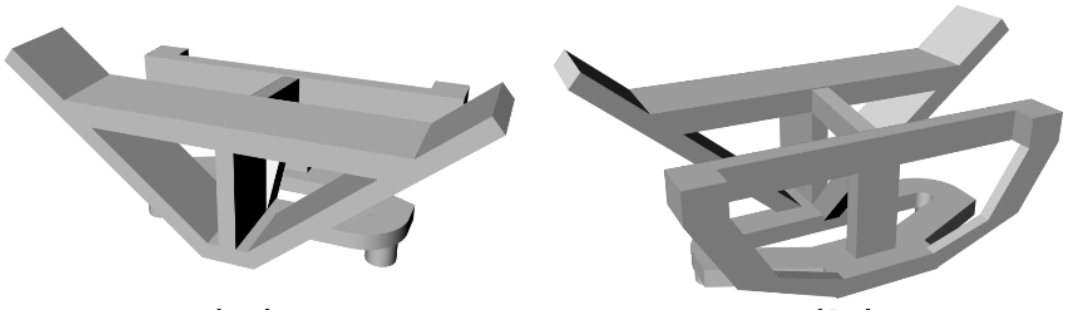

(1) (2)

Fig. 4.21. The CAD model of case 3.

Based on the CAD model, the voxelization and generation of the skeleton are then operated based on the method as mentioned earlier in MATLAB, illustrated in Fig. 4.22. (1). In this research, the medial axis, shown in Fig. 4.22. (2), used for generating the CAD model, is adopted to replace the voxel skeleton for the next steps.

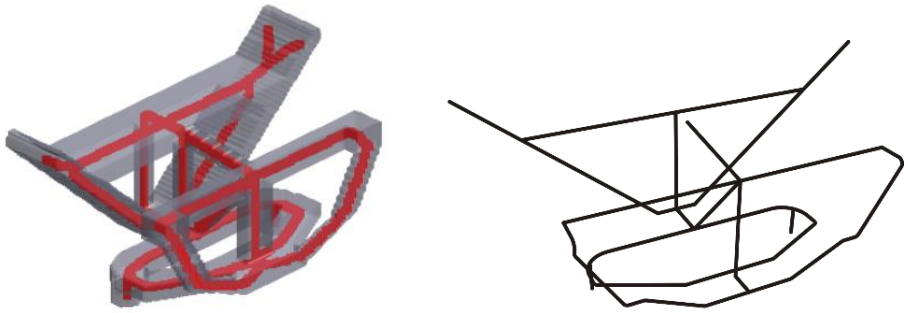

(1) (2)

Fig. 4.22. (1) The voxel skeleton in MATLAB; (2) The medial axis used to generate the CAD model.

4.3.1.2 Generate subparts and determine the optimal branch set

The original subparts can be defined by the branches based on the joint points of the skeleton, similar to the tree model and the previous two cases, and the original subparts are obtained, shown in Fig. 4.23 (1). And the optimal branch set is shown in Fig. 4.23 (2).

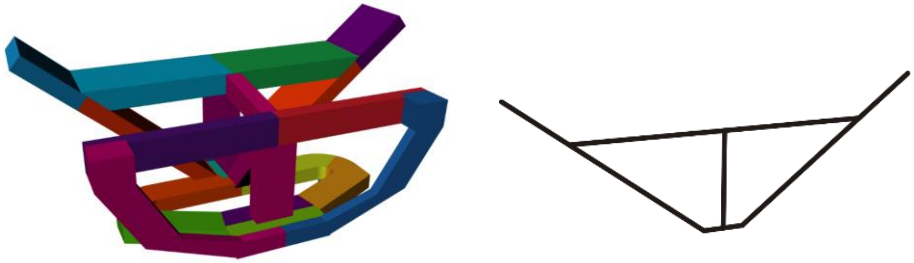

(1) (2)

Fig. 4.23. (1) The original subparts of case 3; (2) The optimal branch set.

4.3.1.4 Generate and optimize initial volumes

The optimization calculation of initial volume considers the constraints mentioned above and the material change rate as the objective function is calculated using the PSO algorithm in Silvereye, one plugin of Grasshopper. The result of each iteration is achieved, shown in Fig. 4.24. The manually selected branch set is shown in Fig. 4.23. (2). for the first step of optimization, and in the second step, the least material change rate of each iteration is obtained, and the result is illustrated in Fig. 4.24.

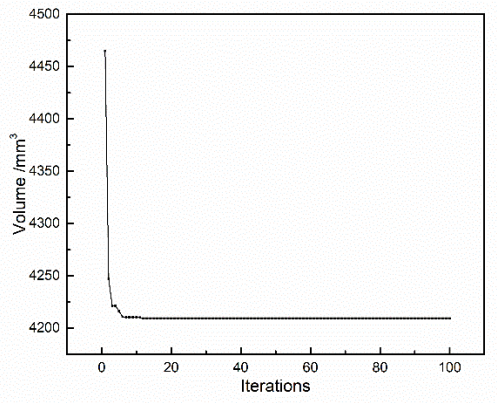

Fig. 4.24. The best result of each iteration in Silvereye.

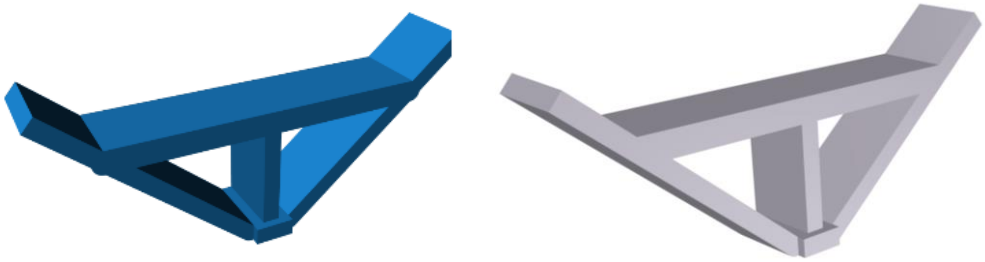

(1) (2)

Fig. 4.25. (1). The original optimal initial volume of case 3; (2). The modified initial volume.

The cross-section in this case study is rectangular so that the initial volume can be obtained directly, illustrated in Fig. 4.25 (1). After the Boolean intersection operation and the adaptation of the film to add onto the original initial volume, the modified initial volume is obtained, illustrated in Fig. 4.25 (2).

4.3.2 The sequence planning for the AM subparts

Except for the initial volume, there are still some volumes left, illustrated in Fig. 4.26. (1) (the volume in grey is the modified optimal initial volume), and based on the adjacent relations, these volumes can be decomposed into AM subparts and classified into three groups, shown in Fig. 4.26. (1), (2).

The sequence planning for the case study is also similar to the tree model and the previous two cases, and the optimization method is the NSGA-II algorithm. The objective functions are the length of the tool switch trajectory and the number of collisions. The parameters set for optimization calculation, in this case, are the same as in table 3.2. These parameters are set in Wallacei X plugin of GH: the generation size is 20; generation count is 40; the population size is 800; the crossover probability is 0.9; mutation probability is 0.3; crossover distribution index is 20; mutation distribution index is 20. After the calculation in GH, the result is obtained.

The third case is very complicated since the decomposition based on the joint point of the skeleton may cause a large number of subparts. To make it simpler, some subparts are combined to reduce the number of AM subparts. This case has three groups of subparts, shown in Fig. 4.26. (1), (2), and the third group (the red subpart in Fig. 4.26. (1)) needs support base.

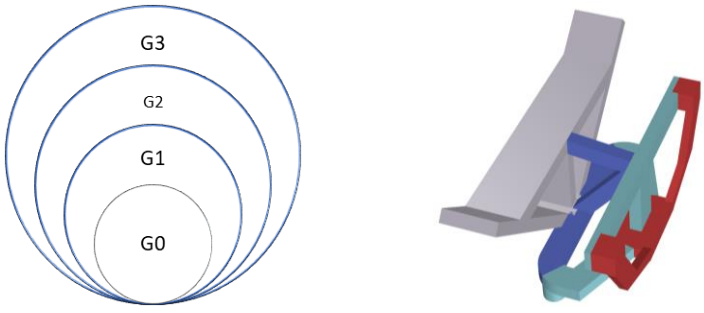

(1) (2)

Fig. 4.26. The AM subparts classified into three groups based on adjacent relations

After calculation, the sequence of each group is as follows in Fig. 4.27., including two groups because the third group is only one subpart and needs support. Moreover, there is one soft collision in the first group, and the details of this collision are illustrated in Fig. 4.28.

After calculation, the sequence of each group is as follows in Fig. 4.27., including two groups because the third group is only one subpart and needs support. Moreover, there is one soft collision in the first group, and the details of this collision are illustrated in Fig. 4.28.

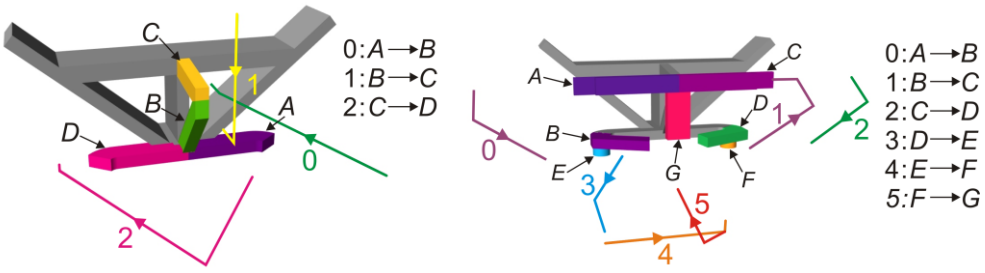

(1) (2)

Fig. 4.27. The sequence of case 3: (1) group 1; (2) group 2.

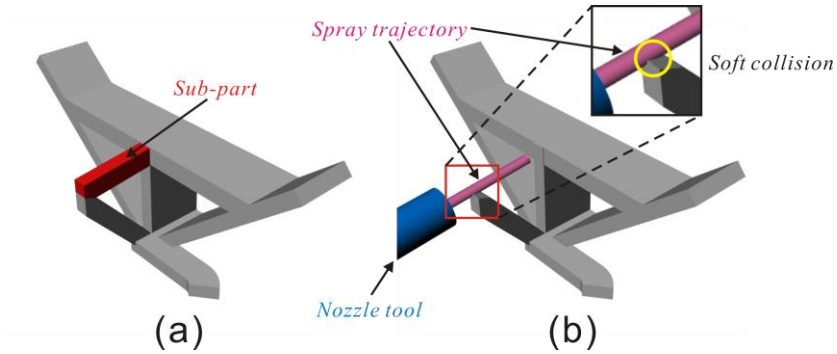

Fig. 4.28. The soft collision in case 3.

4.3.3 The path planning

Based on the optimal sequence of each group, it needs to calculate the best toolpath for the AM subparts which have no collisions. This case also has three groups (illustrated in Fig. 4.26.) as in case 2, and the first subpart in the first group is taken as an example to show the toolpath optimization result, illustrated in Fig. 4.29.

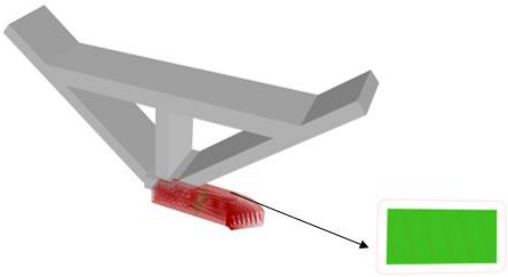

Fig. 4.29. The first AM subpart in group 1 and one layer of the first AM subpart.

All of the AM subparts with no collisions have obtained their corresponding optimal toolpath by optimizing the rastering angles, shown in Fig. 4.30. (1). All the subparts which need support bases are the red ones, shown in Fig. 4.30. (2).

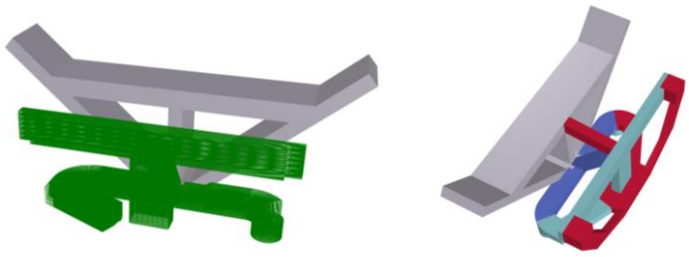

(1) (2)

Fig. 4.30. (1). The toolpath of all subparts which do not have collisions in case 3; (2). The subparts that have collisions

From the case studies, it can be seen that the proposed methods for the optimization of the initial volume, the sequences for the AM subparts, and toolpath optimization can be adopted to save material and fabrication time.

Due to the impact of the virus crisis, only the experiment for case 1 is operated in the CSAM platform at UTBM. The printing result without post-finishing is shown in Fig. 4.31.

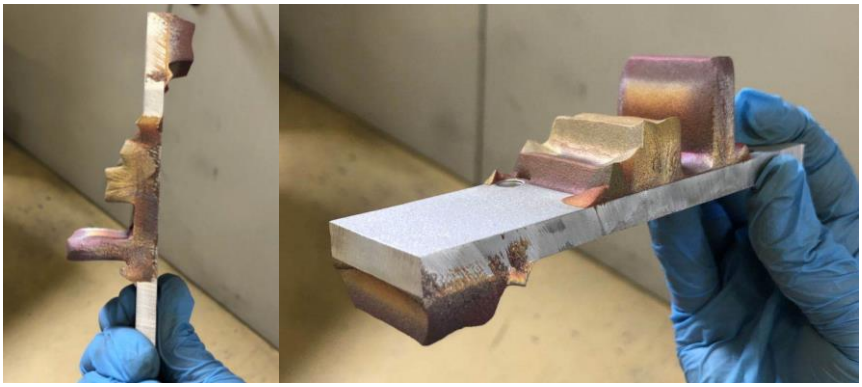

Fig. 4.31. The experiment for Case 1 based on CSAM platform at UTBM.

This chapter employs three cases at different complexity levels to show the three methods proposed for answering the research questions and solving the industrial problems mentioned in chapter 2. Even though the proposed algorithm can work for the three cases, some limitations still need to be improved.

The next chapter comes to an end of this thesis, and the conclusions for the whole work are given, considering the contributions and limitations. Based on the limitations, some future perspectives are proposed to improve the thesis work.

Chapter 5 - Conclusions and Future Work

5.1 The conclusions of this thesis

The primary research of this thesis is on process planning for the AM module of multi-axis HAM, including the generation and optimization of the initial volume, the sequence planning for the AM subpart decomposed from the remaining volumes, and the toolpath optimization. The research takes Cold Spray as an example of AM process, combined with CNC to implement the proposed methods for HAM. This approach can be extended to other multi-axis additive processes like DED, WAAM, etc. Three cases are adopted by MATLAB and Rhino/ Grasshopper to verify the proposed methods. The main contributions of this thesis are as follows:

1. A new method is proposed to generate and optimize the initial volume of a CAD model. The manufacturing process starts from an existing material (i.e., the initial volume). Therefore, much time and material during the whole process can be saved. The initial volume candidates can be generated through the optimal skeleton branch set and the related cross-sections and be optimized by evolutionary optimization algorithms in Grasshopper.

2. A new method is developed to optimize the sequence of AM subparts. Sequence planning is the core stage of this research for process planning because the CAD model is fabricated from an initial volume and some remaining volumes, which are decomposed into AM subparts based on the skeleton. This method is mainly based on classifying the AM subparts to make the previous group act as the support. And the tools change their directions/orientations based on the branch vectors of the skeleton.

3. A new method is improved to optimize toolpath planning. Toolpath is essential for both AM and SM. Because AM and SM have similar path categories, the path planning method can be used for HAM. In this research, the proposed method is the combination of contour and rastering, and the whole toolpath length of one subpart is considered a primary criterion to find an optimized rastering angle for each layer.

However, there are still some limitations and some future work needs to be considered:

1. The skeleton generation method needs to be improved. Skeleton can influence the whole research greatly, so it is crucial to obtain a smoother and more precise skeleton. In this research, the medial axis used to generate a CAD model is adopted to replace the voxel skeleton.

2. The initial volume adaption has not been fully considered. For the optimized result of the initial volume, it is not always expected, and sometimes there are isolated small isles or thin films. In this research, not many details are considered on initial volume adaptation.

3. Decomposition method needs to be improved. Decomposition is essential for initial volume generation and sequence planning, but this method decomposes the model based on the joint of skeleton branches so that the whole CAD model could be decomposed into too many pieces.

4. No consideration of solutions for reducing collisions by decomposing subparts and iteration during the sequence planning. Collisions are very tiresome in the SM and multi-axis AM, but this research only classifies the subparts and uses a tool model to distinguish when collisions occur and use bounding box when switching CS gun.

5. This research can be used only for AM technologies capable of multi-axis manufacturing, including CS, DED, WAAM, etc.

6. This research is also incapable of very complex components whose skeletons are very complicated, like lattice structure.

5.2 The perspectives of thesis work

From the analysis above, there are some limitations of this research. However, some perspectives are given as follows.

1. The methods can be used for other multi-axis AM processes: WAAM, DED.

2. The methods can be introduced to the remanufacturing processing chain.

3. The profile-based toolpath planning can be extended to SM processes.

4. To consider the combination of design for HAM and process planning for HAM. Process planning is only one stage of the product life cycle. CAPP and CAD are mutually influenced by each other, and very two essential steps; consequently, the combination of them is necessary.

Appendix

The visual programming of the tree model in GH

1. The initial volume optimization

The modeling of tree

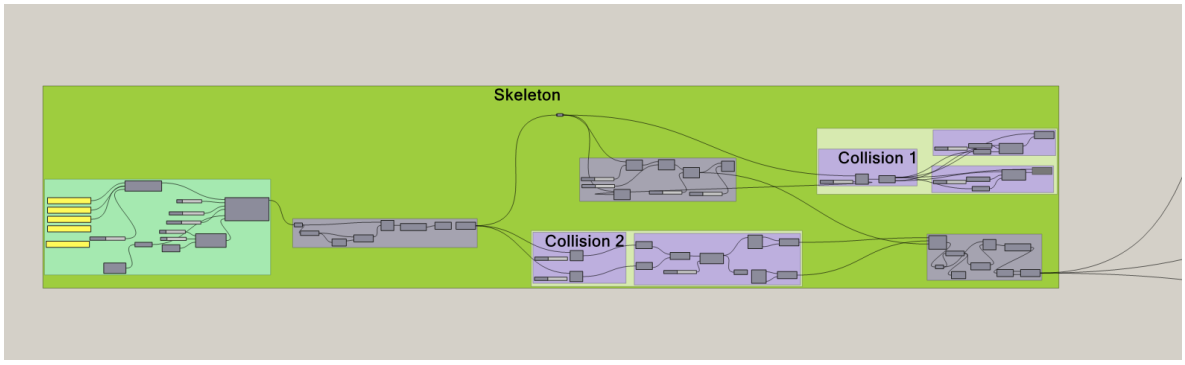

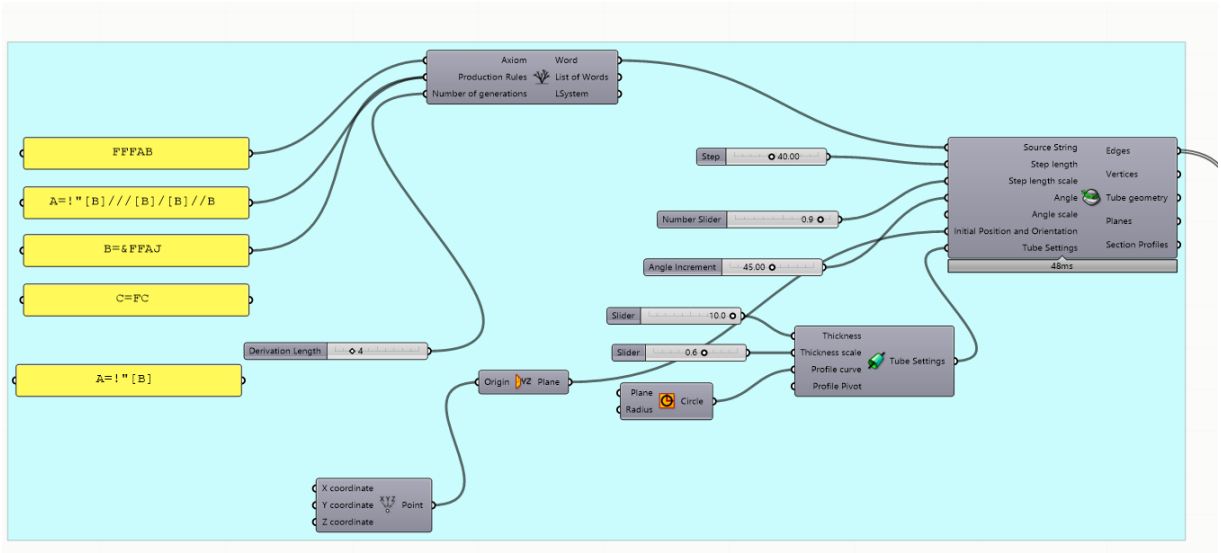

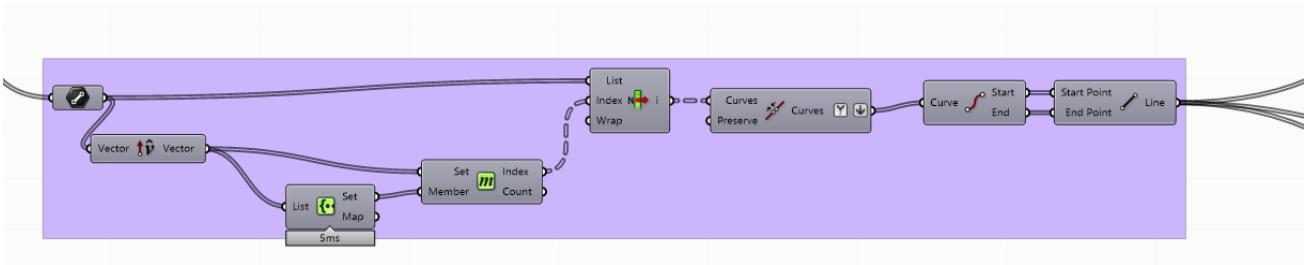

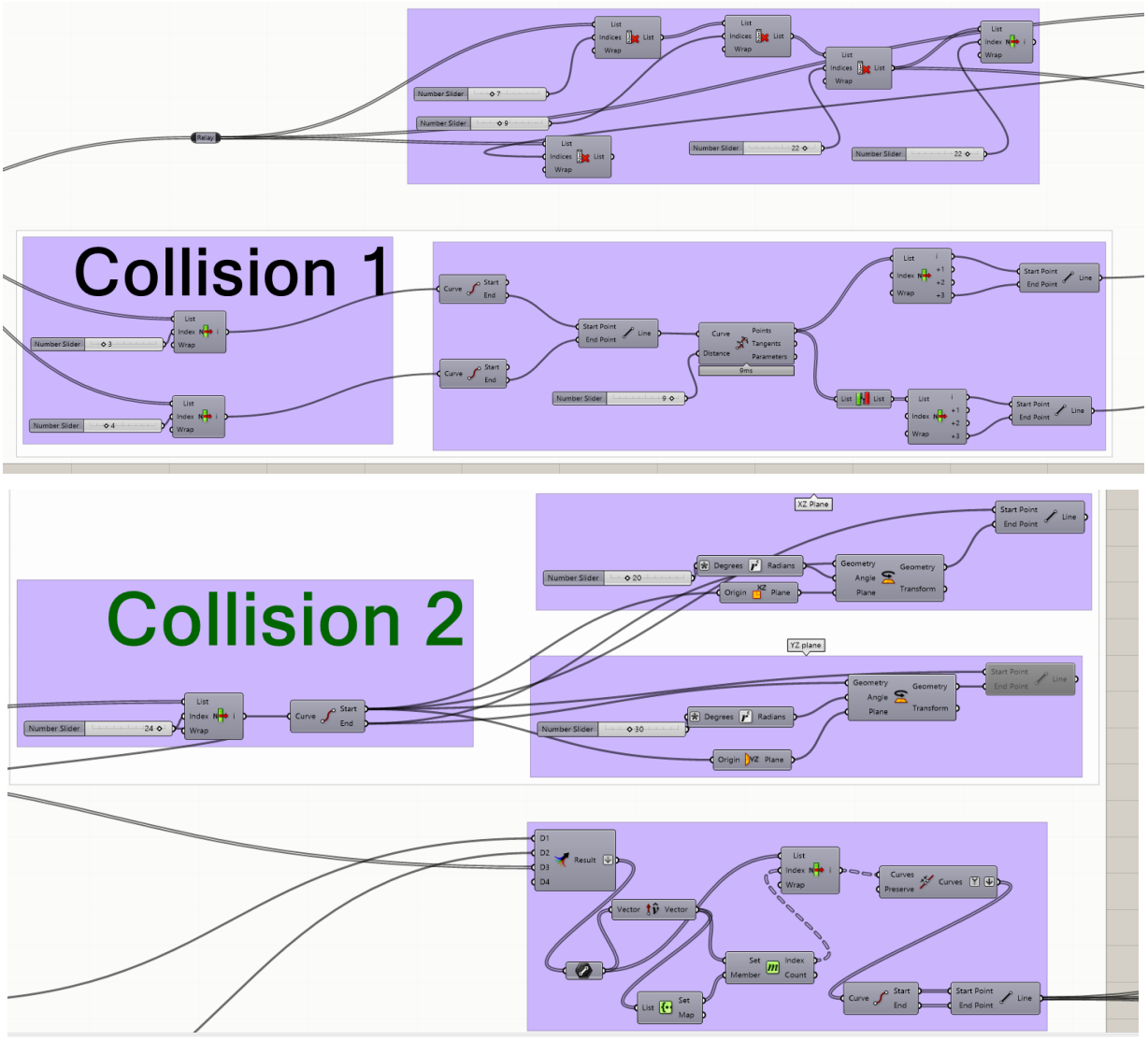

The CAD model of the tree structure

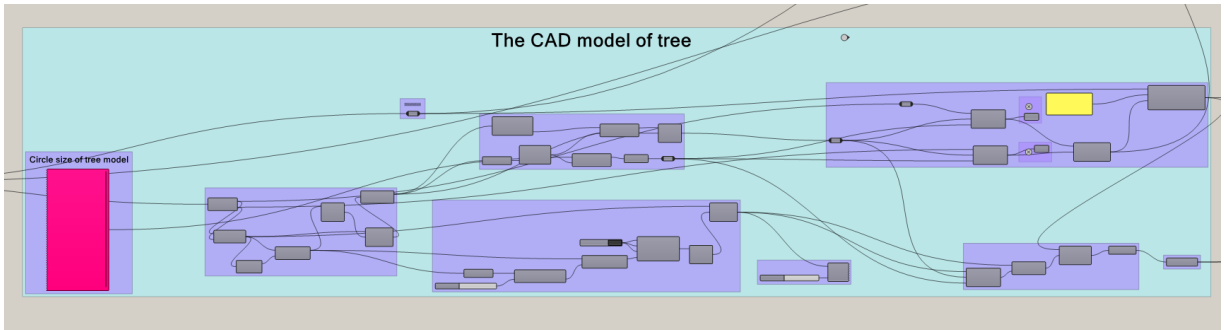

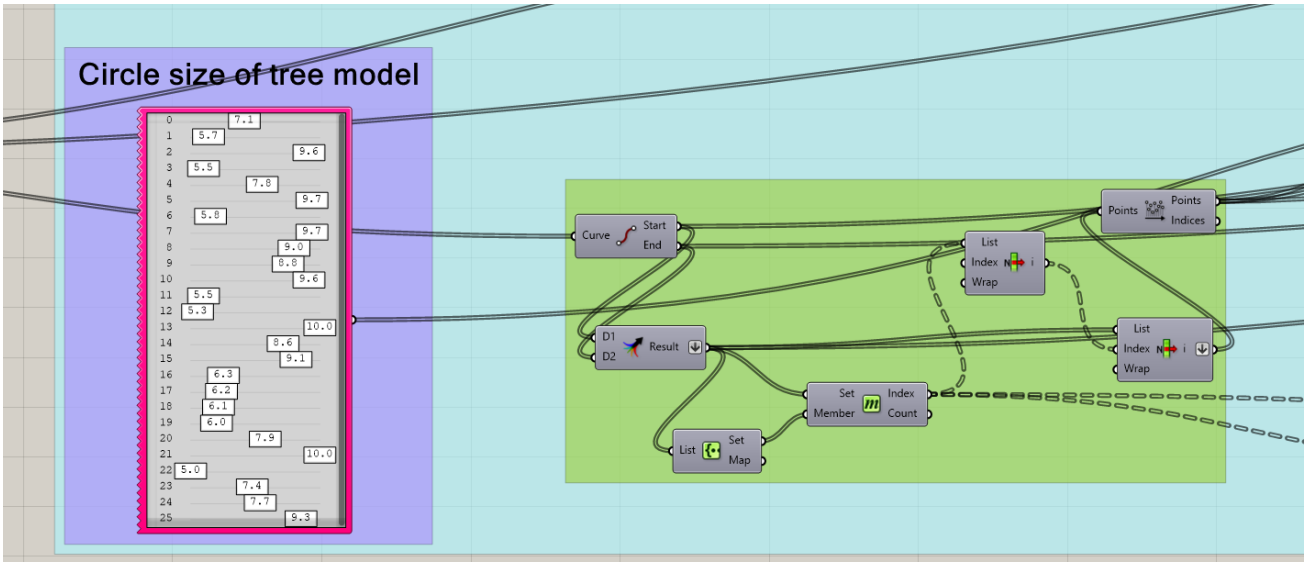
Circle size of tree model
0 7.1
1 5.7
2 9.6
3 5.5
4 7.8
5 9.7
6 5.8
7 9.7
8 9.0
9 8.8
10 9.6
11 5.5
12 5.3
13 10.0
14 8.6
15 9.1
16 6.3
17 6.2
18 6.1
19 6.0
20 7.9
21 10.0
22 5.0
23 7.4
24 7.7
25 9.3
Curve
Start
End
Points
Points
Indices
List
Index
Wrap
D1
D2
Result
Set
Member
Index
Count
List
Set
Map

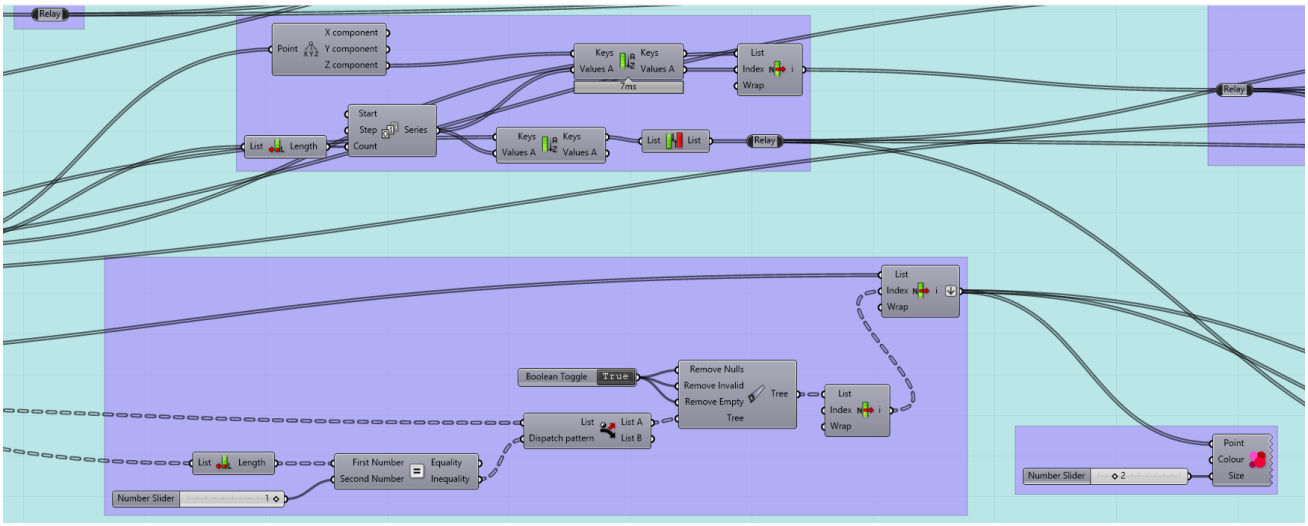
Relay
Point
X component
Y component
Z component
Keys
Values A
Values B
7ms
List
Index
Wrap
Start
Step
Count
Series
List
Length
Relay
Boolean Toggle
True
Remove Nulls
Remove Invalid
Remove Empty
Tree
List
Dispatch pattern
List A
List B
First Number
Second Number
Equality
Inequality
Number Slider
Point
Colour
Size

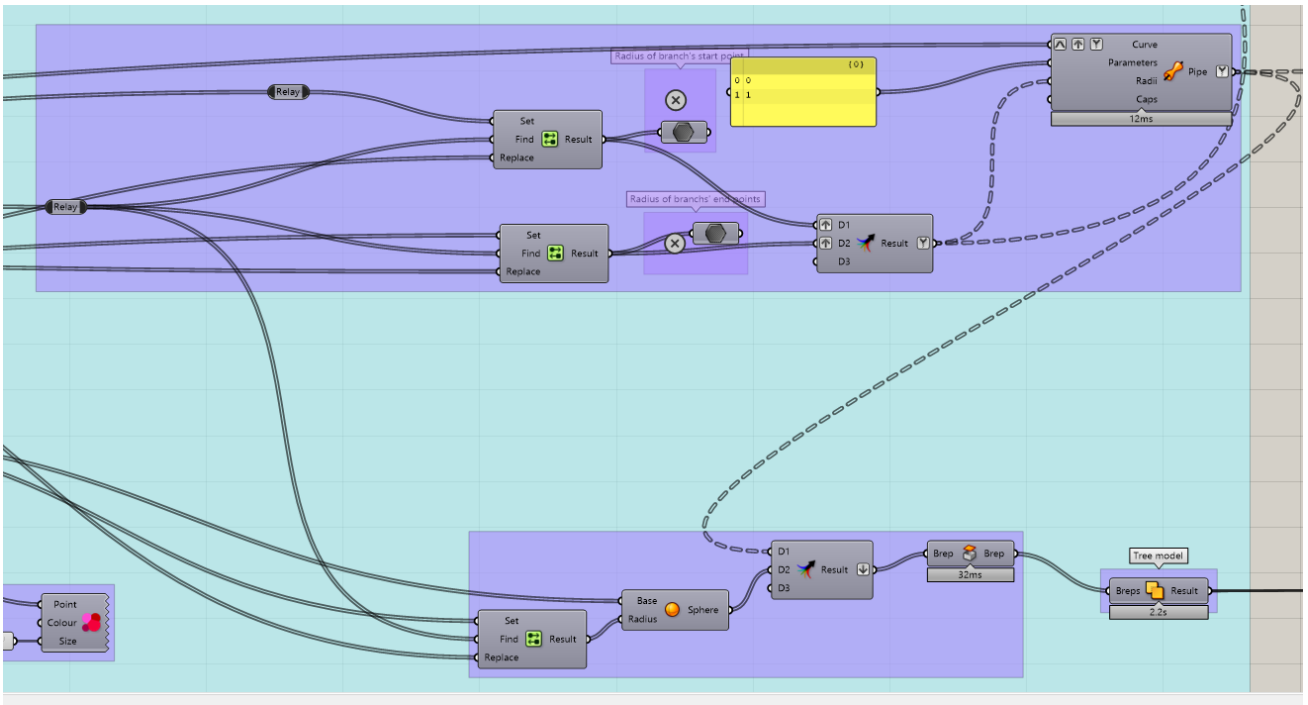
Radius of branch's start point
Radius of branchs' end points
Relay
Set
Find
Replace
Result
Curve
Parameters
Pipe
Radii
Caps
12ms
D1
D2
D3
Base
Radius
Sphere
Brep
32ms
Tree model
Breps
2.2s
Point
Colour
Size

The generation of initial volume

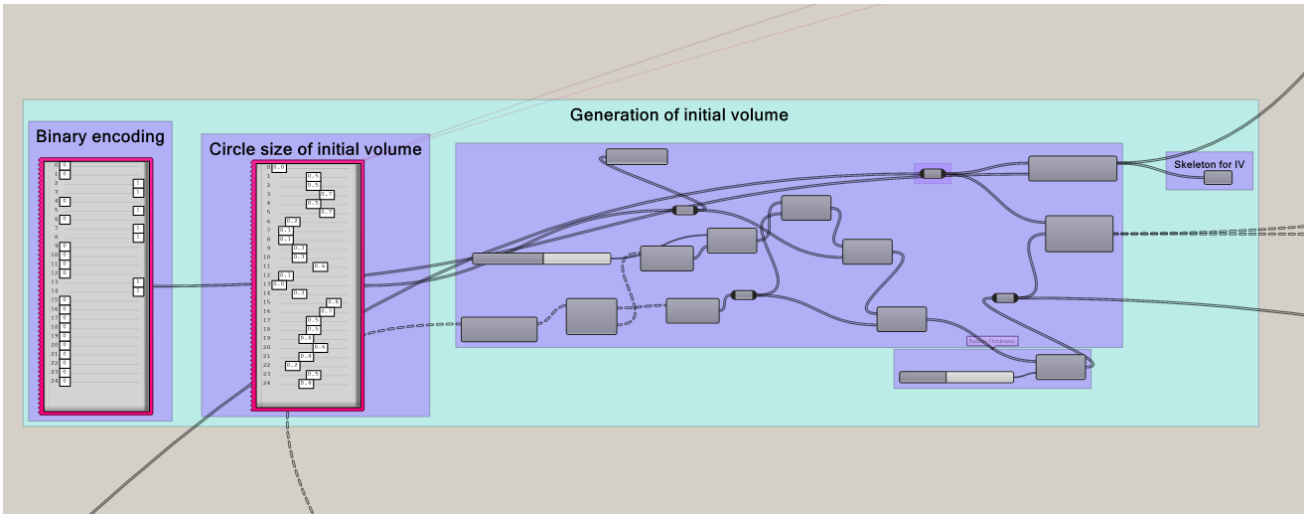

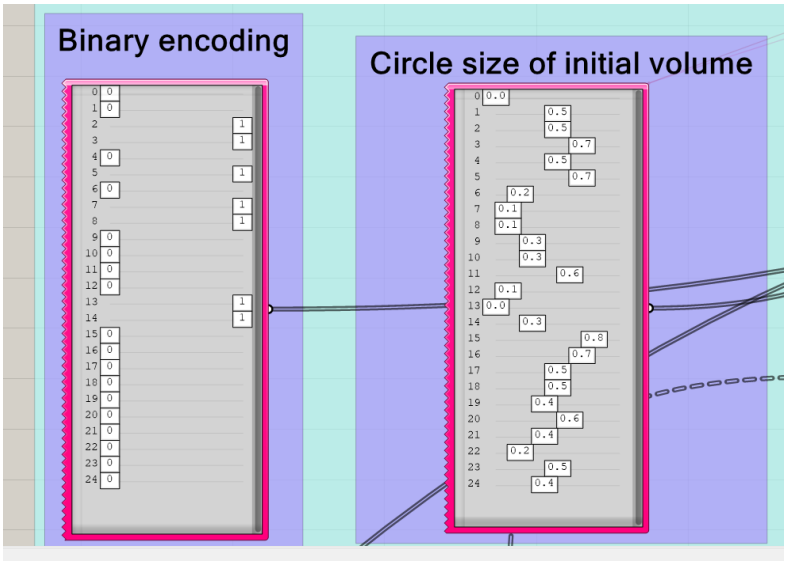

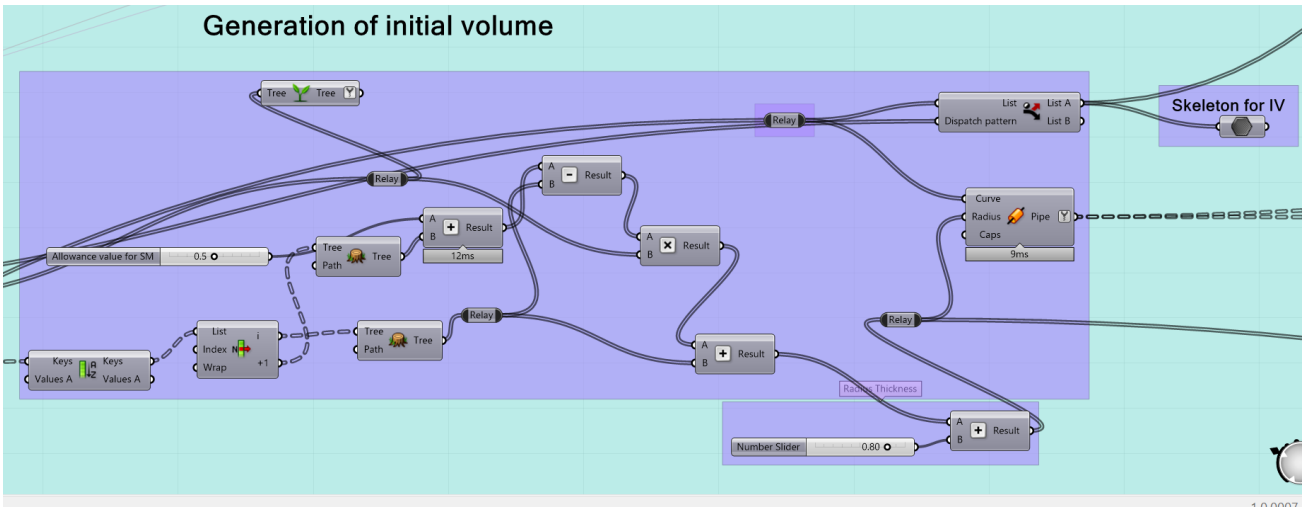

The optimization of initial volume

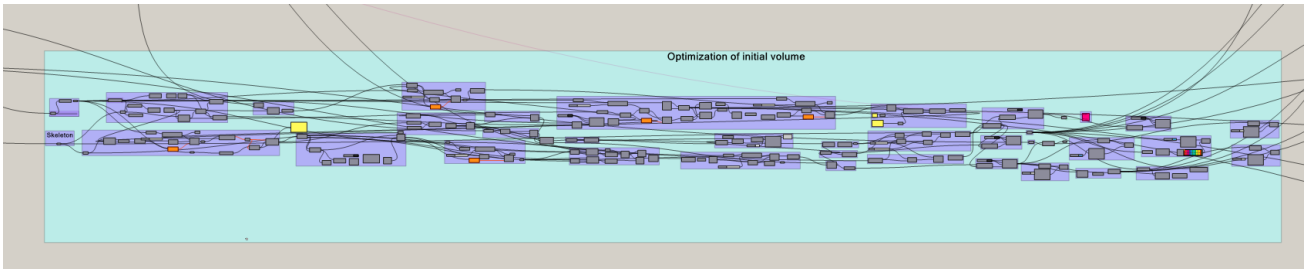

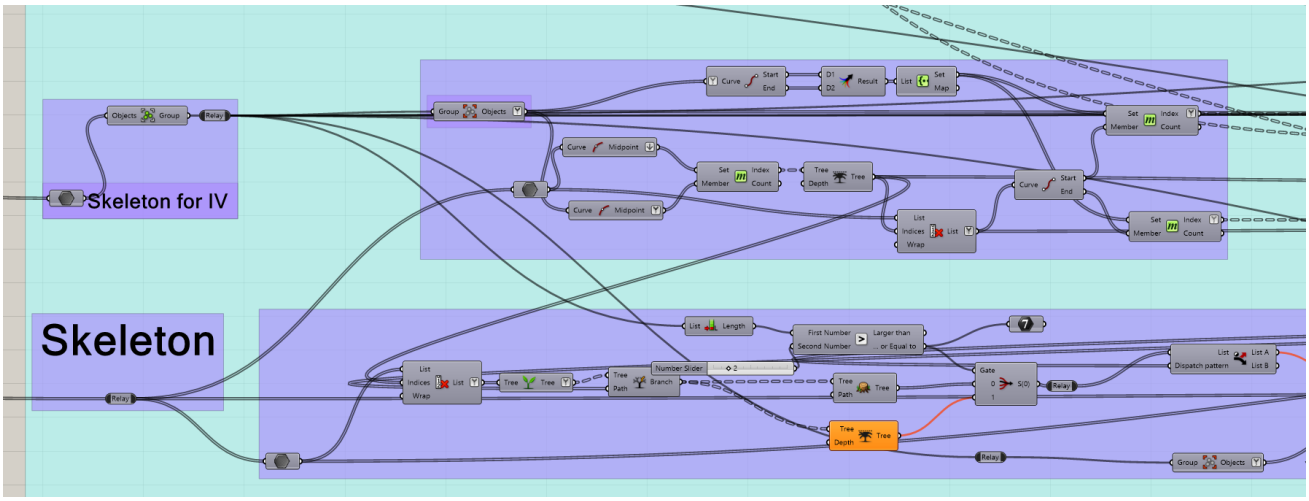

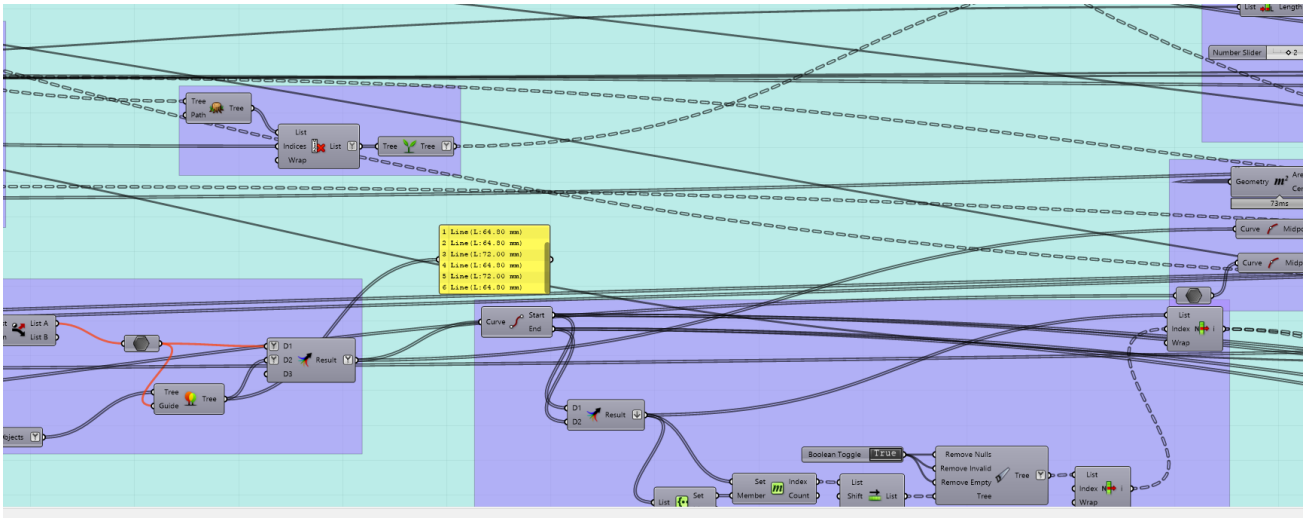

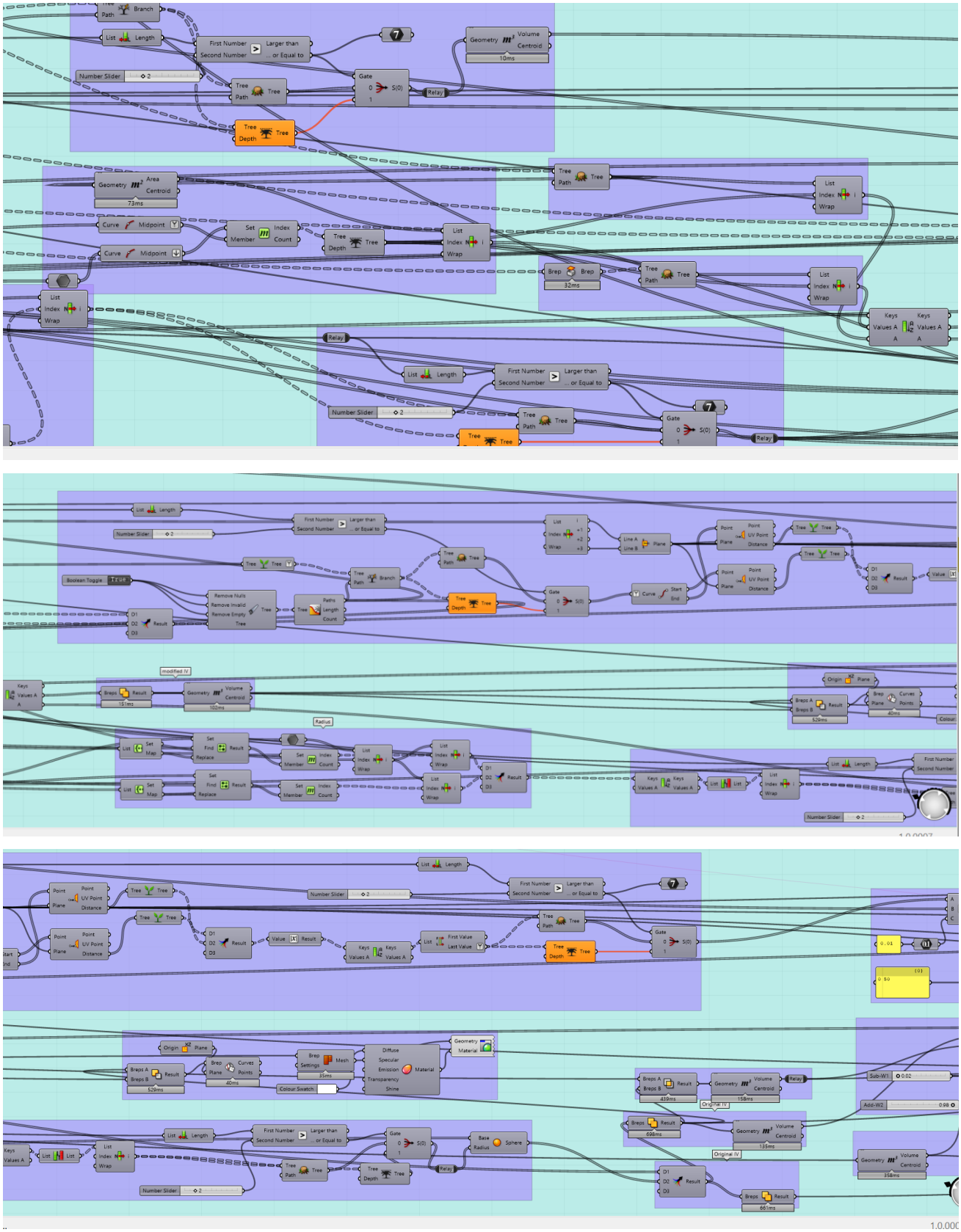

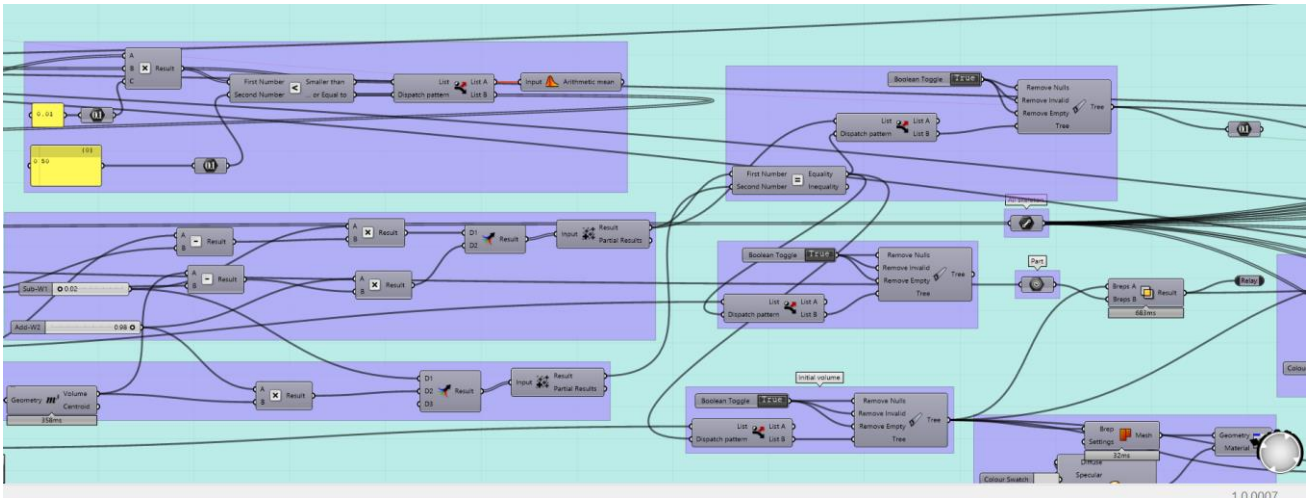

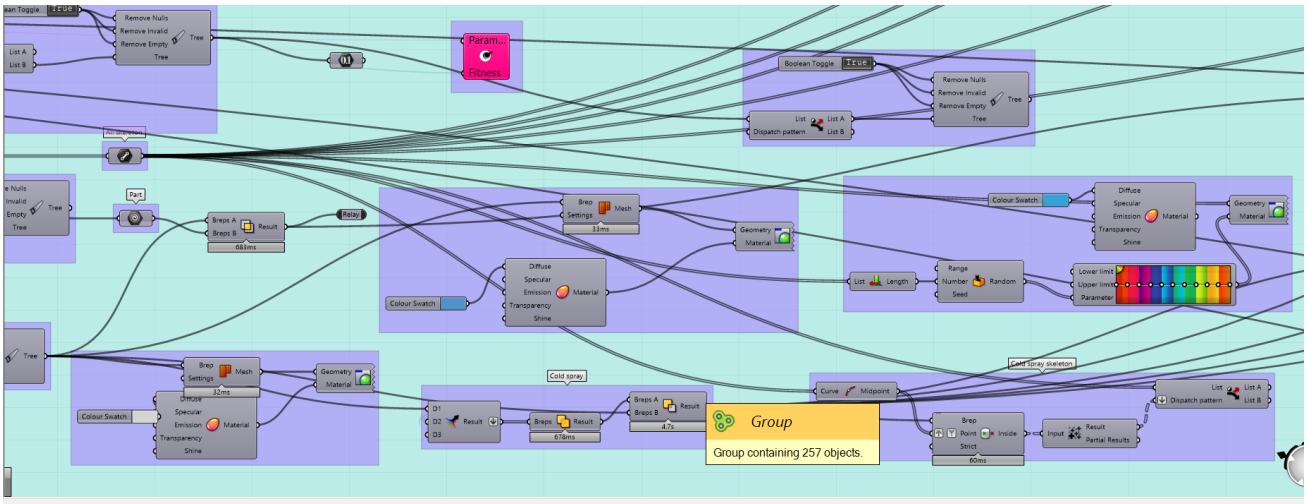
Param...
Fitness
Group
Group containing 257 objects.

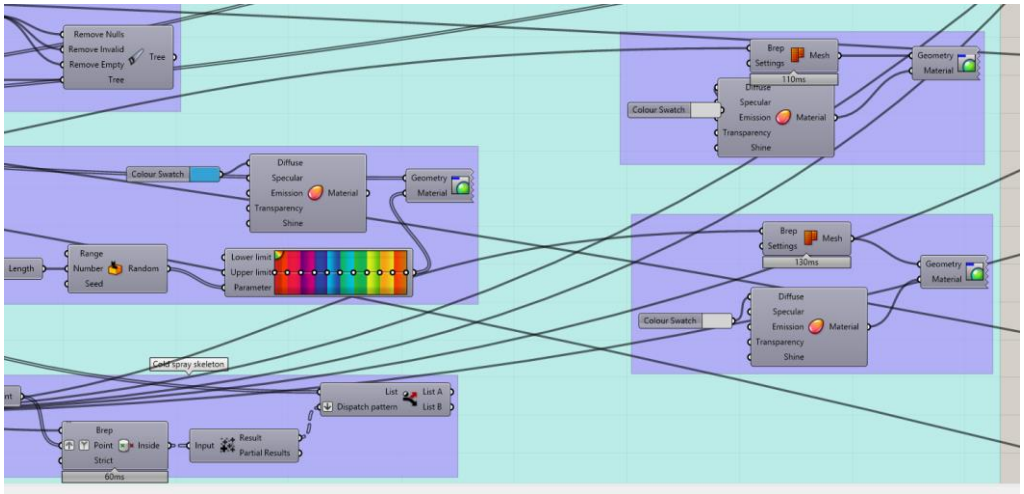

2. The sequence planning

The decomposition & classification

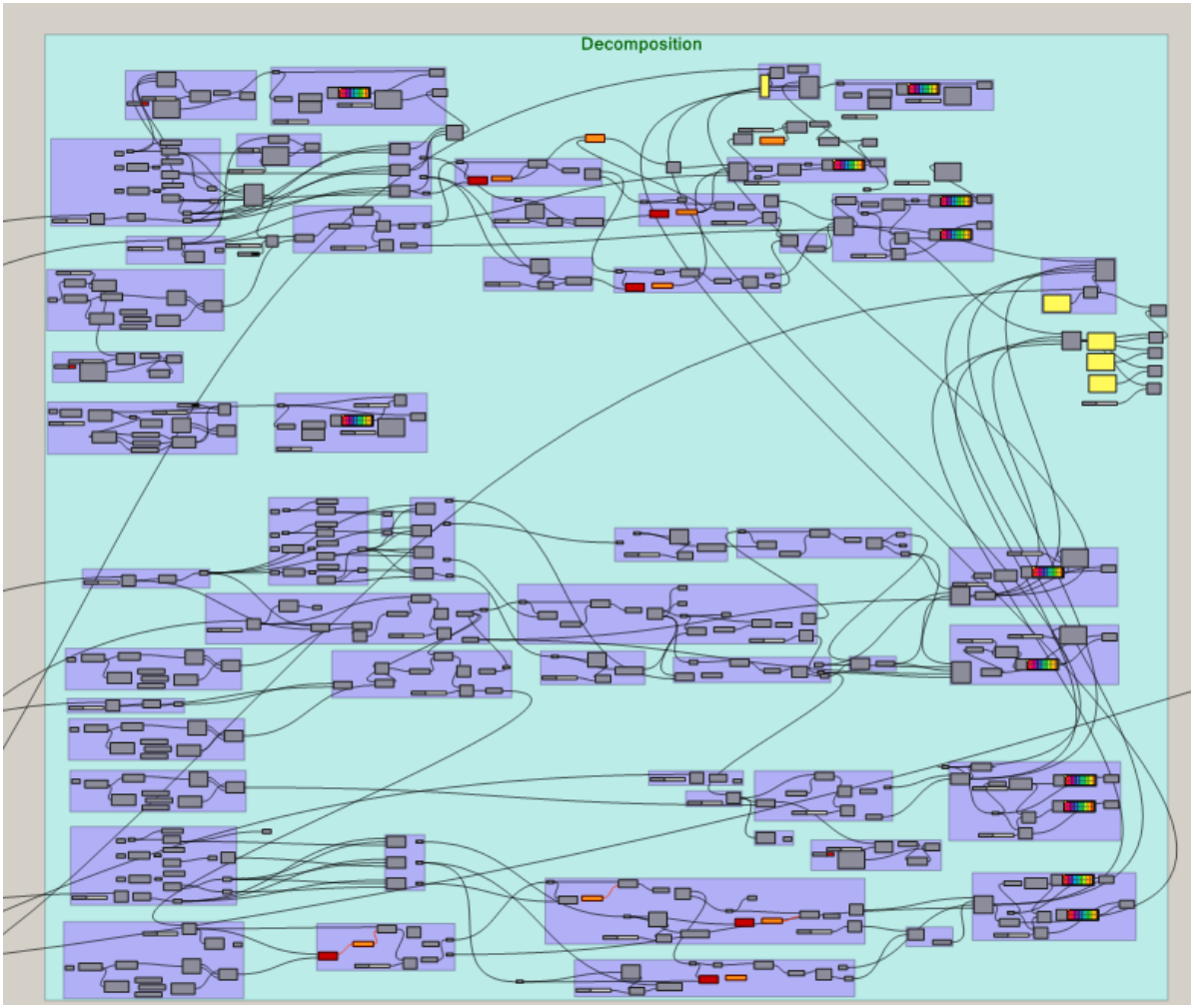

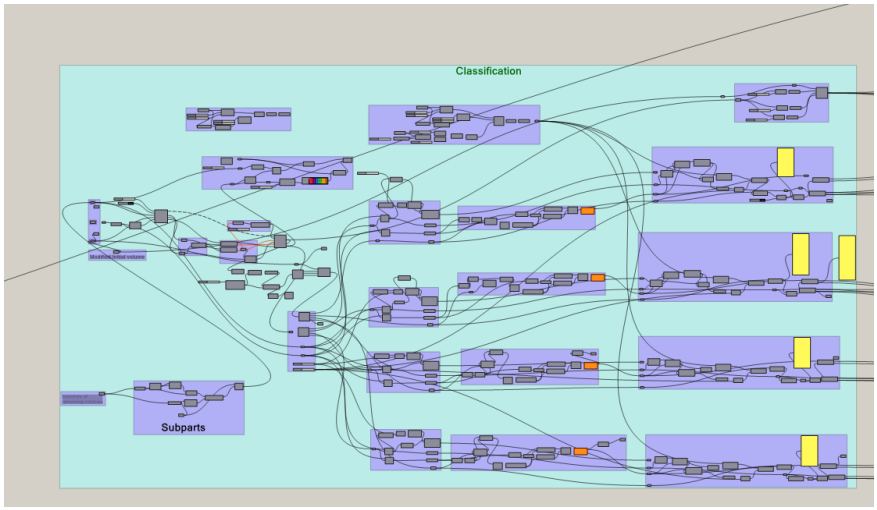

The Collision test & the length of tool switch

Group 1

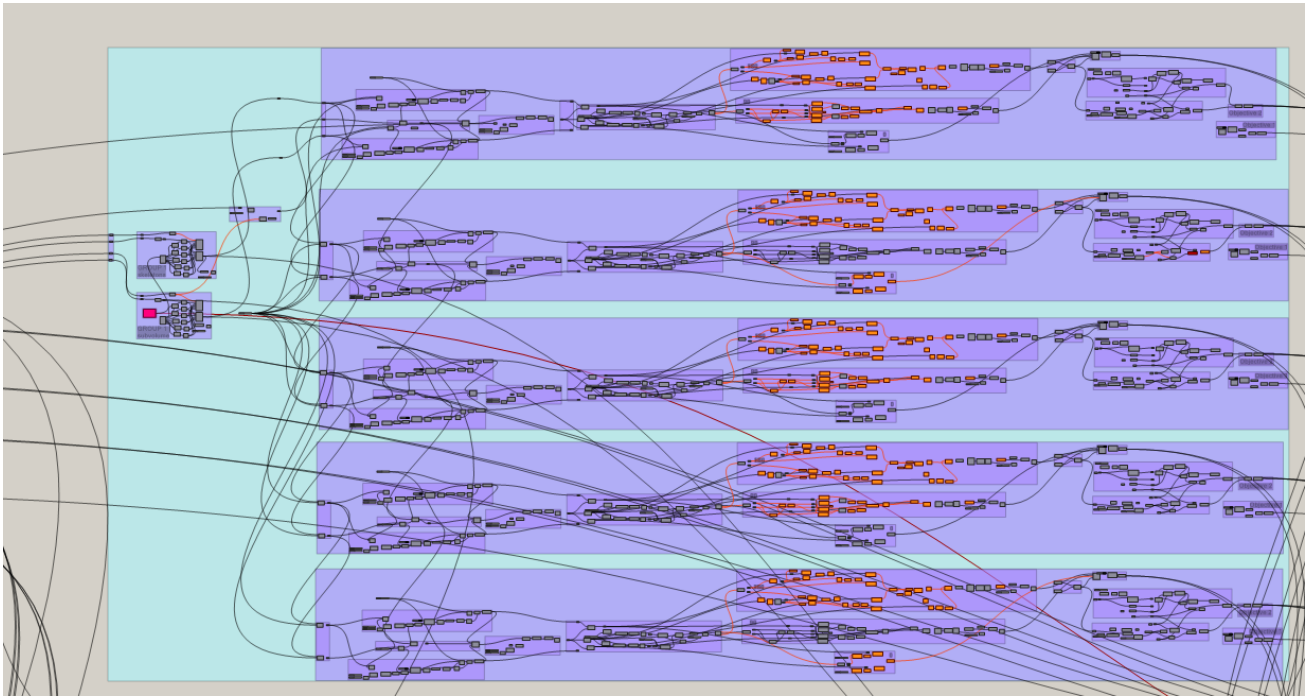

Group 2

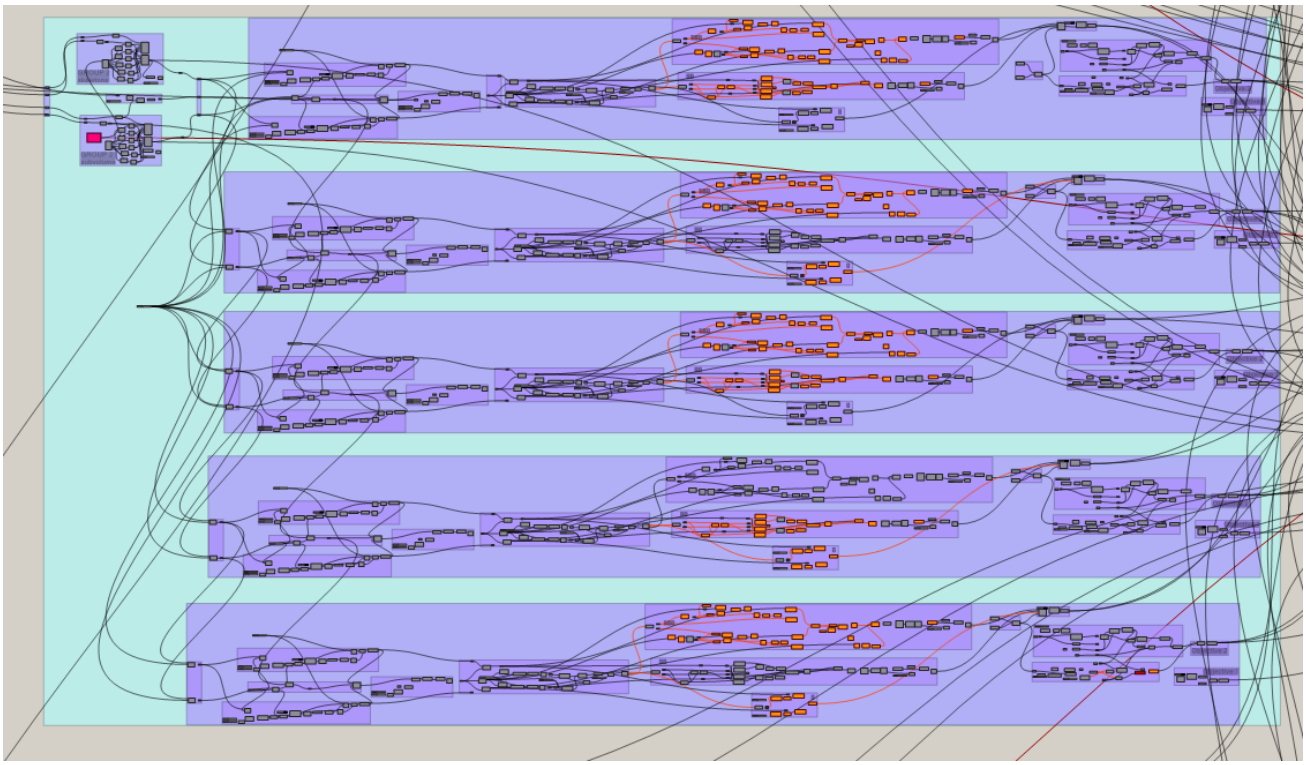

Group 3 & Group 4

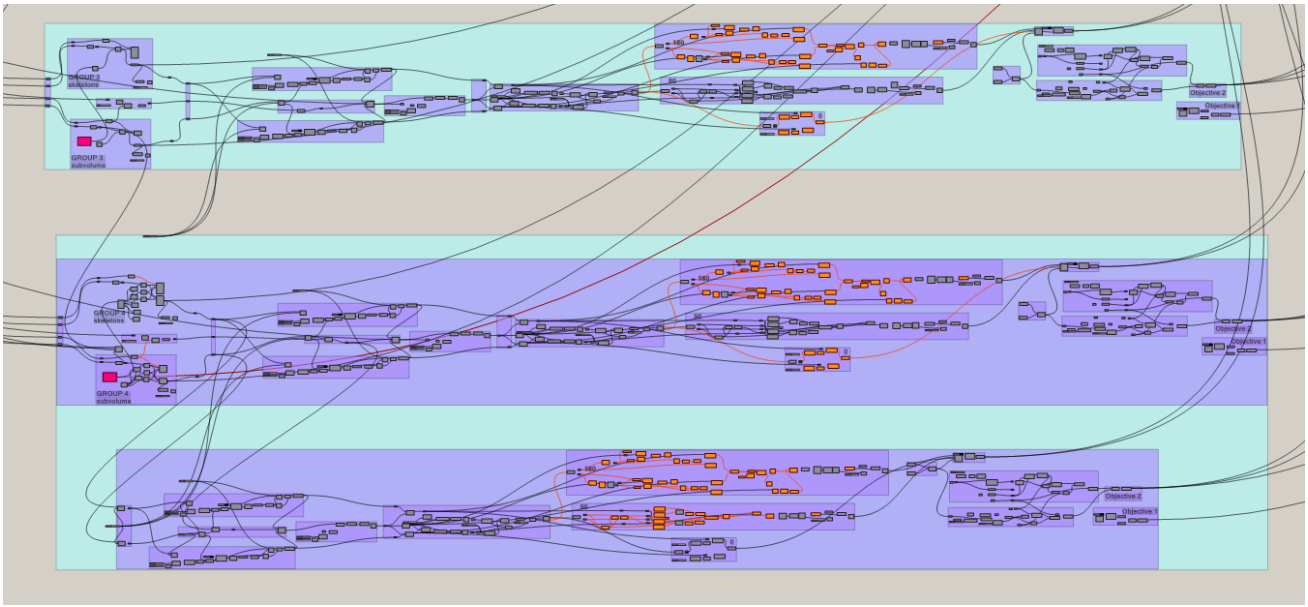

The calculation of objective function

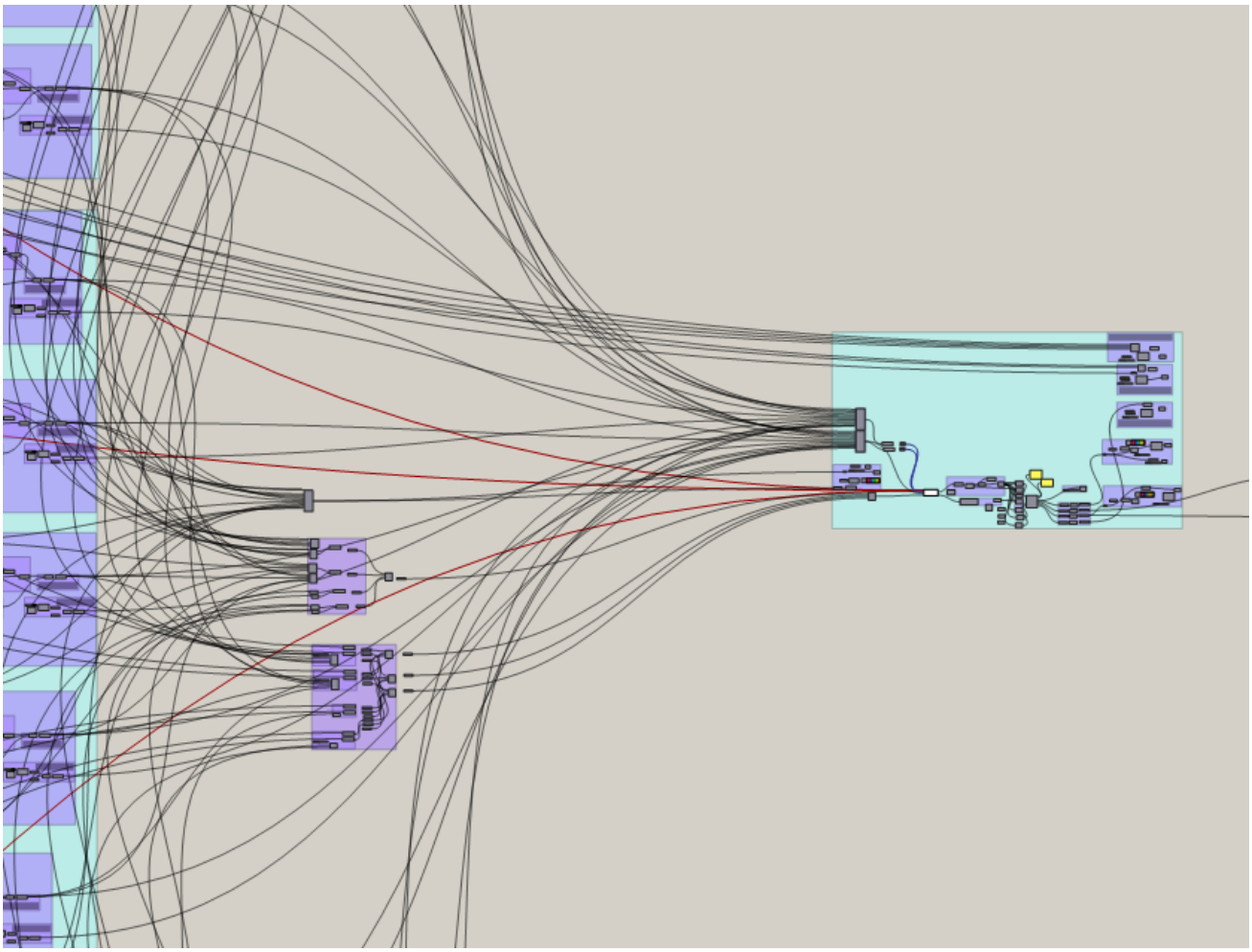

3. The toolpath optimization

The Gaussian distribution profile

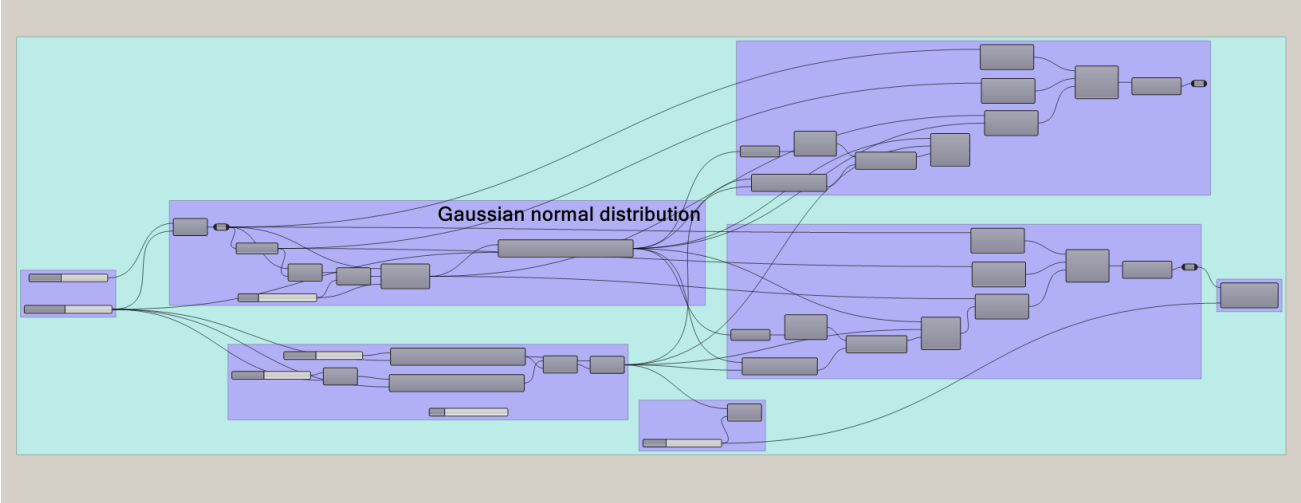

The optimization of toolpath (one subpart is taken as an example)

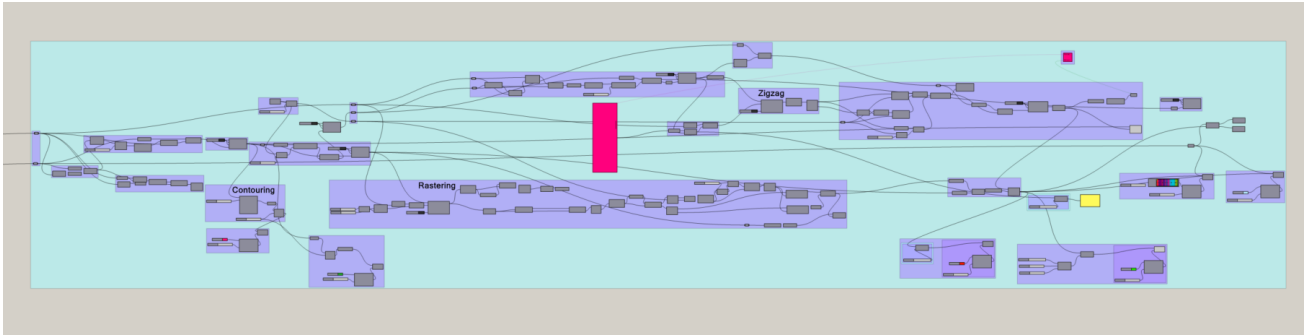

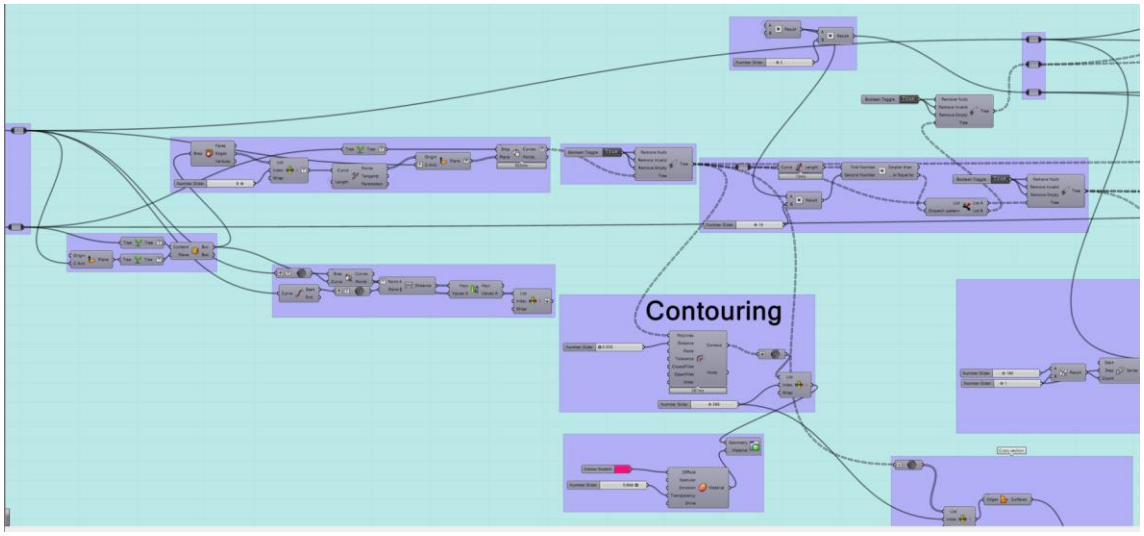

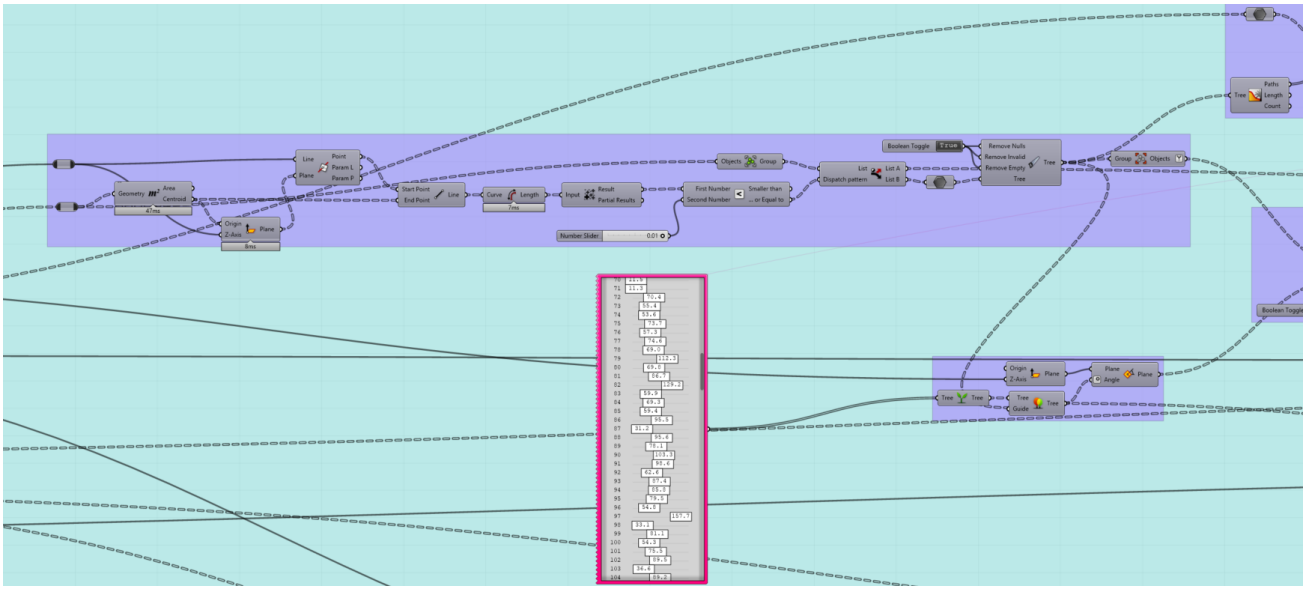

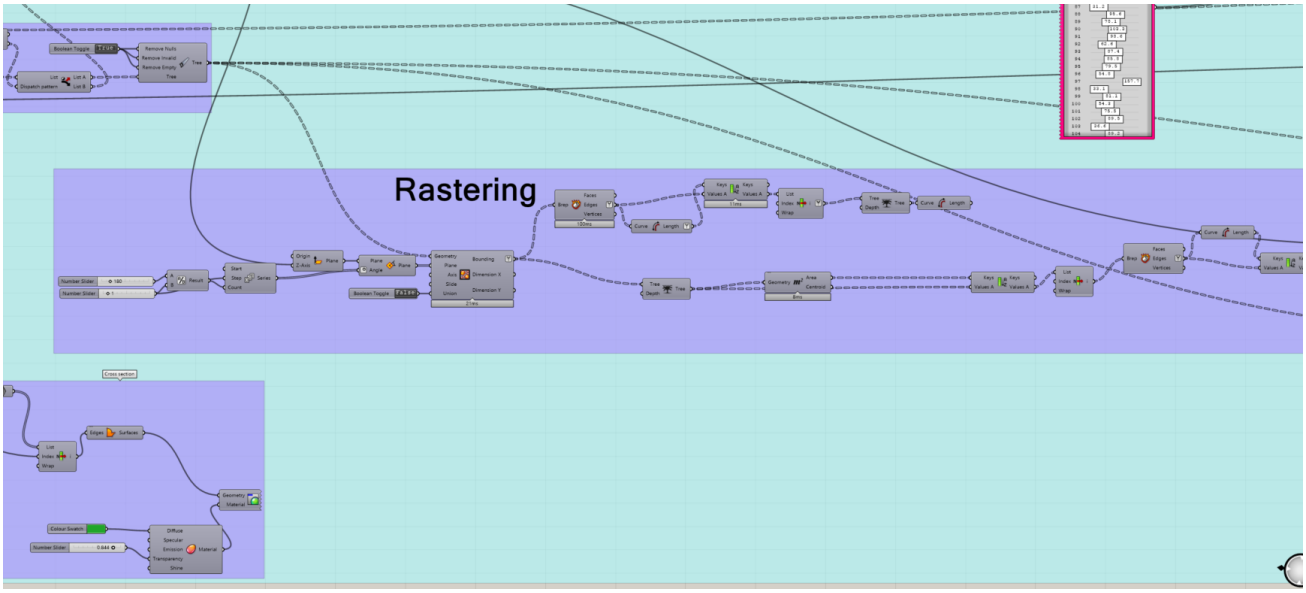
Rastering

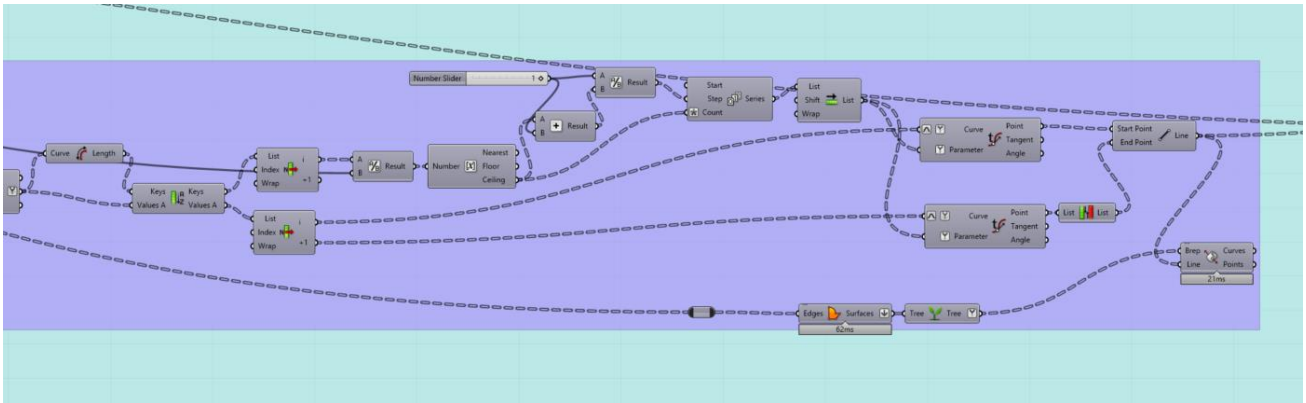

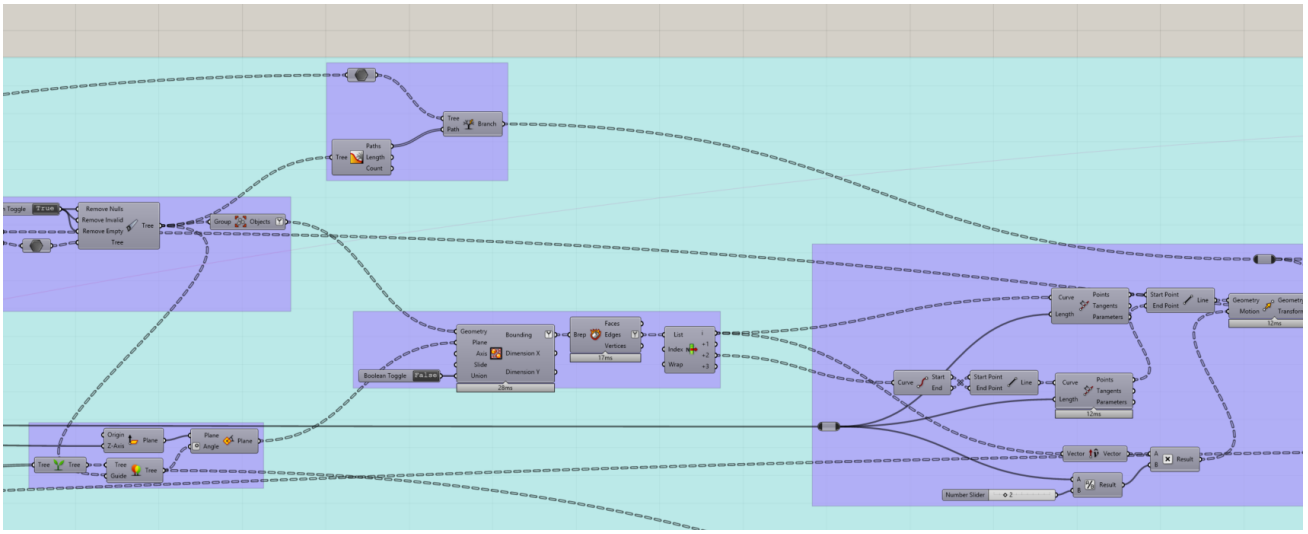

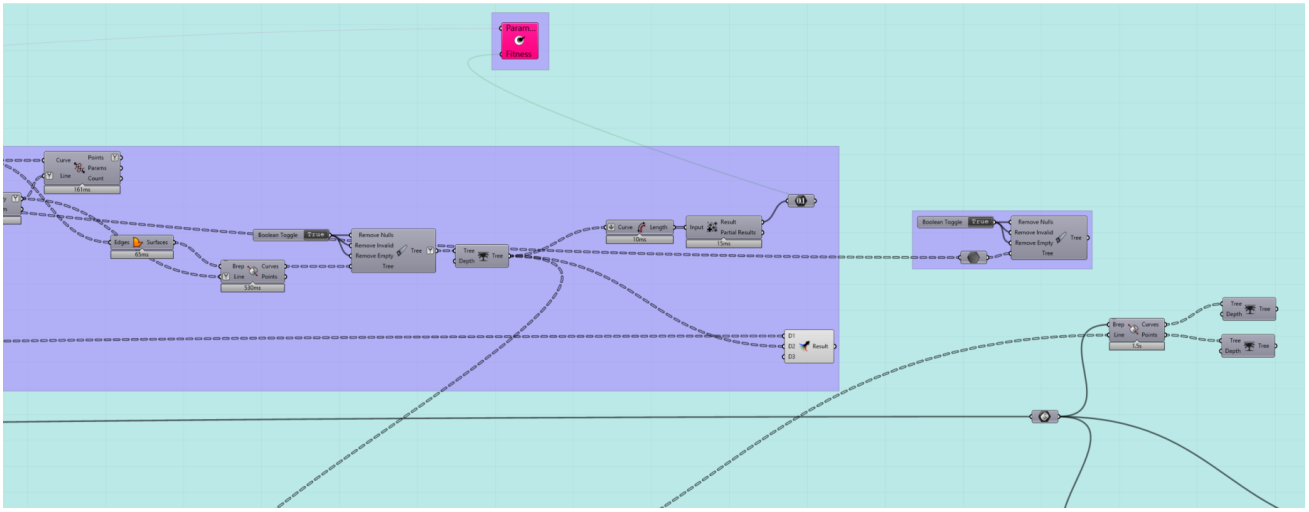

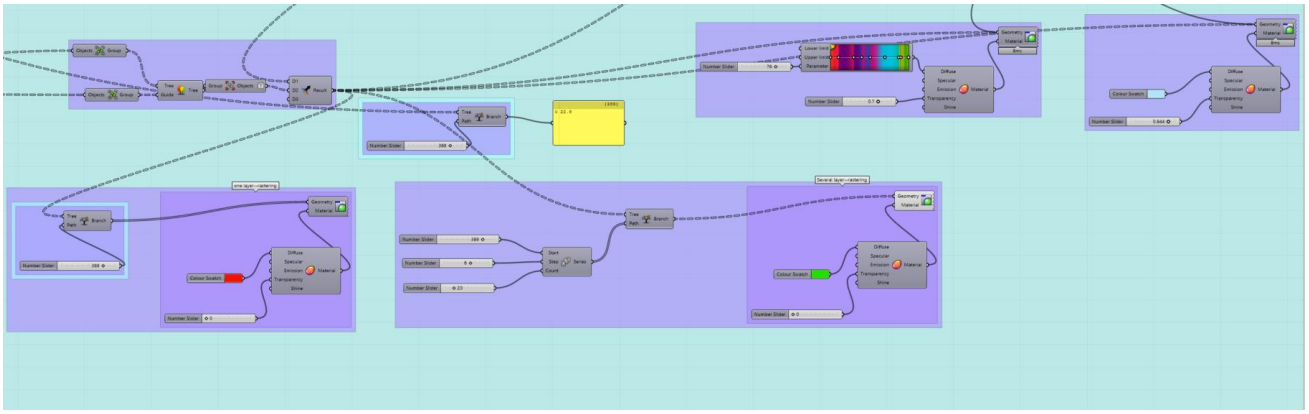

List of References

[1] Esmaeilian, B., Behdad, S., & Wang, B. (2016). The evolution and future of manufacturing: A review. *Journal of Manufacturing Systems*, *39*, 79-100.

[2] Bandyopadhyay, A., Gualtieri, T. P., & Bose, S. (2015). Global engineering and additive manufacturing. *Additive Manufacturing*, *1*, 9-11.

[3] Gao, W., Zhang, Y., Ramanujan, D., Ramani, K., Chen, Y., Williams, C. B., ... & Zavattieri, P. D. (2015). The status, challenges, and future of additive manufacturing in engineering. *Computer-Aided Design*, *69*, 65-89.

[4] Gibson, I., Rosen, D. W., Stucker, B., & Khorasani, M. (2021). *Additive manufacturing technologies* (Vol. 17). Cham, Switzerland: Springer.

[5] Ramaswami, K. (1997). *Process planning for shape deposition manufacturing*. stanford university.

[6] Paris, H., & Mandil, G. (2017). Process planning for combined additive and subtractive manufacturing technologies in a remanufacturing context. *Journal of Manufacturing Systems*, *44*, 243-254.

[7] Thompson, M. K., Moroni, G., Vaneker, T., Fadel, G., Campbell, R. I., Gibson, I., ... & Martina, F. (2016). Design for Additive Manufacturing: Trends, opportunities, considerations, and constraints. *CIRP annals*, *65*(2), 737-760.

[8] Nau, B., Roderburg, A., & Klocke, F. (2011). Ramp-up of hybrid manufacturing technologies. *CIRP Journal of Manufacturing Science and Technology*, *4*(3), 313-316.

[9] Hur, J., Lee, K., & Kim, J. (2002). Hybrid rapid prototyping system using machining and deposition. *Computer-Aided Design*, *34*(10), 741-754.

[10] Flynn, J. M., Shokrani, A., Newman, S. T., & Dhokia, V. (2016). Hybrid additive and subtractive machine tools–Research and industrial developments. *International Journal of Machine Tools and Manufacture*, *101*, 79-101.

[11] Karunakaran, K. P., Suryakumar, S., Pushpa, V., & Akula, S. (2010). Low cost integration of additive and subtractive processes for hybrid layered manufacturing. *Robotics and Computer-Integrated Manufacturing*, *26*(5), 490-499.

[12] Zhu, Z., Dhokia, V. G., Nassehi, A., & Newman, S. T. (2013). A review of hybrid manufacturing processes–state of the art and future perspectives. *International Journal of Computer Integrated Manufacturing*, *26*(7), 596-615.

[13] Jones, J. B., McNutt, P., Tosi, R., Perry, C., & Wimpenny, D. I. (2012). Remanufacture of turbine blades by laser cladding, machining and in-process scanning in a single machine.

[14] Paris, H., & Mandil, G. (2018). Extracting features for manufacture of parts from existing components based on combining additive and subtractive technologies. *International Journal on Interactive Design and Manufacturing (IJIDeM)*, *12*(2), 525-536.

[15] Wang, J., Prakash, S., Joshi, Y., & Liou, F. (2002). Laser aided part repair-a review. In *2002 International Solid Freeform Fabrication Symposium*.

[16] Sealy, M. P., Madireddy, G., Williams, R. E., Rao, P., & Toursangsaraki, M. (2018). Hybrid processes in additive manufacturing. *Journal of manufacturing Science and Engineering*, *140*(6).

[17] Chu, W. S., Kim, C. S., Lee, H. T., Choi, J. O., Park, J. I., Song, J. H., ... & Ahn, S. H. (2014). Hybrid manufacturing in micro/nano scale: A Review. *International journal of precision engineering and manufacturing-green technology*, *1*(1), 75-92.

[18] Patterson, A. E., & Allison, J. T. (2018, August). Manufacturability constraint formulation for design under hybrid additive-subtractive manufacturing. In *International Design Engineering Technical Conferences and Computers and Information in Engineering Conference* (Vol. 51791, p. V004T05A011). American Society of Mechanical Engineers.

[19] Wu, H., Xie, X., Liu, M., Verdy, C., Zhang, Y., Liao, H., & Deng, S. (2020). Stable layer-building strategy to enhance cold-spray-based additive manufacturing. *Additive Manufacturing*, *35*, 101356.

[20] Yin, S., Cavaliere, P., Aldwell, B., Jenkins, R., Liao, H., Li, W., & Lupoi, R. (2018). Cold spray additive manufacturing and repair: Fundamentals and applications. *Additive Manufacturing*, *21*, 628-650.

[21] Lynch, M. E., Gu, W., El-Wardany, T., Hsu, A., Viens, D., Nardi, A., & Klecka, M. (2013). Design and topology/shape structural optimisation for additively manufactured cold sprayed components: this paper presents an additive manufactured cold spray component which is shape optimised to achieve 60% reduction in stress and 20% reduction in weight. *Virtual and Physical Prototyping*, *8*(3), 213-231.

[22] ASTM International. (2013), "F2792-12a - Standard Terminology for Additive Manufacturing Technologies," *Rapid Manuf. Assoc.*, pp. 10–12.

[23] Gao, W., Zhang, Y., Nazzetta, D. C., Ramani, K., & Cipra, R. J. (2015, November). RevoMaker: Enabling multi-directional and functionally-embedded 3D printing using a rotational

cuboidal platform. In *Proceedings of the 28th Annual ACM Symposium on User Interface Software & Technology* (pp. 437-446).

[24] Monette, Z., Kasar, A. K., Daroonparvar, M., & Menezes, P. L. (2020). Supersonic particle deposition as an additive technology: methods, challenges, and applications. *The International Journal of Advanced Manufacturing Technology*, *106*(5), 2079-2099.

[25] Peltola, S. M., Melchels, F. P., Grijpma, D. W., & Kellomäki, M. (2008). A review of rapid prototyping techniques for tissue engineering purposes. *Annals of medicine*, *40*(4), 268-280.

[26] Hutmacher, D. W. (2000). Scaffolds in tissue engineering bone and cartilage. *Biomaterials*, *21*(24), 2529-2543.

[27] Ghadge, A., Karantoni, G., Chaudhuri, A., & Srinivasan, A. (2018). Impact of additive manufacturing on aircraft supply chain performance: A system dynamics approach. *Journal of Manufacturing Technology Management*.

[28] Rochus, P., Plesseria, J. Y., Van Elsen, M., Kruth, J. P., Carrus, R., & Dormal, T. (2007). New applications of rapid prototyping and rapid manufacturing (RP/RM) technologies for space instrumentation. *Acta Astronautica*, *61*(1-6), 352-359.

[29] Pinna, C., Ramundo, L., Sisca, F. G., Angioletti, C. M., Taisch, M., & Terzi, S. (2016). Additive Manufacturing applications within Food industry: an actual overview and future opportunities. In *21st Summer School Francesco Turco 2016* (pp. 18-24). AIDI-Italian Association of Industrial Operations Professors.

[30] Johnson, A., Bingham, G. A., & Wimpenny, D. I. (2013). Additive manufactured textiles for high-performance stab resistant applications. *Rapid Prototyping Journal*.

[31] Geraedts, J., Doubrovski, E., Verlinden, J., & Stellingwerff, M. (2012, May). Three views on additive manufacturing: business, research and education. In *Ninth Int. Symp. Tools Methods Compet. Eng., I. Horváth, A. Albers, M. Behrendt, and Z. Rusák, Eds* (pp. 1-15).

[32] Vanderploeg, A., Lee, S. E., & Mamp, M. (2017). The application of 3D printing technology in the fashion industry. *International Journal of Fashion Design, Technology and Education*, *10*(2), 170-179.

[33] Macdonald, E., Salas, R., Espalin, D., Perez, M., Aguilera, E., Muse, D., & Wicker, R. B. (2014). 3D printing for the rapid prototyping of structural electronics. *IEEE access*, *2*, 234-242.

[34] Busachi, A., Erkoyuncu, J., Colegrove, P., Drake, R., Watts, C., & Martina, F. (2016). Defining next-generation additive manufacturing applications for the ministry of defence (MoD). *Procedia Cirp*, *55*, 302-307.

[35] Hoerber, J., Glasschroeder, J., Pfeffer, M., Schilp, J., Zaeh, M., & Franke, J. (2014). Approaches for additive manufacturing of 3D electronic applications. *Procedia CIRP*, *17*, 806-811.

[36] Paulsen, J. A., Renn, M., Christenson, K., & Plourde, R. (2012, October). Printing conformal electronics on 3D structures with Aerosol Jet technology. In *2012 Future of Instrumentation International Workshop (FIIW) Proceedings* (pp. 1-4). IEEE.

[37] Gardan, N., & Schneider, A. (2015). Topological optimization of internal patterns and support in additive manufacturing. *Journal of Manufacturing Systems*, *37*, 417-425.

[38] Lauwers, B., Klocke, F., Klink, A., Tekkaya, A. E., Neugebauer, R., & Mcintosh, D. (2014). Hybrid processes in manufacturing. *CIRP Annals*, *63*(2), 561-583.

[39] Nassehi, A., Newman, S., Dhokia, V., Zhu, Z., & Asrai, R. I. (2012). Using formal methods to model hybrid manufacturing processes. In *Enabling Manufacturing Competitiveness and Economic Sustainability* (pp. 52-56). Springer, Berlin, Heidelberg.

[40] Chong, L., Ramakrishna, S., & Singh, S. (2018). A review of digital manufacturing-based hybrid additive manufacturing processes. *The International Journal of Advanced Manufacturing Technology*, *95*(5), 2281-2300.

[41] Akula, S., & Karunakaran, K. P. (2006). Hybrid adaptive layer manufacturing: An Intelligent art of direct metal rapid tooling process. *Robotics and Computer-Integrated Manufacturing*, *22*(2), 113-123.

[42] Karunakaran, K. P., Pushpa, V., Akula, S. B., & Suryakumar, S. (2008). Techno-economic analysis of hybrid layered manufacturing. *International journal of intelligent systems technologies and applications*, *4*(1-2), 161-176.

[43] Karunakaran, K. P., Suryakumar, S., Pushpa, V., & Akula, S. (2009). Retrofitment of a CNC machine for hybrid layered manufacturing. *The International Journal of Advanced Manufacturing Technology*, *45*(7-8), 690-703.

[44] Kerschbaumer, M., & Ernst, G. (2004, October). Hybrid manufacturing process for rapid high performance tooling combining high speed milling and laser cladding. In *International Congress on Applications of Lasers & Electro-Optics* (Vol. 2004, No. 1, p. 1710). Laser Institute of America.

[45] Ren, L., Padathu, A. P., Ruan, J., Sparks, T., & Liou, F. W. (2006, August). Three dimensional die repair using a hybrid manufacturing system. In *Proceedings of the 17th Solid Freeform Fabrication Symposium, Austin, TX, USA* (pp. 14-16).

[46] Xiong, X., Zhang, H., & Wang, G. (2009). Metal direct prototyping by using hybrid plasma deposition and milling. *Journal of Materials Processing Technology*, *209*(1), 124-130.

[47] Mognol, P., Jégou, L., Rivette, M., & Furet, B. (2006). High speed milling, electro discharge machining and direct metal laser sintering: A method to optimize these processes in hybrid rapid tooling. *The International Journal of Advanced Manufacturing Technology*, *29*(1-2), 35-40.

[48] Xiangping, W., Haiou, Z., Guilan, W., & Lingpeng, W. (2014). Adaptive slicing for multi-axis hybrid plasma deposition and milling. In *Proceedings of the 2014 Annual International Solid Freeform Fabrication Symposium*.

[49] Song, Y. A., Park, S., Choi, D., & Jee, H. (2005). 3D welding and milling: Part I–a direct approach for freeform fabrication of metallic prototypes. *International Journal of Machine Tools and Manufacture*, *45*(9), 1057-1062.

[50] Jeng, J. Y., & Lin, M. C. (2001). Mold fabrication and modification using hybrid processes of selective laser cladding and milling. *Journal of Materials Processing Technology*, *110*(1), 98-103.

[51] Lamikiz, A., Sanchez, J. A., de Lacalle, L. L., & Arana, J. L. (2007). Laser polishing of parts built up by selective laser sintering. *International Journal of Machine Tools and Manufacture*, *47*(12-13), 2040-2050.

[52] Yasa, E., Kruth, J. P., & Deckers, J. (2011). Manufacturing by combining selective laser melting and selective laser erosion/laser re-melting. *CIRP annals*, *60*(1), 263-266.

[53] Sealy, M. P., Madireddy, G., Li, C., & Guo, Y. B. (2016, January). Finite element modeling of hybrid additive manufacturing by laser shock peening. In *27th Annual International Solid Freeform Fabrication Symposium-An Additive Manufacturing Conference (SFF), Austin, TX, Aug* (pp. 6-8).

[54] Kalentics, N., Burn, A., Cloots, M., & Logé, R. E. (2019). 3D laser shock peening as a way to improve geometrical accuracy in selective laser melting. *The International Journal of Advanced Manufacturing Technology*, *101*(5), 1247-1254.

[55] Kelkar, A., & Koc, B. (2008). Geometric planning and analysis for hybrid re-configurable molding and machining process. *Rapid Prototyping Journal*.

[56] Bariani, P. F., Bruschi, S., Ghiotti, A., & Lucchetta, G. (2007). An approach to modelling the forming process of sheet metal-polymer composites. *CIRP annals*, *56*(1), 261-264.

[57] Friel, R. J., & Harris, R. A. (2013). Ultrasonic additive manufacturing–a hybrid production process for novel functional products. *Procedia Cirp*, *6*, 35-40.

[58] Merz, R., Prinz, F. B., Ramaswami, K., Terk, M., & Weiss, L. E. (1994). Shape deposition manufacturing. In *1994 International Solid Freeform Fabrication Symposium*.

[59] Cooper, A. G., Kang, S., Kietzman, J. W., Prinz, F. B., Lombardi, J. L., & Weiss, L. E. (1999). Automated fabrication of complex molded parts using mold shape deposition manufacturing. *Materials & design*, *20*(2-3), 83-89.

[60] Song, Y., & Chen, Y. H. (2000, September). Layer Based Robot Machining for Rapid Prototyping. In *International Design Engineering Technical Conferences and Computers and Information in Engineering Conference* (Vol. 35135, pp. 215-223). American Society of Mechanical Engineers.

[61] Chen, Y. H., & Song, Y. (2001). The development of a layer based machining system. *Computer-Aided Design*, *33*(4), 331-342.

[62] Yang, Z. Y., Chen, Y. H., & Sze, W. S. (2001). Determining build orientation for layer-based machining. *The international journal of advanced manufacturing technology*, *18*(5), 313-322.

[63] Yang, Z. Y., Chen, Y. G., & Sze, W. S. (2002). Layer-based machining: recent development and support structure design. *Proceedings of the Institution of Mechanical Engineers, Part B: Journal of Engineering Manufacture*, *216*(7), 979-991.

[64] Eiamsa-ard, K., Zhang, J., & Liou, F. W. (2001). Skeleton-based Geometric Reasoning for Adaptive Slicing in a Five-axis Laser Aided manufacturing Process System. In *2001 International Solid Freeform Fabrication Symposium*.

[65] Cormier, D., & Taylor, J. (2001). A process for solvent welded rapid prototype tooling. *Robotics and Computer-Integrated Manufacturing*, *17*(1-2), 151-157.

[66] Taylor, J. B., Cormier, D. R., Joshi, S., & Venkataraman, V. (2001). Contoured edge slice generation in rapid prototyping via 5-axis machining. *Robotics and Computer-Integrated Manufacturing*, *17*(1-2), 13-18.

[67] Zhu, Z., Dhokia, V., & Newman, S. T. (2012, December). A novel process planning approach for hybrid manufacturing consisting of additive, subtractive and inspection processes. In *2012 IEEE International Conference on Industrial Engineering and Engineering Management* (pp. 1617-1621). IEEE.

[68] Zhang, H. O., Rui, D. M., Xie, Y., & Wang, G. L. (2013, August). Study on Metamorphic Rolling Mechanism for Metal Hybrid Additive Manufacturing. In *Solid Freeform Fabrication Symposium (SFF), Austin, TX, Aug* (pp. 12-14).

[69] Zhang, H. O., Xie, Y., Rui, D. M., & Wang, G. L. (2013). Hybrid deposition and micro rolling manufacturing method of metallic parts. In *Solid Freeform Fabrication Symposium (SFF), Austin, TX, Aug* (pp. 12-14).

[70] Manogharan, G., Wysk, R., Harrysson, O., & Aman, R. (2015). AIMS–a metal additive-hybrid manufacturing system: system architecture and attributes. *Procedia Manufacturing*, *1*, 273-286.

[71] Frank, M. C., Harrysson, O., Wysk, R. A., Chen, N., Srinivasan, H., Hou, G., & Keough, C. (2017, September). Direct additive subtractive hybrid manufacturing (DASH)—an out of envelope method. In *28th Annual International Solid Freeform Fabrication Symposium*.

[72] Li, F., Chen, S., Shi, J., Tian, H., & Zhao, Y. (2017). Evaluation and optimization of a hybrid manufacturing process combining wire arc additive manufacturing with milling for the fabrication of stiffened panels. *Applied Sciences*, *7*(12), 1233.

[73] Fessler, J. R., Merz, R., Nickel, A. H., Prinz, F. B., & Weiss, L. E. (1996). Laser deposition of metals for shape deposition manufacturing. In *1996 International Solid Freeform Fabrication Symposium*.

[74] Amon, C. H., Beuth, J. L., Weiss, L. E., Merz, R., & Prinz, F. B. (1998). Shape deposition manufacturing with microcasting: processing, thermal and mechanical issues.

[75] Hartmann, K., Krishnan, R., Merz, R., Neplotnik, G., Prinz, F. B., Schultz, L., ... & Weiss, L. E. (1994, May). Robot-assisted shape deposition manufacturing. In *Proceedings of the 1994 IEEE international conference on robotics and automation* (pp. 2890-2895). IEEE.

[76] Kao, J. H., & Prinz, F. B. (1998, September). Optimal motion planning for deposition in layered manufacturing. In *International Design Engineering Technical Conferences and Computers and Information in Engineering Conference* (Vol. 80364, p. V006T06A018). American Society of Mechanical Engineers.

[77] Pinilla, J. M., Kao, J. H., & Prinz, F. B. (1998). Process planning and automation for additive-subtractive solid freeform fabrication. In *1998 International Solid Freeform Fabrication Symposium*.

[78] Gupta, S. K., Tian, Q., & Weiss, L. (1999). Finding near-optimal build orientations for shape deposition manufacturing. In *Machining impossible shapes* (pp. 208-216). Springer, Boston, MA.

[79] Chang, Y. C., Pinilla, J. M., Kao, J. H., Dong, J., Ramaswami, K., & Prinz, F. B. (1999). Automated layer decomposition for additive/subtractive solid freeform fabrication. In *1999 International Solid Freeform Fabrication Symposium*.

[80] Lanzetta, M., & Cutkosky, M. R. (2008). Shape deposition manufacturing of biologically inspired hierarchical microstructures. *CIRP annals*, *57*(1), 231-234.

[81] Karunakaran, K. P., Sreenathbabu, A., & Pushpa, V. (2004). Hybrid layered manufacturing: direct rapid metal tool-making process. *Proceedings of the Institution of Mechanical Engineers, Part B: Journal of Engineering Manufacture*, *218*(12), 1657-1665.

[82] Sreenathbabu, A., Karunakaran, K. P., & Amarnath, C. (2005). Statistical process design for hybrid adaptive layer manufacturing. *Rapid prototyping journal*.

[83] Zhu, Z., Dhokia, V., & Newman, S. T. (2013). The development of a novel process planning algorithm for an unconstrained hybrid manufacturing process. *Journal of manufacturing processes*, *15*(4), 404-413.

[84] Newman, S. T., Zhu, Z., Dhokia, V., & Shokrani, A. (2015). Process planning for additive and subtractive manufacturing technologies. *CIRP Annals*, *64*(1), 467-470.

[85] Zhu, Z., Dhokia, V., Newman, S. T., & Nassehi, A. (2014). Application of a hybrid process for high precision manufacture of difficult to machine prismatic parts. *The International Journal of Advanced Manufacturing Technology*, *74*(5-8), 1115-1132.

[86] Xie, Y., Zhang, H., & Zhou, F. (2016). Improvement in geometrical accuracy and mechanical property for arc-based additive manufacturing using metamorphic rolling mechanism. *Journal of Manufacturing Science and Engineering*, *138*(11), 111002.

[87] Zhou, X., Zhang, H., Wang, G., Bai, X., Fu, Y., & Zhao, J. (2016). Simulation of microstructure evolution during hybrid deposition and micro-rolling process. *Journal of materials science*, *51*(14), 6735-6749.

[88] Fu, Y., Zhang, H., Wang, G., & Wang, H. (2017). Investigation of mechanical properties for hybrid deposition and micro-rolling of bainite steel. *Journal of materials processing technology*, *250*, 220-227.

[89] Popov, V. V., & Fleisher, A. (2020). Hybrid additive manufacturing of steels and alloys. *Manufacturing Review*, *7*, 6.

[90] Yi, L., Gläßner, C., & Aurich, J. C. (2019). How to integrate additive manufacturing technologies into manufacturing systems successfully: A perspective from the commercial vehicle industry. *Journal of Manufacturing Systems*, *53*, 195-211.

[91] Häfele, T., Schneberger, J. H., Kaspar, J., Vielhaber, M., & Griebsch, J. (2019). Hybrid additive manufacturing–Process chain correlations and impacts. *Procedia CIRP*, *84*, 328-334.

[92] Zhu, Z., Dhokia, V., & Newman, S. T. (2012, December). A novel process planning approach for hybrid manufacturing consisting of additive, subtractive and inspection processes. In *2012 IEEE International Conference on Industrial Engineering and Engineering Management* (pp. 1617-1621). IEEE.

[93] Urbanic, R. J., Hedrick, R. W., & Burford, C. G. (2017). A process planning framework and virtual representation for bead-based additive manufacturing processes. *The International Journal of Advanced Manufacturing Technology*, *90*(1), 361-376.

[94] Zhang, Y., & Bernard, A. (2014, August). AM feature and knowledge based process planning for additive manufacturing in multiple parts production context. In *Proceedings of 25th Annual International Solid Freeform Fabrication Symposium* (Vol. 44, No. 4, pp. 1259-1276).

[95] Zhang, Y., Bernard, A., Gupta, R. K., & Harik, R. (2014). Evaluating the design for additive manufacturing: a process planning perspective. *Procedia Cirp*, *21*, 144-150.

[96] Goguelin, S., Colaco, J., Dhokia, V., & Schaefer, D. (2017). Smart manufacturability analysis for digital product development. *Procedia Cirp*, *60*, 56-61.

[97] Byun, H. S., & Lee, K. H. (2006). Determination of optimal build direction in rapid prototyping with variable slicing. *The International Journal of Advanced Manufacturing Technology*, *28*(3), 307-313.

[98] Zhang, Y., Bernard, A., Harik, R., & Karunakaran, K. P. (2017). Build orientation optimization for multi-part production in additive manufacturing. *Journal of Intelligent Manufacturing*, *28*(6), 1393-1407.

[99] Zhang, Y., Harik, R., De Backer, W., Bernard, A., & IRCCyN, E. C. D. N. (2016). A facet cluster-based method for alternative build orientation generation in additive manufacturing. In *Solid Freeform Fabrication Symposium* (pp. 23-35).

[100] Zhang, Y., Bernard, A., Gupta, R. K., & Harik, R. (2016). Feature based building orientation optimization for additive manufacturing. *Rapid Prototyping Journal*.

[101] Luo, Z., Yang, F., Dong, G., Tang, Y., & Zhao, Y. F. (2016, August). Orientation optimization in layer-based additive manufacturing process. In *International Design Engineering Technical Conferences and Computers and Information in Engineering Conference* (Vol. 50077, p. V01AT02A039). American Society of Mechanical Engineers.

[102] Li, Y., Tang, K., He, D., & Wang, X. (2021). Multi-Axis Support-Free Printing of Freeform Parts with Lattice Infill Structures. *Computer-Aided Design*, *133*, 102986.

[103] Xu, K., Chen, L., & Tang, K. (2018). Support-free layered process planning toward 3+ 2-axis additive manufacturing. *IEEE Transactions on Automation Science and Engineering*, *16*(2), 838-850.

[104] Xu, J., Gu, X., Ding, D., Pan, Z., & Chen, K. (2018). A review of slicing methods for directed energy deposition based additive manufacturing. *Rapid Prototyping Journal*.

[105] Jin, Y., Du, J., & He, Y. (2017). Optimization of process planning for reducing material consumption in additive manufacturing. *Journal of Manufacturing Systems*, *44*, 65-78.

[106] Ding, D., Pan, Z., Cuiuri, D., Li, H., & Larkin, N. (2016). Adaptive path planning for wire-feed additive manufacturing using medial axis transformation. *Journal of Cleaner Production*, *133*, 942-952.

[107] Kulkarni, P., Marsan, A., & Dutta, D. (2000). A review of process planning techniques in layered manufacturing. *Rapid prototyping journal*.

[108] Zhang, Y., & Bernard, A. (2018). A KBE CAPP framework for qualified additive manufacturing. *CIRP Annals*, *67*(1), 467-470.

[109] Zhang, Y., & Bernard, A. (2014, August). AM feature and knowledge based process planning for additive manufacturing in multiple parts production context. In *Proceedings of 25th Annual International Solid Freeform Fabrication Symposium* (Vol. 44, No. 4, pp. 1259-1276).

[110] Zhang, Y., Xu, Y., & Bernard, A. (2014). A new decision support method for the selection of RP process: knowledge value measuring. *International journal of computer integrated manufacturing*, *27*(8), 747-758.

[111] Zhang, Y., & Bernard, A. (2014). An integrated decision-making model for multi-attributes decision-making (MADM) problems in additive manufacturing process planning. *Rapid Prototyping Journal*.

[112] Zhang, Y., & Bernard, A. (2014). Grouping parts for multiple parts production in Additive Manufacturing. *Procedia Cirp*, *17*, 308-313.

[113] Zhang, Y., Gupta, R. K., & Bernard, A. (2016). Two-dimensional placement optimization for multi-parts production in additive manufacturing. *Robotics and Computer-Integrated Manufacturing*, *38*, 102-117.

[114] Zhang, Y., Bernard, A., Harik, R., & Fadel, G. (2018). A new method for single-layer-part nesting in additive manufacturing. *Rapid Prototyping Journal*.

[115] Jin, Y., He, Y., & Shih, A. (2016). Process planning for the fuse deposition modeling of ankle-foot-othoses. *Procedia Cirp*, *42*, 760-765.

[116] Ruan, J., Eiamsa-ard, K., & Liou, F. W. (2005, January). Automatic multi-axis slicing based on centroidal axis computation. In *International Design Engineering Technical Conferences and Computers and Information in Engineering Conference* (Vol. 47403, pp. 383-393).

[117] Zhang, J., & Liou, F. (2004). Adaptive slicing for a multi-axis laser aided manufacturing process. *J. Mech. Des.*, *126*(2), 254-261.

[118] Kirschman, C. F., & Jara-Almonte, C. C. (1992). A parallel slicing algorithm for solid freeform fabrication processes. In *1992 International Solid Freeform Fabrication Symposium*.

[119] Jin, Y. A., He, Y., Fu, J. Z., Gan, W. F., & Lin, Z. W. (2014). Optimization of tool-path generation for material extrusion-based additive manufacturing technology. *Additive manufacturing*, *1*, 32-47.

[120] Zhang, Y., & Bernard, A. (2015). A Parallel 2D Nesting Method for Machine's Work Space Planning in Additive Manufacturing. In *14ème Colloque National: Produits, Procédés, Systèmes Intelligents et Durables*.

[121] Oh, Y., Witherell, P., Lu, Y., & Sprock, T. (2020). Nesting and scheduling problems for additive manufacturing: a taxonomy and review. *Additive Manufacturing*, 101492.

[122] Karunakaran, K. P., Shanmuganathan, P. V., Jadhav, S. J., Bhadauria, P., & Pandey, A. (2000). Rapid prototyping of metallic parts and moulds. *Journal of materials processing technology*, *105*(3), 371-381.

[123] Liou, F. W., Choi, J., Landers, R. G., Janardhan, V., Balakrishnan, S. N., & Agarwal, S. (2001). Research and development of a hybrid rapid manufacturing process. In *2001 International Solid Freeform Fabrication Symposium*.

[124] Eiamsa-ard, K., Liou, F. W., Landers, R. G., & Choset, H. (2003, January). Toward automatic process planning of a multi-axis hybrid laser aided manufacturing system: skeleton-based offset edge generation. In *International Design Engineering Technical Conferences and Computers and Information in Engineering Conference* (Vol. 37009, pp. 227-235).

[125] Ruan, J., Eiamsa-ard, K., & Liou, F. W. (2005). Automatic process planning and toolpath generation of a multiaxis hybrid manufacturing system. *Journal of manufacturing processes*, *7*(1), 57-68.

[126] Ren, L., Sparks, T., Ruan, J., & Liou, F. (2010). Integrated process planning for a multiaxis hybrid manufacturing system. *Journal of Manufacturing Science and Engineering*, *132*(2).

[127] Zhu, Z., Dhokia, V., & Newman, S. T. (2017). A novel decision-making logic for hybrid manufacture of prismatic components based on existing parts. *Journal of Intelligent Manufacturing*, *28*(1), 131-148.

[128] Behandish, M., Nelaturi, S., & de Kleer, J. (2018). Automated process planning for hybrid manufacturing. *Computer-Aided Design*, *102*, 115-127.

[129] Manogharan, G., Wysk, R. A., & Harrysson, O. L. (2016). Additive manufacturing–integrated hybrid manufacturing and subtractive processes: economic model and analysis. *International Journal of Computer Integrated Manufacturing*, *29*(5), 473-488.

[130] Chen, L., Lau, T. Y., & Tang, K. (2020). Manufacturability analysis and process planning for additive and subtractive hybrid manufacturing of Quasi-rotational parts with columnar features. *Computer-Aided Design*, *118*, 102759.

[131] Kerbrat, O., Mognol, P., & Hascoet, J. Y. (2010). Manufacturing complexity evaluation at the design stage for both machining and layered manufacturing. *CIRP Journal of Manufacturing Science and Technology*, *2*(3), 208-215.

[132] Chen, L., Lau, T. Y., & Tang, K. (2020). Manufacturability analysis and process planning for additive and subtractive hybrid manufacturing of Quasi-rotational parts with columnar features. *Computer-Aided Design*, *118*, 102759.

[133] Wei, X., Qiu, S., Zhu, L., Feng, R., Tian, Y., Xi, J., & Zheng, Y. (2017). Toward support-free 3D printing: A skeletal approach for partitioning models. *Ieee Transactions on visualization and computer graphics*, *24*(10), 2799-2812.

[134] Wang, X., Chen, L., Lau, T. Y., & Tang, K. (2020). A skeleton-based process planning framework for support-free 3+ 2-axis printing of multi-branch freeform parts. *The International Journal of Advanced Manufacturing Technology*, *110*(1), 327-350.

[135] Zheng, Y., & Ahmad, R. (2020). Feature extraction and process planning of integrated hybrid additive-subtractive system for remanufacturing. *Mathematical Biosciences and Engineering*, *17*(6), 7274-7301.

[136] Eldakroury, M. A., Chen, N., & Frank, M. C. (2018). A new method for locating candidate substrates for multi axis hybrid manufacturing systems. *Rapid Prototyping Journal*.

[137] N Chen, N., & Frank, M. (2019). Process planning for hybrid additive and subtractive manufacturing to integrate machining and directed energy deposition. *Procedia Manufacturing*, *34*, 205-213.

[138] Reichler, A. K., Gerbers, R., Falkenberg, P., Türk, E., Dietrich, F., Vietor, T., & Dröder, K. (2019). Incremental Manufacturing: Model-based part design and process planning for Hybrid Manufacturing of multi-material parts. *Procedia Cirp*, *79*, 107-112.

[139] Ruan, J., Zhang, J., & Liou, F. (2009, January). Selection of part orientation for multi-axis hybrid manufacturing process. In *International Design Engineering Technical Conferences and Computers and Information in Engineering Conference* (Vol. 49026, pp. 587-596).

[140] Wu, H., Xie, X., Liu, M., Chen, C., Liao, H., Zhang, Y., & Deng, S. (2020). A new approach to simulate coating thickness in cold spray. *Surface and Coatings Technology*, *382*, 125151.

[141] Hao, J., Chen, X., Liu, H., & Ye, S. (2018). A novel process planning algorithm for additive and subtractive manufacturing based on skeleton tree matching. *Rapid Prototyping Journal*.

[142] Xie, F., Bi, D., & Tang, K. (2020). A potential field based multi-axis printing path generation algorithm. *International Journal of Computer Integrated Manufacturing*, *33*(12), 1277-1299.

[143] Ren, L., Ruan, J., Eiamsa-ard, K., & Liou, F. (2007, January). Adaptive deposition coverage toolpath planning for metal deposition process. In *International Design Engineering Technical Conferences and Computers and Information in Engineering Conference* (Vol. 48078, pp. 413-419).

[144] Ren, L., Eiamsa-ard, K., Ruan, J., & Liou, F. (2007, January). Part repairing using a hybrid manufacturing system. In *International Manufacturing Science and Engineering Conference* (Vol. 42908, pp. 1-8).

[145] Calleja, A., Tabernero, I., Fernández, A., Celaya, A., Lamikiz, A., & De Lacalle, L. L. (2014). Improvement of strategies and parameters for multi-axis laser cladding operations. *Optics and Lasers in Engineering*, *56*, 113-120.

[146] Choi, S. H., & Cheung, H. H. (2006). A topological hierarchy-based approach to toolpath planning for multi-material layered manufacturing. *Computer-Aided Design*, *38*(2), 143-156.

[147] Jin, G. Q., Li, W. D., Tsai, C. F., & Wang, L. (2011). Adaptive tool-path generation of rapid prototyping for complex product models. *Journal of manufacturing systems*, *30*(3), 154-164.

[148] Han, W., Jafari, M. A., Danforth, S. C., & Safari, A. (2002). Tool path-based deposition planning in fused deposition processes. *J. Manuf. Sci. Eng.*, *124*(2), 462-472.

[149] Jin, Y. A., He, Y., & Fu, J. Z. (2013). An adaptive tool path generation for fused deposition modeling. In *Advanced Materials Research* (Vol. 819, pp. 7-12). Trans Tech Publications Ltd.

[150] Jin, Y. A., He, Y., Fu, J. Z., Gan, W. F., & Lin, Z. W. (2014). Optimization of tool-path generation for material extrusion-based additive manufacturing technology. *Additive manufacturing*, *1*, 32-47.

[151] Patil, S., & Ravi, B. (2005, December). Voxel-based representation, display and thickness analysis of intricate shapes. In *Ninth International Conference on Computer Aided Design and Computer Graphics (CAD-CG'05)* (pp. 6-pp). IEEE.

[152] Bertrand, G., & Malandain, G. (1995). A Note on" Building Skeleton Models via 3-D Medial Surface/Axis Thinning Algorithms". *Graphical Models and Image Processing*, *57*(6), 537-538.

[153] Kennedy, J., & Eberhart, R. (1995, November). Particle swarm optimization. In *Proceedings of ICNN'95-international conference on neural networks* (Vol. 4, pp. 1942-1948). IEEE.

[154] Cichocka, J. M., Migalska, A., Browne, W. N., & Rodriguez, E. (2017, July). SILVEREYE–the implementation of Particle Swarm Optimization algorithm in a design optimization tool. In *International Conference on Computer-Aided Architectural Design Futures* (pp. 151-169). Springer, Singapore.

[155] Chandrakar, A., Zhang, Y., Laroche, F., & Bernard, A. (2017). Physical assembly sequence optimisation for developing an integrated 3D reconstruction method. *Virtual and Physical Prototyping*, *12*(2), 173-190.

[156] Deb, K., Pratap, A., Agarwal, S., & Meyarivan, T. A. M. T. (2002). A fast and elitist multiobjective genetic algorithm: NSGA-II. *IEEE transactions on evolutionary computation*, *6*(2), 182-197.

Titre : CAPP pour la Fabrication Additive Hybride

Mots clés: CAPP, HAM, volume initial, séquence de dépôt, trajectoire de dépôt, optimisation évolutive.

Résumé: La fabrication additive hybride (HAM) devient de plus en plus importante pour obtenir des produits d'utilisation finale. Cependant, quelques problèmes persistent à toutes les étapes de la chaîne de traitement de HAM et cette thèse rapporte les études sur la planification des processus. L'ensemble de la recherche propose des méthodes pour trois tâches clés de la planification des processus en HAM à un niveau relativement général. Les principales méthodes proposées comprennent la génération et l'optimisation du volume initial, la planification des séquences et la planification des trajectoires. Pour démontrer ces méthodes proposées, un ensemble de cas de simulation numérique est utilisé pour la démonstration. Un procédé HAM spécial, la pulvérisation à froid avec usinage CNC, est adopté pour définir les exigences de l'application et les contraintes de fabrication dans le calcul. Cependant, l'objectif de cette recherche est de développer des méthodes génériques pour plus de processus HAM, où des systèmes multi-axes sont appliqués. En modifiant les contraintes de fabrication, les méthodes proposées et les algorithmes mis en œuvre pourraient être adoptés pour de larges applications CAPP dans différents processus HAM.

Title: CAPP for Hybrid Additive Manufacturing

Keywords: CAPP, HAM, initial volume, sequence planning, path planning, evolutionary optimization.

Abstract: Hybrid additive manufacturing (HAM) is becoming increasingly important to obtain end-use products. However, a couple of problems still exist in all the stages of HAM's processing chain and this thesis reports the studies on process planning. The whole research proposes some methods for three key tasks of process planning in HAM at a relatively general level. The main proposed methods include generation and optimization of the initial volume, sequence planning, and path planning. To demonstrate these proposed methods, a set of numerical simulation cases are used for demonstration. A special HAM process, cold spraying with CNC machining, is adopted to set the application requirements and manufacturing constrains in computation. However, the objective of this research is to develop generic methods for more HAM processes, where multi-axis systems are applied. By changing the manufacturing constraints, the proposed methods and implemented algorithms could be adopted for wide CAPP applications in different HAM processes.